TBK1 deficiency leads to TDP-43 pathology driven by endo-lysosomal dysfunction in human-induced motor neurons

Citation

Hao, Jin. 2022. TBK1 deficiency leads to TDP-43 pathology driven by endo-lysosomal dysfunction in human-induced motor neurons. Doctoral dissertation, Harvard University Graduate School of Arts and Sciences.

Permanent link

https://nrs.harvard.edu/URN-3:HUL.INSTREPOS:37371944

Terms of Use

Share Your Story

Accessibility

HARVARD UNIVERSITY
Graduate School of Arts and Sciences

DISSERTATION ACCEPTANCE CERTIFICATE

The undersigned, appointed by the

Department of Biological Sciences in Dental Medicine

have examined a dissertation entitled

"TBK1 deficiency leads to TDP-43 pathology driven by endo-lysosomal dysfunction in human-induced motor neurons"
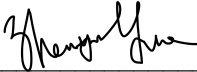
presented by Jin Hao,

candidate for the degree of Doctor of Philosophy and hereby certify that it is worthy of acceptance.

Signature _____

Typed name: Prof. Clifford J. Woolf

Signature _____

Typed name: Prof. Brian Wainger

Signature _____

Typed name: Prof. Zhenyu Yue

Date: April 14, 2022

TBK1 deficiency leads to TDP-43 pathology driven by endo-lysosomal

dysfunction in human-induced motor neurons

A dissertation presented by

Jin Hao

to

The Department of Biological Sciences in Dental Medicine

in partial fulfillments of the requirements

for the degree of

Doctor of Philosophy

in the subject of

Biology

Harvard University

Cambridge, Massachusetts

April 2022

TBK1 deficiency leads to TDP-43 pathology driven by endo-lysosomal dysfunction in human-induced motor neurons

Abstract

Amyotrophic lateral sclerosis (ALS) is a fatal neurodegenerative disease characterized by motor neuron loss accompanied by cytoplasmic localization of TDP-43 proteins and their insoluble accumulations. Over the past decades, the development of whole-genome sequencing and whole exome sequencing have substantially advanced our understanding of the genetic etiology of ALS. Haploinsufficiency of TBK1 has been found to associate with or cause ALS by recent exome sequencing. However, the exact mechanism of this connection remains elusive. Here, we generated a human stem cell model harboring loss-of-function mutations of *TBK1* by gene editing. We found that TBK1 deficiency was sufficient to cause TDP-43 pathology in human-induced motor neurons. In addition, TBK1 interacted with endosomes and was required for normal endosomal maturation and subsequent lysosomal acidification. Surprisingly, TDP-43 pathology resulted from the dysfunctional endo-lysosomal pathway rather than the impaired autophagosome formation mechanism. Restoring TBK1 levels in TBK1 deficient cells re-sustained endo-lysosomal function and TDP-43 homeostasis and maintained motor neuron physiological functions. Notably, using patient-derived motor neurons, we found that haploinsufficiency of TBK1 sensitized neurons to lysosomal stress, and chemical regulators of the endo-lysosomal pathway rescued the neurodegenerative process. Together, our results revealed that the mechanisms of TBK1 in maintaining TDP-43 and motor neuron homeostasis and modulating endosomal maturation might be able to rescue neurodegenerative disease phenotypes caused by TBK1 deficiency.

Table of Contents

Acknowledgements

First, I would like to thank my primary advisor, Dr. Kevin Eggan, for his kind support and guidance throughout the first five years of my Ph.D. career. Before I came to Harvard, I was trained to be a doctor with limited access to basic scientific research. Therefore, when I first stepped in Kevin's office seeking an opportunity for lab rotation, I was worried and nervous about the fitness of my background into his lab. However, instead of asking me about basic scientific questions, he was more interested in the personality and determination. He encouraged me a lot by offering me the rotation and the opportunity to participate in an amazing project. This experience helped build my confidence and encouraged me to devote into basic science.

I would also like to thank every former Eggan lab member for helping me out when I had trouble with experiments, for cheering me up when I was feeling upset, and for working together with me in this long march towards the degree. In particular, I would like to thank Maura Charlton and Joanie Mok for organizing the lab and supporting my routine experiments. I would also like to mention Feng Tian, Yingying Zhang, Menglu Qian, Atsushi Fukuda, Jingyuan Wang, Francesco Limone, and Irune Guerra for being good friends and bench neighbors. We spent a lot of time together during the past years, and they were the best peers in the world. In addition, I would like to thank my collegues, Dia Ghosh, Jana Mitchell, Kevin Smith, Joe Klim, Michael Wells, Daniel Mordes, Gengle Niu, Werner Neuhaus, Kanchana Gamage, Olli Pietilainen, Ralda Nehme, Greta Pintacuda, Brian Joseph, Yenal Lakes, Alex Couto, Leslie Nash, Marcel Leyton, and every former Eggan lab member who I have worked with, for their intellectual support for my project.

Second, I would like to thank Dr. Zhixun Dou, who served as my second advisor when Kevin left Harvard. Zhixun is very energetic and smart, and he always has fantastic ideas for research. When he was still the member of my dissertation advisory committee, he offered me a lot of insightful ideas and technical tricks that could take me five years to figure out without his

help. In addition, the research atmosphere in the Dou lab is very supportive and pleasing. I would like to thank Yanxin Xu, Takuya Kumazawa, Angelique Onorati for their support and help.

I would like to acknowledge the members of my Dissertation Advisory Committee, Dr. Lee Rubin and Dr. Clifford Woolf, for their insightful advice and guidance on my research project and academic development.

Furthermore, I would like to thank my program, Biological Sciences in Dental Medicine. I want to thank Leanne Jacobellis, the administrative staff of our program, for her supportive work and help. I would also like to thank Dr. Yingzi Yang and Dr. Francesca Gori for their help and guidance.

In closing, I would like to express my most sincere gratitude to my families, without whom I would never be able to come this far. I want to thank them for their unconditional support for every decision I have made in this journey, and their company and encouragement for me to fulfill my dreams.

March 2022

Cambridge, MA

CHAPTER 1: Introduction

Author Contributions:

This chapter was unpublished work by Jin Hao.

1.1 Introduction to Amyotrophic Lateral Sclerosis

Amyotrophic lateral sclerosis (ALS), also known as Lou Gehrig's disease in the United States, is a progressive and fatal neurodegenerative disease affecting the motor neurons, resulting in paralysis and death [1,2]. ALS is currently the most common cause of neurologic deaths in adults [3], and the disease is incurable with no current Food and Drug Administration (FDA) approved drugs that could extend the lifespan to more than one year [4,5]. The term amyotrophic lateral sclerosis, was originated from a French neurologist named Jean-Martin Charcot in 1874 and reflected how clinicians described the disease in the 19th century based on autopsy findings and clinical symptoms [1]. The initial symptom of ALS can vary between patients: some patients initiate with a bulbar-onset disease, which is depicted by dysarthria (inability to speak) and dysphagia (inability to swallow), while some other patients present with a spinal-onset disease, which is characterized by muscle weakness. As the disease progresses, these symptoms will spread to other parts of the body and result in paralysis and death due to respiratory failure, usually within five years of diagnosis [6,7].

In most cases, the primary cause of ALS is unclear. Some patients may have familial history linked to mutations of genes that have various functions. However, even in familial ALS, some of the ALS-implicated genes are not completely penetrant, and in some rare cases, the genotype does not necessarily predict the phenotype [8]. Currently, treatment of ALS focuses on symptom management and respiratory support, which provides limited benefits in some patients, and there is no cure or effective treatment for ALS patients [9,10].

Our understanding of ALS and its pathologies has advanced over the past decades. With the advancement of the next-generation sequencing techniques, most ALS cases can be classified as sporadic (SALS) and familial (FALS) due to the identification of several causative genes. Many novel pathological concepts have emerged based on the genetics of ALS, and new therapeutic strategies are being developed targeting these genetic forms.

1.2 The genetics of amyotrophic lateral sclerosis

Although the disease was described more than one century ago, the genes whose mutations are associated with ALS have not been known until 1993. Superoxide dismutase 1 (*SOD1*) was the first gene identified to associate with FALS [11]. More than one hundred mutations in *SOD1* have been identified to cause ALS, counting for 12%-23.5% of FALS cases and about 1% of SALS cases [12,13]. Another two very critical gene mutations found in ALS were the *FUS* and *TARDBP* [14,15], which encode RNA binding proteins. Mutations in each gene count for 1% SALS and 4% FALS patients [12,16]. Many other genes have been identified with the help of sequencing and molecular biology techniques [12]. Mutations of a GGGGCC hexanucleotide repeat expansion (HRE) located between exon1 and the alternative exon1b of chromosome 9 open reading frame 72 (*C9ORF72*) were identified in 2011 [17], which counted for 40% of FALS and 7% of SALS patients. Nowadays, there are over 30 genes found to cause ALS (Table 1) (http://alsod.iop.kcl.ac.uk/), and more than a dozen genes are recognized as ALS risk genes or disease modifiers [18-21]. Although most ALS cases are identified as sporadic, and FASL only represents 5%-10% of the total cases, this prevalence may be undervalued due to the variable definitions used. Currently, *SOD1*, *C9ORF72*, *TARDBP*, and *FUS* are the most mutated genes in the ALS population, but the frequency of these mutations largely depends on their ancestral origins [22]. For example, in the population of European FALS patients, *C9ORF72* represents 33.7%, *SOD1* represents 14.8%, *TARDBP* counts for 4.2%, and *FUS* represents 2.8% of the total cases. However, in the Asian FALS patient pool, these genes present a different repartition of the total cases, with *SOD1* having 30%, *FUS* presenting 6.4%, *C9ORF72* presenting 2.3%, and *TARDBP* showing in 1.5% of the patients [22]. These observations indicate the population-specific genetic risk factors in ALS. In addition, while most of these genes are autosomal dominant (not always with complete penetrance), some are recessive, like *SOD1, OPTN, and FUS* [23]. Others can represent only autosomal recessive or X-linked inheritance (Table 1) [23].

Table 1. Classification of inherited genetic factors in ALS

Inheritance mode	OMIM	Gene name	Chromosome	Proposed denomination	Current denomination
Autosomal Dominant (AD)	105400	SOD1 (superoxide dismutase 1)	21q22.11	AD-ALS-SOD1	ALS1
	606640	Unknown	18q21	AD-ALS-unknown	ALS3
	602433	SETX (senataxin)	9q34.13	AD-ALS-SETX	ALS4
	608030	FUS/LTS (Fused in sarcoma/translated in liposarcoma)	16q11.2	AD-ALS-FUS	ALS6
	608031	Unknown	20p13	AD-ALS-Unknown	ALS7
	608627	VAPB (vesicle-associated membrane protein B angiogenin)	20q13.32	AD-ALS-VAPB	ALS8
	611895	ANG (angiogenin)	14q11.2	AD-ALS-ANG	ALS9
	612069	TARDBP (TAR DNA-binding protein 43)	1p36.22	AD-ALS-TARDBP	ALS10
	612577	FIG. 4 (phosphoinositide 5-phosphatase)	6q21	AD-ALS-FIG. 4	ALS11
	613435	OPTN (optineurin)	10p13	AD-ALS-OPTN	ALS12
	183090	ATXN2 (ataxin-2)	12q24.12		ALS13
	613954	VCP (valosin-containing protein)	9p13.3	AD-ALS-VCP	ALS14
	614696	CHMP2B (charged multivesicular body protein 2B)	3p11.2	AD-ALS-CHMP2B	ALS17
	614808	PFN1 (Profilin-1)	17p13.2	AD-ALS-PFN1	ALS18
	615515	ERBB4 (chorion protein gene ErB.4)	2q34	AD-ALS-ERBB4	ALS19
	615426	HNRNPA1 (heterogeneous nuclear ribonucleoprotein A1)	12q13	AD-ALS-HNRNPA1	ALS20
	606070	MATR3 (matrin-3)	5q31.2	AD-ALS-MATR3	ALS21
	616208	TUBA4A (tubulin alpha-4A)	2q35	AD-ALS-TUBA4A	ALS22

4

	617839	ANXA11 (annexin A11)	10q22.3	AD-ALS-ANXAII	ALS23
	-	DAO (D-amino acid oxidase)	12q24	AD-ALS-DAO	-
	-	KIAA0693/CREST (calcium-responsive transactivator)/SS18L1 (synovial sarcoma translocation gene on chromosome 18-like 1)	20q13	-	-
	105550	C9ORF72 (chromosome 9 open reading frame 72)	9p21.2	AD-ALS-C9ORF72	FTD-ALS1
	615911	CHCHD10 (coiled-coil-helix-coiled-coil-helix domain containing protein 10)	22q11.23	AD-ALS-CHCHD10	FTD-ALS2
	616437	SQSTM1 /p62 (sequestosome-1)	5q35.3	AD-ALS-SQSMT1	FTD-ALS3
	616439	TBK1 (TANK-binding kinase 1)	12q14.2	AD-ALS-TBK1	FTD-ALS4
Autosomal Recessive (AR)	105400	SOD1 (superoxide dismutase 1)	21q22.11	AR-ALS-SOD1	ALS1
	205100	KIAA1563 (alsin)	2q33.1	AR-ALS-KIAA1563	ALS2
	602099	KIAA1840/SPG11 (spastacin)	15q15–21.1	AR-ALS-KIAA1840	ALS5
	608030	FUS/LTS (Fused in sarcoma/translated in liposarcoma)	16q11.2	AR-ALS-FUS	ALS6
	613435	OPTN (optineurin)	10p13	AR-ALS-OPTN	ALS12
	614373	SIGMAR1 (Sigma nonopioid intracellular receptor 1)	9p13.3	AR-ALS-SIGMAR1	ALS16
	611890	GLE1 (GLE1, RNA export mediator)	9q34.11	AR-ALS-GLE1	LAHCDA
X-linked (XL)	300857	UBQLN2 (Ubiquilin-2)	Xp11.21	XL-ALS-UBQLN2	ALS15

Another important finding in the FALS population is the low penetrance rate of ALS-causing mutations and the genetic pleiotropy. In addition, evidence has shown that both polygenic and oligogenic inheritance can be found in SALS [24,25]. In such cases, some isolated FALS patients may be identified as SALS, and mutations that are found to cause FALS are repeatedly observed in SALS [26]. Therefore, genetic mutations could account for 7.4% of total ALS cases in the European cohort (primarily *C9ORF72*) and 2.9% in the Asian population (mainly *SOD1*) [22].

1.3 Molecular mechanisms in ALS pathology

To date, the cause and mechanism of ALS remain elusive. However, the advances in genetic studies, as well as the development of *in vitro* and *in vivo* models, revealed common pathways that could be disrupted in ALS or contributed to the onset and progression of the disease. Consensus is yet to be reached regarding the causal mechanisms of different forms of disease pathology, including in familial and sporadic cases.

1.3.1 Impaired protein homeostasis

Protein aggregates positive for TDP-43 have been identified in about 95% of total ALS cases, being widely recognized as a hallmark of ALS [27]. In addition, protein aggregation of SOD1 [28], FUS [14], and neurofilament [29] have also been identified in ALS patients, suggesting the impairment of protein quality control and the imbalance between protein synthesis and degradation in diseased cells. The presence of protein aggregates in ALS patients was first found in the anterior horn cells [30], and these protein aggregates were described as ubiquitin-positive [31]. Later, the ubiquitinated inclusions were found to be immunoreactive for SOD1 [32] and p62 [33], and up to 98% of the total ALS cases show TDP-43 positive inclusions [16]. Therefore, the presence of protein aggregations in ALS suggests the critical role of impaired protein degradation pathway in ALS pathogenesis.

The discovery of mutations in genes encoding *UBQLN2* and *VCP*, both involved in protein

clearance through the ubiquitin-proteasome system (UPS), leads to the theory of dysregulated UPS in ALS pathology [34,35]. In addition, subsequent studies have reported that the mutations in *SOD1, VABP, SQSTM1, OPTN, CCNF*, and *C9ORF72* caused reduced activation of the UPS [36-38]. Similarly, C9ORF72-derived DPR proteins, FUS, and SOD1 have been reported to produce toxic aggregates positive for proteasome components [39,40], suggesting the involvement of UPS in ALS pathogenesis.

The ubiquitinated protein can be degraded through the auto-lysosomal pathway. This process involves four tightly regulated steps: 1) the bilayer vacuole initiates and extends into phagophores; 2) the selective autophagic cargoes (protein aggregates and damaged organelles) are transported; 3) the phagophores mature into autophagosomes; and 4) the autophagosomes fuse with lysosomes, where degradation of the cargoes is proceeded [41]. The impaired auto-lysosomal pathway has been found in many ALS cases with the mutations for *OPTN, SQSTM1, FUS, VCP, CHMP2B*, and *TBK1* [42-45]. In addition, the mutations of *C9ORF72* have been reported to interfere with the autophagy pathway. Autophagy activity is inhibited when C9ORF72 expression is eliminated, resulting in an increased number of p62 and TDP-43 inclusions [46,47]. The accumulation of cytotoxic DPR proteins could also lead to impaired autophagy and, ultimately, neuronal death [48]. Furthermore, autophagy induction has been reported to increase the turnover of TDP-43 aggregates and thus improve motor neuron survival [49].

These studies demonstrate the significance of autophagy on the clearance of aggregated or misfolded proteins and indicate the underlying mechanisms of impaired proteostasis in mediating ALS pathology.

1.3.2 Endoplasmic reticulum stress and unfolded protein response

In diseased cells, the defective proteins could be transported to the endoplasmic reticulum (ER) initiated by the unfolded-protein response (UPR) for proper folding [50]. The accumulation of misfolded proteins in the ER will activate ER stress response to clear misfolded proteins, also

known as the ER-associated protein degradation (ERAD) pathway [50]. Previous research has reported the accumulation of SOD1 aggregates in the ER, which co-localized with unfolded protein response (UPR) markers [51]. In *C9ORF72* ALS patients, the aggregation of poly (GA) was shown to induce ER stress and inhibit proteasome activity [52]. In addition, accumulations of ER stress markers were found in the cerebrospinal fluid (CSF) of SALS patients [51]. When exposed to the CSF of ALS patients, healthy neurons displayed ER fragmentation and caspase-dependent apoptosis activation, indicating increased ER stress [53].

The mutations of vesicle-associated membrane protein-associated protein B (VAPB) have also been associated with ALS, leading to accumulations of misfolded proteins in the ER [54]. The VAPB has been found to localize with ER membrane and play a key role in vesicle trafficking [55]. Notably, VAPB accumulations have also been identified in the ER of mononuclear cells from the peripheral blood of sporadic ALS patients [56]. In addition, in *OPTN* mutant FALS patients, optineurin has been found to diffuse in the cytosol, leading to increased Golgi apparatus fragmentation and elevated ER stress [57].

Therefore, these studies evidenced that protein degradation could be impaired in ALS, leading to protein aggregation and accumulation, which, in turn, could cause defects in the functions of organelles like mitochondria and ER. However, it remains unclear whether ER stress and the UPR are a cause of ALS or a result of neurodegeneration.

1.3.3 Oxidative stress and mitochondria dysfunction

Oxidative stress results from the imbalance between the production and clearance of reactive oxygen species (ROS) and the inability to repair ROS-mediated toxicity [58]. In both *SOD1* and sporadic ALS patients, elevated levels of oxidized proteins have been found in the post-mortem tissue, serum, urine, and the CSF [59]. SOD1 has been identified as an antioxidant enzyme that can catalyze radical superoxide anions into hydrogen peroxide and molecular oxygen [60]. In familial *SOD1* patients, there is a 42% reduction in SOD1 activity, causing a potential imbalance

between ROS production and elimination [61]. This imbalance could be worsened by impaired Nuclear erythroid 2-Related Factor—antioxidant response element (NRF2-ARE) signaling pathway that mediated the expression of antioxidant proteins in *SOD1* patients [62,63]. In addition, oxidative damage has been observed in the motor neurons from *SOD1* mutant mice and *SOD1* familial ALS patients [64,65].

In normal cells, oxidative stress and induced DNA damage are recurrent throughout life, which can be reversed by activating the DNA damage repair. The fact that mutations of several genes encoding for proteins involved in DNA damage repair are also associated with ALS, including *C21ORF2, SETX*, and *NEK1* [66-68], further supported this theory. Mutations in these genes may lead to dysregulated DNA damage repair machinery and increase the susceptibility of motor neurons to oxidative stress and neuronal death [69].

Triggering by several mechanisms, mitochondria dysfunction has also been described in the dorsal root ganglion cells of sporadic ALS patients [70]. The mutations in coiled-coil helix coiled-coil helix domain-containing protein 10 (CHCHD10), which has been shown to associate with ALS, have been reported to cause increased mitochondria fragmentation and impaired mitochondria repair [71,72]. The biogenesis of mitochondria can also be affected in FUS mutants [73], which has been found to accumulate in the cytosol and affect the normal function of mitochondria [14,15].

Abnormal swollen mitochondria morphology has also been identified in other FALS patients with *SOD1* and *C9ORF72* mutations and in SOD1^{G93A} and TDP-43^{A315T} mouse models [6,74], which could be the consequence of mutated protein aggregates in these mutants. For instance, the insoluble form of mutant *SOD1* was found to aggregate in the mitochondria in the spinal cord of *SOD1* mutants, leading to impaired mitochondria respiration, reduced energy production, and elevated levels of oxidative stress [75,76]. Furthermore, an increase in the complex I and III activity of mitochondria, which increases mitochondrial ROS production, has been observed in the motor cortex in ALS patients with *SOD1* mutation [77].

The damaged mitochondria can be targeted by PTEN-induced putative kinase protein 1

(PINK1)-E3 ubiquitin ligase parkin for degradation in the lysosome [78]. The engulfment process of damaged mitochondria with autophagosomes is mediated by OPTN and TBK1 [79]. Therefore, the ALS-associated mutations in *OPTN* and *TBK1* may affect mitophagy and result in accumulated nonfunctional mitochondria, causing stress and motor neuron death [80]. In addition, alterations in mitochondria due to damage can impair calcium homeostasis, increasing the vulnerability of motor neurons to glutamate excitotoxicity [81].

1.3.4 Defective axonal transport

The motor neurons typically have extremely long axons, about 1 m in length, placing exceptional demands on cellular functions that require axonal transport. This process and the conduction of electrical impulses are highly regulated by the neurofilament structures [82]. The disruption of neurofilament network organization has been reported in both SALS and FALS patients [83]. In motor neurons, neurofilaments link not only with each other but also with microtubules and actin filaments, and the linked protein network contributes to the maintenance of the axonal structures [84]. Mutations in the *PFN1* gene, which encodes profilin-I that binds to actin, are found to result in disrupted actin polymerization and associate with ALS [85,86].

Impaired distal axonal transport has been identified in *SOD1* mutant mice, with a reduction in kinesin expression and a subsequent decrease in dynein expression [87]. The impaired axonal transport may lead to the accumulation of damaged mitochondria, causing reduced ATP production and impaired calcium homeostasis at distal sites in both mouse models and human patients [88-90]. Furthermore, the kinesin-dynein complex has been affected in SALS, where reduced KIF3Aβ and KIF1Bβ expression has been observed in the motor cortex of SALS patients [91]. In addition, mutations in *KIF5A*, which may disrupt axonal transport, are associated with ALS [92].

In summary, mutations that can alter cytoskeleton dynamics and affect axonal transport have been identified to associate with ALS. In addition, impaired axonal transport has also been found in other ALS patients without mutations in cytoskeletal-related genes. Mechanistically,

defects in the axonal transport pathway may disrupt mitochondria metabolism, RNA transport, and protein degradation, posing risks to motor neurons.

1.3.5 Aberrant RNA metabolism

The mutations in many RNA-binding proteins are associated with ALS, including *TDP-43* and FUS [14,93], and the mutated RNA-binding proteins may lead to disrupted downstream RNA processing mechanisms. In most ALS cases, dysregulated RNA metabolism is a prominent disease feature, including defects in RNA biogenesis and transcription, changes in alternate splicing, formation of stress granules, and disrupted RNA transport.

FUS, TDP-43, MATR3, and *hnRNPA2B1* were reported to associate with ALS and participated in pre-mRNA processing [94,95]. Previous research has shown that knockdown of TDP-43 can cause dysregulated alternate splicing [96], and FUS deficiency can cause defects in splicing events [97], demonstrating the critical role of alternative splicing events in ALS. In addition, changes in alternate splicing have been found in neuronal genes involved in axonal guidance, axon growth, and cytoskeleton organization in *FUS* ALS patients [98,99].

In addition to aberrant RNA splicing, the formation of RNA foci is frequently observed in *C9ORF72* ALS patient cells [100]. The RNA foci may sequester RNA-binding proteins and affect RNA processing and metabolism throughout the central nervous system [101]. Furthermore, the antisense RNA foci have been observed to co-localize with cytoplasmic TDP-43 aggregates in the *C9ORF72* mutant motor neurons [102]. In *C9ORF72* ALS post-mortem tissues, 24.9% of the glial cells and 78.7% of the neurons were found positive for antisense RNA foci in the spinal cord and motor brain regions [102].

RNA granules, also named stress granules, are produced in response to stress. The stress granules have been observed to recruit TDP-43 and FUS, and mutations in both genes showed increased stress granules in the cytoplasm [103,104]. The stress granules were reported to inhibit mRNA translation, thus contributing to ALS progression [104]. The heterogeneous nuclear

ribonucleoprotein particle proteins, named hnRNPA2/B1 and hnRNPA1, are the binding partners of TDP-43 and can mediate multiple RNA processing events, including the mRNA nucleocytoplasmic transport, miRNA maturation, and RNA metabolism [105]. Increased fibril formation and aggregation have been found in hnRNPA2/B1 and hnRNPA1 mutants, resulting in increased stress granule assembly [106,107]. Stress granules can be targeted to the lysosome for degradation through the autophagy mechanism involving VCP, and inhibition of VCP showed reduced stress granule clearance. In addition, accumulations of stress granules, also positive for TDP-43, have been identified in cells expressing *VCP* mutations [108].

Collectively, these studies indicate the critical role of proper RNA metabolism in maintaining the homeostasis of the nervous system. Therefore, the alterations in RNA processing events, including RNA splicing and translation, RNA transport, and RNA stress granules, may contribute to neurodegeneration and ALS pathogenesis.

1.3.6 Disrupted glutamate excitotoxicity

In motor neurons, excitotoxicity is mainly caused by the excessive neurotransmitter glutamate, which leads to atypical activation of glutamate receptors and increased neuronal firing [109]. The excitotoxicity is a consequence of disrupted glutamate uptake and transport, which results in excessive Ca^{2+} intake, increased levels of ROS, and mitochondria dysfunction [110,111]. Motor neurons are particularly susceptible to glutamate excitotoxicity as they have an increased number of glutamate-gated AMPA receptors and reduced ability to buffer calcium influx [112]. The increased AMPA receptor activation has been evidenced to cause paralysis and motor neuron death in animal models, demonstrating the vulnerability of motor neurons to calcium dysregulation [113]. In ALS patients, spinal motor neurons have shown reduced expression of GluA2 compared to dorsal horn neurons, suggesting a selective susceptibility theory in motor neurons [114]. In addition, reduced adenosine deaminase acting on RNA 2 (ADAR2) activity, which mediates the transcriptional editing of GluA2 into the impermeable calcium subunit, has been observed in

sporadic ALS cases, leading to increased TDP-43 aggregation in spinal motor neurons [115].

In addition to the dysfunctional GluA2 subunit, impaired glutamate transport has also been reported in ALS. Physiologically, glutamate is cleared by the excitatory amino acid transporter (EAAT2), an astrocyte glutamate importer. Loss of EAAT2 has been found in the affected areas of ALS patient sample [116], while activation of EAAT2 by small molecules rescued motor neuron death and delayed paralysis in SOD1^{G93A} mice [117,118], highlighting the dysfunctional glutamate uptake and transport mechanisms in ALS pathogenesis. Increased glutamate release has also been found in SOD1^{G93A} mice, where the mutation of *SOD1* decreased the astrocytic GluA2 and diminished the protection from astrocytes against motor neuron excitotoxicity [119]. In addition, elevated glutamate levels have been found in the CSF of *C9ORF72* ALS patients, which may result from the impaired glutamate clearance caused by aberrant splicing of EAAT2 [120]. Furthermore, the anti-glutamatergic drug Riluzole has been developed and approved for treating ALS patients through the glutamate excitotoxicity mechanism. However, Riluzole failed to prevent death or delay disease progression over a long period in ALS, suggesting that glutamate excitotoxicity might not be the sole mechanism for ALS pathogenesis.

1.3.7 Impaired endosomal and vesicle trafficking pathway

There are different types of extracellular vesicles, including micro-vesicles, exosomes, and apoptotic vesicles, all of which are involved in maintaining intracellular communications and physiological function [121]. Over the last decade, the relevance of exosomes to ALS has been intensively investigated, either as disease biomarkers or in disease propagation [122,123]. In *SOD1* and *C9ORF72* mutant ALS cases, exosomes secreted by neurons, astrocytes, and microglia carry toxic elements, such as dipeptide repeat proteins (DPRs), and cause motor neuron degeneration [122,124]. These findings suggest the importance of extracellular vesicle secretion and the vesicle trafficking pathway in ALS.

The biogenesis of exosomes starts from the formation of the multivesicular body (MVB)

inward buds, with subsequent fission and release as vesicles in the MVB lumen. This process can be mediated by the Endosomal Sorting Complex Required for Transport (ESCRT), which consists of four complexes, ESCRT-0 to ESCRT-III. Intriguingly, the charged multivesicular protein 2B (*CHMP2B*), the mutation of which has been identified to associate with ALS, is a component of ESCRT-III [125]. The mutations and dysregulation of the ESCRT-III component cause dysmorphic and aberrant endosomes in FTD patients [126]. This finding suggests the potential role of exosome regulation in neurodegenerative diseases like ALS and FTD, however, more evidence is still needed clinically and experimentally.

In addition to exosome, endocytosis and vesicle trafficking are also implicated in ALS. For example, Alsin, an ALS-associated protein, is a guanine nucleotide exchange factor that mediates endosomal motility and endo-lysosomal fusion [127]. The mutations of *Alsin* cause an increased number of RAB5+ vesicles and enhanced lysosomal degradation of endosomal vesicles in hippocampal neurons [128]. In *C9ORF72* mutant models, defective autophagy, impaired endosomal trafficking, and aberrant exosome secretion were observed [120], suggesting the involvement of autophagy and the vesicle trafficking pathway in ALS pathology.

The formation of MVB is a critical mechanism at the crossroad between autophagic degradation and exosome secretion pathway [129]. One example of this pathway involved in ALS is the case of VCP. VCP is the valosin-containing protein involved in the formation of early endosomes by interacting with clathrin [130]. The mutations of *VCP* have been found to affect the endosomal pathway and associate with ALS [35], suggesting the potential role of the endosomal pathway in ALS pathogenesis.

A less well-studied case that may potentially be characterized in this group is the vesicle-associated membrane protein-associated protein B (VAPB), the mutations of which have been found in a small population of ALS [131]. VAPB has been identified to interact with CD63 and RAB7, both involved in exosome biogenesis and late endosome formation [132].

1.4 TDP-43 pathology as a hallmark of amyotrophic lateral sclerosis

TDP-43 is an RNA binding protein of 414 amino acids, and the protein contains two RNA recognition motifs and a carboxy-terminal glycine-rich domain. In the post-mortem tissues of ALS patients, pathological TDP-43 has been identified to form ubiquitinated or phosphorylated insoluble aggregates in the cytoplasm, indicating the nucleocytoplasmic relocation in the formation of aggregation [133,134]. Aggregation of TDP-43 has been identified in both sporadic and familial ALS patients and is now considered the histopathological hallmark of ALS [135]. In addition, mutations of *TDP-43* have been documented in 1.5% of sporadic and 3% of familial ALS cases [136], suggesting that about 95% of patients with TDP-43 aggregation do not carry any mutation of this protein [137]. Although TDP-43 pathology is a universal disease hallmark in ALS, whether this pathology directly causes motor neuron degeneration is still debatable. Therefore, it is critical to understand the mechanistic link between TDP-43 pathology and ALS pathogenesis.

1.4.1 Physiological functions of TDP-43

As an RNA binding protein, the most studied function of TDP-43 is its regulation in RNA processing. Transcriptome-wide analysis evidenced the role of TDP-43 in mediating the splicing of more than 6,000 transcripts, which is about 30% of the whole transcriptome [138,139]. Traditional RNA immunoprecipitation also identified specific RNA targets of TDP-43 [140], suggesting a broad role of TDP-43 in regulating mRNA processing.

Previous research has evidenced that TDP-43 can localize to the sites of RNA splicing [141], suggesting its role in splicing events. Indeed, TDP-43 has been observed to regulate the splicing patterns of many essential genes, including *CFTR*, *FUS*, and *SNCA* [138,142]. The nuclear depletion of TDP-43 has been found to cause aberrant mRNA splicing [143] and generate widespread dysregulated splicing events in motor neurons [144]. In addition, ALS-associated mutations of *TDP-43*, like M337V and Q331K, have been evidenced to affect mRNA splicing [97,138], suggesting a prominent role of TDP-43 in regulating RNA splicing events. In addition to its role in regulating

RNA splicing, TDP-43 has also been found to mediate mRNA maturation and stability by binding to the mRNA transcripts [145]. In this case, TDP-43 can interact with the regulatory 3' UTR of the mRNAs and regulate their half-life either positively or negatively [93,145,146]. Another critical role of TDP-43 is its ability to generate ribonucleoprotein (RNP) granules by associating with RNA molecules. The RNP granules can transport mRNA to distal areas in the axonal cells [147]. In fact, impaired transportation of the RNP granules was observed in ALS patients with *TDP-43* mutations [147,148].

In addition to the ability of TDP-43 in regulating RNA splicing, stability, and transport, TDP-43 has also been found to assemble into stress granules, indicating the protective role of TDP-43 against cellular stress [149]. TDP-43 has been reported to regulate vital nucleating proteins of stress granules, including the T cell-restricted intracellular antigen-1 (TIA-1) and the rasGAP SH3 domain-binding protein 1 (G3BP) [150]. More details about stress granule formation and the function of TDP-43 were described in Chapter 1.3.5.

1.4.2 Pathological forms of TDP-43 aggregation

The histopathological hallmark of ALS and FTLD-TDP is the identification of dense TDP-43 aggregates in affected neural cells [151]. In age-related neurodegenerative diseases, the observation of abnormal protein aggregates is a common theme, while whether these aggregates are detrimental or beneficial remains debatable. Previous studies have characterized the oligomerization of TDP-43 and suggested that physiological TDP-43 exists typically in a dimeric form in the nucleus [152]. Recently, TDP-43 has been found to display multiple forms of oligomerization by cross-linking experiments in normal human brains [153]. However, pathological forms of TDP-43 are structurally distinct, with the N-terminal region acting as an intermolecular interacting domain to form an 86 kDa dimerization form [154]. Another study reported the ability of full-length TDP-43 to form ring-like oligomers and spheroidal structures with cytotoxicity in neurons [155]. The importance of the diversity of oligomeric forms is unknown.

TDP-43 protein has been evidenced to be prone to aggregation, which is consistent with the observation of TDP-43 inclusions in models of TDP-43 pathology [156]. The biochemical correlation of TDP-43 inclusions is the identification of insoluble TDP-43 accumulations, with most of the sarkosyl-insoluble TDP-43 proteins being those of 43 kDa molecular weight in normal and diseased brain samples. However, other insoluble TDP-43 have also been observed in diseased brains as a phosphorylated 45 kDa form and CTFs of the 20-25 kDa form [133].

TDP-43 inclusions have also been found in transgenic mouse models expressing full-length TDP-43 [157]. However, no correlation between the number of TDP-43 inclusions and the extent of neurodegeneration was found [158], indicating that TDP-43 aggregation may not seem to be an absolute indicator for neurodegeneration. The effect of TDP-43 aggregation on neuronal pathology and viability is still unknown. Although experimental evidence has demonstrated that TDP-43 aggregates are not absolutely necessary for TDP-43 mediated neuronal death, the aggregates may still contribute to the dysfunction of neurons. For example, the prion-like cell-to-cell transmission theory of TDP-43 aggregation is worthy of being validated, and more evidence for TDP-43 proteinopathies could advance our understanding of how TDP-43 aggregation could contribute to the progression of the disease.

1.4.3 Emerging mechanisms of TDP-43 induced cytotoxicity

TDP-43 has been reported to regulate autophagy induction by interacting with the mRNA of ATG7, and ALS-associated mutations of *TDP-43* were shown to abolish this binding ability, thus impairing the autophagy induction pathway [159]. In addition, TDP-43 can regulate the localization of TFEB, which mediates the autophagosome-lysosome fusion pathway in neuronal cells [160]. In addition, increased TDP-43 aggregates have been observed in autophagy-deficient cells [161]. However, it is still unclear about the role of autophagy in rescuing TDP-43 induced toxicity, as suggested by conflicting data.

In addition to its role in autophagy, abnormal levels of TDP-43 have also been found to

cause defective endocytosis [162]. Increased TDP-43 aggregation has been linked with impaired endocytosis, while re-sustained endocytic function reversed TDP-43 aggregation and motor neuron dysfunction [162]. In an independent study, loss of TDP-43 activity in human-induced neurons can specifically decrease the number and motilities of recycling endosomes [163]. In addition, TDP-43 expression can affect the activity of the endo-lysosomal pathway, which could contribute to TDP-43 clearance independent of autophagy [163,164].

The expression of mutant TDP-43 has been documented to cause mitochondrial dysfunction, suggesting the role of mitochondria in mediating TDP-43 cytotoxicity [165,166]. Overexpression of TDP-43 has been reported to affect the mitochondrial length and movement [167], and mutant TDP-43 expression leads to aberrant mitochondrial distribution and transport [74]. In addition, the presence of functional mitochondria has been found to increase the detrimental effects of TDP-43 toxicity, suggesting that mitochondria could be a target of TDP-43 pathology [165,168].

These studies implicate the important role of TDP-43 induced toxicity in neurons, highlighting the importance of TDP-43 in ALS pathogenesis. Many other mechanisms of TDP-43 induced pathologies have also been revealed, including dysregulated metal ion homeostasis and interference with chromatin remodeling. Investigations into these mechanisms will help uncover the mechanistic link between TDP-43 and the pathogenesis of neurodegenerative diseases.

1.5 Identification of TBK1 in amyotrophic lateral sclerosis

TBK1 is an IKK family kinase previously identified for a central role in controlling type-I interferon production in response to viral infection. It also regulates multiple cellular pathways, including inflammation [169], immune response [170], and cell proliferation [171]. A recent study using the whole-exome sequencing technique has identified the heterozygous loss-of-function mutations of TBK1 in ALS and FTD patients [66,172]. Additional TBK1 (OMIM 604834) variants have also been

found in patients with ALS or FTD (Table 2), making TBK1 mutations the third or fourth most frequent cause of the diseases in the studied populations [173-177]. Like many other ALS and FTD-associated genes, TBK1 variants have been related to the full phenotypic spectrum of ALS and FTD syndromes even within the same family [172,173]. Although loss-of-function mutations of TBK1 have been evidenced to cause ALS with well-documented cosegregation data, which downstream mechanism of TBK1 is relevant to the development of ALS and FTD is still unknown.

1.5.1 TBK1 in autophagy

The autophagy pathway is the most recognized mechanism of TBK1 mutations to be implicated in ALS. TBK1 has been described as a critical player in autophagy, which is well-documented for mediating the degradation of protein aggregates and the clearance of intracellular pathogens [178]. More details about the role of autophagy in ALS development are described in 1.3.1.

The first evidence for TBK1 to be implicated in autophagy and ALS was the finding that TBK1 could co-localize with OPTN and protein aggregates with Hela cells and the SOD1 mouse models of ALS [179]. The role of TBK1 in mediating protein aggregates recycling and autophagy activity has been shown by its ability to phosphorylate autophagy receptors, like p62 and optineurin [179]. TBK1 has also been reported to mediate the elimination of invading intracellular pathogens through the autophagic clearance in human and mouse cells [180-182]. In addition, TBK1 has been shown to promote autophagosome maturation, leading to autophagic degradation of p62 and the associated cargo [182]. Therefore, loss of TBK1 activity could contribute to impaired autophagy pathway, leading to compromised clearance of protein aggregates and pathogens in ALS. However, experimental evidence is still needed to elucidate whether impaired autophagy is the most direct disease-relevant mechanism for developing disease pathology in ALS patients with TBK1 mutations.

Variant type	Mutation type	Expression				Function		Disease
		mRNA level		Protein level		OPTN binding	IFN signaling	
		Allele specific	Patient cells	Allele Specific	Patient cells			
Missense	p.R47H	-	-	Normal	Normal	Normal	Impaired	ALS-FTD
	p.R271L	-	Normal	-	Normal	-	-	FTD
	p.K291E	-	Normal	-	Normal	-	-	FTD
	p.L306I	-	-	-	Normal	-	-	FTD
	p.R308Q	-	-	Normal	-	Normal	Normal	ALS-FTD
	p.H322Y	-	Normal	-	Normal	-	-	ALS
	p.R357Q	-	-	Normal	-	Reduced	Impaired	ALS-FTD
	p.K401E	-	-	-	Reduced	-	-	FTD
	p.I515T	-	Normal	-	Normal	-	-	ALS
	p.A535T	-	Normal	-	Normal	-	-	FTD
	p.M559R	-	-	Normal	-	Impaired	Impaired	ALS-FTD
	p.M598V	-	-	-	Normal	-	-	ALS-FTD
	p.E696K	-	-	Normal	Reduced	Impaired	Normal	ALS-FTD; FTD
Nonsense	p.Y185X	-	Reduced	-	-	-	-	ALS-FTD
	p.R117X	-	Reduced	-	Reduced	-	-	FTD
	p.A417X	-	Reduced	-	Reduced	-	-	ALS-FTD
Frameshift	p.T77WfsX4	-	Reduced	-	Reduced	-	-	ALS-FTD
	p.T320QfsX40	-	-	No	-	Impaired	Impaired	ALS-FTD
	p.S398PfsX11	-	Reduced	-	Reduced	-	-	ALS
	p.I450KfsX15	-	Reduced	Truncated	Reduced	Impaired	Impaired	ALS-FTD
	p.V479EfsX4	-	-	Truncated	-	Impaired	Impaired	ALS-FTD
	p.S518LfsX32	-	Reduced	-	Reduced	-	-	ALS
Deletion	p.D167del	-	Normal	-	Normal	-	-	ALS
	p.G272_T331del	-	Reduced	-	Reduced	-	-	FTLD
	p.E643del	-	Normal	-	Reduced	-	-	ALS-FTD
	p.690-713del	-	Normal	Normal truncated	Normal and truncated	Impaired	Normal	ALS-FTD

Table 2. TBK1 variants reported in ALS/FTD

1.5.2 TBK1 in neuroinflammation

TBK1 was first identified to regulate the NF-kB-mediated responses as described in HEK293T cells using luciferase reporter assays [183]. However, unlike the canonical IKKs that control the activation of the NF-kB pathway, TBK1 is a noncanonical IKK that activates the transcription factors of the IFN-regulatory factor (IRF) family [184]. In the IFN regulatory pathway, invading pathogens are recognized by RIG-I-like receptors (RLRs) and cytosolic DNA receptors, resulting in the production of IFNs [185]. Subsequently, innate immune sensors were engaged in this process, and cytokines were produced to alert neighboring cells for foreign invasion. The TLR3 then recruited TIR domain-containing adaptor-inducing IFN-b (TRIF) in response to dsRNA, which activated TBK1 for IRF3 phosphorylation [185,186]. The phosphorylated IRF3 induced the expression of type I and type III IFNs in the nucleus [186].

The two pathways of autophagy and inflammation are not mutually exclusive. For example, cGAS has been shown to interact with Beclin-1 in response to HSV1 infection, leading to reduced IFN production and increased autophagic clearance of viral DNA [187]. Similarly, type I IFN could be induced upon mycobacterial infection to activate autophagosomal clearance of pathogen in a TBK1-dependent manner [188]. A previous study has shown that the reduced Tbk1 expression synergizes with aging mediated RIPK1 inhibition to promote neuroinflammation and neurodegeneration in mouse models [189]. In this study, heterozygous *Tbk1* mutations might function as a genetic risk factor that predisposes neuroinflammation and neurodegeneration under specific environmental or physiological stresses. Additional studies also reported that loss-of-function mutations of *Tbk1* in mouse motor neurons do not display any neurodegeneration phenotype, but TBK1 might contribute to the onset of disease in SOD1^{G93A} mouse models [190,191].

In summary, TBK1 is involved in various ALS-relevant mechanisms, including autophagy and neuroinflammation. Although mouse models of TBK1 deficiency advanced our understanding of TBK1 functions in mediating autophagy and neuroinflammation, ALS-relevant phenotypes, such as TDP-43 pathology, have not been assessed in motor neurons.

1.6 Dissertation overview

This dissertation tries to elucidate the cell-autonomous functions of TBK1 in human motor neurons and the downstream mechanism of TBK1 that contributes to ALS development. This remains critical for three reasons: 1) it could provide insights into whether the reduction of TBK1 protein found in ALS patients directly contributes to motor neuron pathology; 2) efforts are being made to develop therapeutics targeting autophagy [192], which is considered a central disease mechanism for TBK1 mutation related ALS/FTD. In addition, ongoing clinical trials are using autophagy inducers, like Rapamycin, to treat ALS patients. Therefore, determining whether loss of autophagy activity downstream of TBK1 mutations is the crucial disease-causing mechanism, specifically in motor neurons, could be therapeutically beneficial; 3) TDP-43 pathology has been observed in the spinal cord of patients with TBK1 mutations [193], but not in Tbk1 mutant mice [190]. Thus, it is necessary to systematically evaluate the effects of loss-of-function mutations of TBK1 in human cell models, focusing on the TDP-43 pathology.

In Chapter 2, we generated human embryonic stem cells (ESCs) harboring loss-of-function mutations of TBK1 by CRISPR/Cas9 as our experimental model. We found that TBK1$^{-/-}$ cells showed impaired autophagic flux in human cellular models and increased cytoplasmic and insoluble TDP-43 in TBK1$^{-/-}$ motor neurons. Functional analysis using MEA and axotomy also validated the roles of TBK1 in early-stage disease progression. Therefore, our model successfully recapitulated the ALS-relevant pathology in human motor neurons. In addition, our results provided strong evidence that TBK1 was associated with ALS pathology in a loss-of-function manner.

In Chapter 3, we tried to elucidate the detailed mechanism of TDP-43 pathology, the most disease-relevant phenotype in ALS, in our TBK1 deficient model. Surprisingly, in contrast to the previous recognition, inhibition of autophagy induction by ATG7 shRNA hairpin failed to reproduce TDP-43 pathology found in TBK1$^{-/-}$ motor neurons, suggesting a mechanism independent of autophagosome formation. Using the phosphoproteomics approach, we identified abnormal

phosphorylation activities in the endosomal transport pathway in TBK1$^{-/-}$ motor neurons. We validated that loss of TBK1 activity led to impaired endosomal maturation and subsequent lysosomal dysfunction. Disruption of the endo-lysosomal pathway could phenocopy the TDP-43 pathology observed in TBK1 deficient motor neurons, suggesting a mechanistic link between TBK1 deficiency and TDP-43 pathology.

In Chapter 4, we further validated our endo-lysosomal theory and explored methods to therapeutically manipulate this process using patient-derived iPSCs. First, we found that restoring TBK1 protein expression in the loss-of-function models restored lysosomal functions and attenuated TDP-43 pathology and ALS-relevant phenotypes. Furthermore, small molecules targeting the endosomal trafficking pathway rescued neurodegenerative disease phenotypes in TBK1 patient-derived motor neurons. Most importantly, TBK1 mutations sensitized motor neurons to lysosomal stress, and Rapamycin, an autophagy inducer, failed to rescue TDP-43 pathology and neurodegenerative phenotypes in these patient-derived motor neurons.

Therefore, we conclude that loss-of-function mutations of TBK1 are sufficient to cause TDP-43 pathology in human motor neurons through endo-lysosomal pathways. Our results also provide preliminary evidence that restoration of the functional TBK1 expression and small molecules targeting the endosomal trafficking might be therapeutically beneficial for ALS and FTD patients with TBK1 mutations.

References:

1   Brown, R. H. & Al-Chalabi, A. Amyotrophic Lateral Sclerosis. *N Engl J Med* **377**, 162-172, doi:10.1056/NEJMra1603471 (2017).

2   Kiernan, M. C. *et al.* Amyotrophic lateral sclerosis. *Lancet* **377**, 942-955, doi:10.1016/S0140-6736(10)61156-7 (2011).

3   Kusui, K. [Epidemiological study on amyotrophic lateral sclerosis (ALS) and other neighboring motor neuron diseases in Kii Peninsula]. *Seishin Shinkeigaku Zasshi* **64**, 85-

99 (1962).

4   Kanning, K. C., Kaplan, A. & Henderson, C. E. Motor neuron diversity in development and disease. *Annu Rev Neurosci* **33**, 409-440, doi:10.1146/annurev.neuro.051508.135722 (2010).

5   Krivickas, L. S. Amyotrophic lateral sclerosis and other motor neuron diseases. *Phys Med Rehabil Clin N Am* **14**, 327-345, doi:10.1016/s1047-9651(02)00119-5 (2003).

6   Hardiman, O. *et al.* Amyotrophic lateral sclerosis. *Nat Rev Dis Primers* **3**, 17071, doi:10.1038/nrdp.2017.71 (2017).

7   Goutman, S. A. Diagnosis and Clinical Management of Amyotrophic Lateral Sclerosis and Other Motor Neuron Disorders. *Continuum (Minneap Minn)* **23**, 1332-1359, doi:10.1212/CON.0000000000000535 (2017).

8   Al-Chalabi, A., van den Berg, L. H. & Veldink, J. Gene discovery in amyotrophic lateral sclerosis: implications for clinical management. *Nat Rev Neurol* **13**, 96-104, doi:10.1038/nrneurol.2016.182 (2017).

9   Petrov, D., Mansfield, C., Moussy, A. & Hermine, O. ALS Clinical Trials Review: 20 Years of Failure. Are We Any Closer to Registering a New Treatment? *Front Aging Neurosci* **9**, 68, doi:10.3389/fnagi.2017.00068 (2017).

10   de Carvalho, M., Costa, J. & Swash, M. Clinical trials in ALS: a review of the role of clinical and neurophysiological measurements. *Amyotroph Lateral Scler Other Motor Neuron Disord* **6**, 202-212, doi:10.1080/14660820510011997 (2005).

11   Rosen, D. R. *et al.* Mutations in Cu/Zn superoxide dismutase gene are associated with familial amyotrophic lateral sclerosis. *Nature* **362**, 59-62, doi:10.1038/362059a0 (1993).

12   Renton, A. E., Chio, A. & Traynor, B. J. State of play in amyotrophic lateral sclerosis genetics. *Nat Neurosci* **17**, 17-23, doi:10.1038/nn.3584 (2014).

13   Chio, A. *et al.* Prevalence of SOD1 mutations in the Italian ALS population. *Neurology* **70**, 533-537, doi:10.1212/01.wnl.0000299187.90432.3f (2008).

14   Vance, C. *et al.* Mutations in FUS, an RNA processing protein, cause familial amyotrophic lateral sclerosis type 6. *Science* **323**, 1208-1211, doi:10.1126/science.1165942 (2009).

15   Kwiatkowski, T. J., Jr. *et al.* Mutations in the FUS/TLS gene on chromosome 16 cause familial amyotrophic lateral sclerosis. *Science* **323**, 1205-1208, doi:10.1126/science.1166066 (2009).

16   Ling, S. C., Polymenidou, M. & Cleveland, D. W. Converging mechanisms in ALS and FTD: disrupted RNA and protein homeostasis. *Neuron* **79**, 416-438, doi:10.1016/j.neuron.2013.07.033 (2013).

17   DeJesus-Hernandez, M. *et al.* Expanded GGGGCC hexanucleotide repeat in noncoding region of C9ORF72 causes chromosome 9p-linked FTD and ALS. *Neuron* **72**, 245-256, doi:10.1016/j.neuron.2011.09.011 (2011).

18   Alsultan, A. A., Waller, R., Heath, P. R. & Kirby, J. The genetics of amyotrophic lateral sclerosis: current insights. *Degener Neurol Neuromuscul Dis* **6**, 49-64, doi:10.2147/DNND.S84956 (2016).

19   Souza, P. V., Pinto, W. B., Chieia, M. A. & Oliveira, A. S. Clinical and genetic basis of familial amyotrophic lateral sclerosis. *Arq Neuropsiquiatr* **73**, 1026-1037, doi:10.1590/0004-282X20150161 (2015).

20   Volk, A. E., Weishaupt, J. H., Andersen, P. M., Ludolph, A. C. & Kubisch, C. Current knowledge and recent insights into the genetic basis of amyotrophic lateral sclerosis. *Med Genet* **30**, 252-258, doi:10.1007/s11825-018-0185-3 (2018).

21   Zhang, S. *et al.* Genome-wide identification of the genetic basis of amyotrophic lateral sclerosis. *Neuron* **110**, 992-1008 e1011, doi:10.1016/j.neuron.2021.12.019 (2022).

22   Zou, Z. Y. *et al.* Genetic epidemiology of amyotrophic lateral sclerosis: a systematic review and meta-analysis. *J Neurol Neurosurg Psychiatry* **88**, 540-549, doi:10.1136/jnnp-2016-315018 (2017).

23   Zufiria, M. *et al.* ALS: A bucket of genes, environment, metabolism and unknown

ingredients. *Prog Neurobiol* **142**, 104-129, doi:10.1016/j.pneurobio.2016.05.004 (2016).

24 McCann, E. P. *et al.* Evidence for polygenic and oligogenic basis of Australian sporadic amyotrophic lateral sclerosis. *J Med Genet*, doi:10.1136/jmedgenet-2020-106866 (2020).

25 van Blitterswijk, M. *et al.* Evidence for an oligogenic basis of amyotrophic lateral sclerosis. *Hum Mol Genet* **21**, 3776-3784, doi:10.1093/hmg/dds199 (2012).

26 Kenna, K. P. *et al.* Delineating the genetic heterogeneity of ALS using targeted high-throughput sequencing. *J Med Genet* **50**, 776-783, doi:10.1136/jmedgenet-2013-101795 (2013).

27 Feneberg, E., Gray, E., Ansorge, O., Talbot, K. & Turner, M. R. Towards a TDP-43-Based Biomarker for ALS and FTLD. *Mol Neurobiol* **55**, 7789-7801, doi:10.1007/s12035-018-0947-6 (2018).

28 Gill, C. *et al.* SOD1-positive aggregate accumulation in the CNS predicts slower disease progression and increased longevity in a mutant SOD1 mouse model of ALS. *Sci Rep* **9**, 6724, doi:10.1038/s41598-019-43164-z (2019).

29 Butti, Z. & Patten, S. A. RNA Dysregulation in Amyotrophic Lateral Sclerosis. *Front Genet* **9**, 712, doi:10.3389/fgene.2018.00712 (2018).

30 Sun, C. N., Araoz, C., Lucas, G., Morgan, P. N. & White, H. J. Amyotrophic lateral sclerosis. Inclusion bodies in a case of the classic sporadic form. *Ann Clin Lab Sci* **5**, 38-44 (1975).

31 Leigh, P. N. *et al.* Ubiquitin-immunoreactive intraneuronal inclusions in amyotrophic lateral sclerosis. Morphology, distribution, and specificity. *Brain* **114 (Pt 2)**, 775-788, doi:10.1093/brain/114.2.775 (1991).

32 Shibata, N. *et al.* Intense superoxide dismutase-1 immunoreactivity in intracytoplasmic hyaline inclusions of familial amyotrophic lateral sclerosis with posterior column involvement. *J Neuropathol Exp Neurol* **55**, 481-490, doi:10.1097/00005072-199604000-00011 (1996).

33 Matsumoto, G., Wada, K., Okuno, M., Kurosawa, M. & Nukina, N. Serine 403

phosphorylation of p62/SQSTM1 regulates selective autophagic clearance of ubiquitinated proteins. *Mol Cell* **44**, 279-289, doi:10.1016/j.molcel.2011.07.039 (2011).

34   Teyssou, E. *et al.* Novel UBQLN2 mutations linked to amyotrophic lateral sclerosis and atypical hereditary spastic paraplegia phenotype through defective HSP70-mediated proteolysis. *Neurobiol Aging* **58**, 239 e211-239 e220, doi:10.1016/j.neurobiolaging.2017.06.018 (2017).

35   Johnson, J. O. *et al.* Exome sequencing reveals VCP mutations as a cause of familial ALS. *Neuron* **68**, 857-864, doi:10.1016/j.neuron.2010.11.036 (2010).

36   Saeki, Y. Ubiquitin recognition by the proteasome. *J Biochem* **161**, 113-124, doi:10.1093/jb/mvw091 (2017).

37   Ryan, T. A. & Tumbarello, D. A. Optineurin: A Coordinator of Membrane-Associated Cargo Trafficking and Autophagy. *Front Immunol* **9**, 1024, doi:10.3389/fimmu.2018.01024 (2018).

38   Katsuragi, Y., Ichimura, Y. & Komatsu, M. p62/SQSTM1 functions as a signaling hub and an autophagy adaptor. *FEBS J* **282**, 4672-4678, doi:10.1111/febs.13540 (2015).

39   Kabashi, E., Agar, J. N., Taylor, D. M., Minotti, S. & Durham, H. D. Focal dysfunction of the proteasome: a pathogenic factor in a mouse model of amyotrophic lateral sclerosis. *J Neurochem* **89**, 1325-1335, doi:10.1111/j.1471-4159.2004.02453.x (2004).

40   Wen, X. *et al.* Antisense proline-arginine RAN dipeptides linked to C9ORF72-ALS/FTD form toxic nuclear aggregates that initiate in vitro and in vivo neuronal death. *Neuron* **84**, 1213-1225, doi:10.1016/j.neuron.2014.12.010 (2014).

41   Yu, L., Chen, Y. & Tooze, S. A. Autophagy pathway: Cellular and molecular mechanisms. *Autophagy* **14**, 207-215, doi:10.1080/15548627.2017.1378838 (2018).

42   Ramesh, N. & Pandey, U. B. Autophagy Dysregulation in ALS: When Protein Aggregates Get Out of Hand. *Front Mol Neurosci* **10**, 263, doi:10.3389/fnmol.2017.00263 (2017).

43   Nassif, M. & Hetz, C. Targeting autophagy in ALS: a complex mission. *Autophagy* **7**, 450-453, doi:10.4161/auto.7.4.14700 (2011).

44   Oakes, J. A., Davies, M. C. & Collins, M. O. TBK1: a new player in ALS linking autophagy and neuroinflammation. *Mol Brain* **10**, 5, doi:10.1186/s13041-017-0287-x (2017).

45   Navone, F., Genevini, P. & Borgese, N. Autophagy and Neurodegeneration: Insights from a Cultured Cell Model of ALS. *Cells* **4**, 354-386, doi:10.3390/cells4030354 (2015).

46   Waite, A. J. *et al.* Reduced C9orf72 protein levels in frontal cortex of amyotrophic lateral sclerosis and frontotemporal degeneration brain with the C9ORF72 hexanucleotide repeat expansion. *Neurobiol Aging* **35**, 1779 e1775-1779 e1713, doi:10.1016/j.neurobiolaging.2014.01.016 (2014).

47   Allen, S. P. *et al.* Astrocyte adenosine deaminase loss increases motor neuron toxicity in amyotrophic lateral sclerosis. *Brain* **142**, 586-605, doi:10.1093/brain/awy353 (2019).

48   Boivin, M. *et al.* Reduced autophagy upon C9ORF72 loss synergizes with dipeptide repeat protein toxicity in G4C2 repeat expansion disorders. *EMBO J* **39**, e100574, doi:10.15252/embj.2018100574 (2020).

49   Barmada, S. J. *et al.* Autophagy induction enhances TDP43 turnover and survival in neuronal ALS models. *Nat Chem Biol* **10**, 677-685, doi:10.1038/nchembio.1563 (2014).

50   Stolz, A. & Wolf, D. H. Endoplasmic reticulum associated protein degradation: a chaperone assisted journey to hell. *Biochim Biophys Acta* **1803**, 694-705, doi:10.1016/j.bbamcr.2010.02.005 (2010).

51   Atkin, J. D. *et al.* Endoplasmic reticulum stress and induction of the unfolded protein response in human sporadic amyotrophic lateral sclerosis. *Neurobiol Dis* **30**, 400-407, doi:10.1016/j.nbd.2008.02.009 (2008).

52   Zhang, Y. J. *et al.* Aggregation-prone c9FTD/ALS poly(GA) RAN-translated proteins cause neurotoxicity by inducing ER stress. *Acta Neuropathol* **128**, 505-524, doi:10.1007/s00401-014-1336-5 (2014).

53   Vijayalakshmi, K. *et al.* Evidence of endoplasmic reticular stress in the spinal motor neurons exposed to CSF from sporadic amyotrophic lateral sclerosis patients. *Neurobiol*

Dis **41**, 695-705, doi:10.1016/j.nbd.2010.12.005 (2011).

54   Yamanaka, T., Nishiyama, R., Shimogori, T. & Nukina, N. Proteomics-Based Approach Identifies Altered ER Domain Properties by ALS-Linked VAPB Mutation. *Sci Rep* **10**, 7610, doi:10.1038/s41598-020-64517-z (2020).

55   Lev, S., Ben Halevy, D., Peretti, D. & Dahan, N. The VAP protein family: from cellular functions to motor neuron disease. *Trends Cell Biol* **18**, 282-290, doi:10.1016/j.tcb.2008.03.006 (2008).

56   Cadoni, M. P. L. *et al.* VAPB ER-Aggregates, A Possible New Biomarker in ALS Pathology. *Cells* **9**, doi:10.3390/cells9010164 (2020).

57   Sundaramoorthy, V. *et al.* Defects in optineurin- and myosin VI-mediated cellular trafficking in amyotrophic lateral sclerosis. *Hum Mol Genet* **24**, 3830-3846, doi:10.1093/hmg/ddv126 (2015).

58   Kandlur, A., Satyamoorthy, K. & Gangadharan, G. Oxidative Stress in Cognitive and Epigenetic Aging: A Retrospective Glance. *Front Mol Neurosci* **13**, 41, doi:10.3389/fnmol.2020.00041 (2020).

59   Mitsumoto, H. *et al.* Oxidative stress biomarkers in sporadic ALS. *Amyotroph Lateral Scler* **9**, 177-183, doi:10.1080/17482960801933942 (2008).

60   Juarez, J. C. *et al.* Superoxide dismutase 1 (SOD1) is essential for H2O2-mediated oxidation and inactivation of phosphatases in growth factor signaling. *Proc Natl Acad Sci U S A* **105**, 7147-7152, doi:10.1073/pnas.0709451105 (2008).

61   Saccon, R. A., Bunton-Stasyshyn, R. K., Fisher, E. M. & Fratta, P. Is SOD1 loss of function involved in amyotrophic lateral sclerosis? *Brain* **136**, 2342-2358, doi:10.1093/brain/awt097 (2013).

62   Kirby, J. *et al.* Mutant SOD1 alters the motor neuronal transcriptome: implications for familial ALS. *Brain* **128**, 1686-1706, doi:10.1093/brain/awh503 (2005).

63   Johnson, J. A. *et al.* The Nrf2-ARE pathway: an indicator and modulator of oxidative stress

in neurodegeneration. *Ann N Y Acad Sci* **1147**, 61-69, doi:10.1196/annals.1427.036 (2008).

64   Andrus, P. K., Fleck, T. J., Gurney, M. E. & Hall, E. D. Protein oxidative damage in a transgenic mouse model of familial amyotrophic lateral sclerosis. *J Neurochem* **71**, 2041-2048, doi:10.1046/j.1471-4159.1998.71052041.x (1998).

65   Hall, E. D., Andrus, P. K., Oostveen, J. A., Fleck, T. J. & Gurney, M. E. Relationship of oxygen radical-induced lipid peroxidative damage to disease onset and progression in a transgenic model of familial ALS. *J Neurosci Res* **53**, 66-77, doi:10.1002/(SICI)1097-4547(19980701)53:1<66::AID-JNR7>3.0.CO;2-H (1998).

66   Cirulli, E. T. *et al.* Exome sequencing in amyotrophic lateral sclerosis identifies risk genes and pathways. *Science* **347**, 1436-1441, doi:10.1126/science.aaa3650 (2015).

67   van Rheenen, W. *et al.* Genome-wide association analyses identify new risk variants and the genetic architecture of amyotrophic lateral sclerosis. *Nat Genet* **48**, 1043-1048, doi:10.1038/ng.3622 (2016).

68   Chen, Y. Z. *et al.* DNA/RNA helicase gene mutations in a form of juvenile amyotrophic lateral sclerosis (ALS4). *Am J Hum Genet* **74**, 1128-1135, doi:10.1086/421054 (2004).

69   Higelin, J. *et al.* NEK1 loss-of-function mutation induces DNA damage accumulation in ALS patient-derived motoneurons. *Stem Cell Res* **30**, 150-162, doi:10.1016/j.scr.2018.06.005 (2018).

70   Sasaki, S., Horie, Y. & Iwata, M. Mitochondrial alterations in dorsal root ganglion cells in sporadic amyotrophic lateral sclerosis. *Acta Neuropathol* **114**, 633-639, doi:10.1007/s00401-007-0299-1 (2007).

71   Genin, E. C. *et al.* CHCHD10 mutations promote loss of mitochondrial cristae junctions with impaired mitochondrial genome maintenance and inhibition of apoptosis. *EMBO Mol Med* **8**, 58-72, doi:10.15252/emmm.201505496 (2016).

72   Genin, E. C. *et al.* Loss of MICOS complex integrity and mitochondrial damage, but not

TDP-43 mitochondrial localisation, are likely associated with severity of CHCHD10-related diseases. *Neurobiol Dis* **119**, 159-171, doi:10.1016/j.nbd.2018.07.027 (2018).

73   Deng, J. *et al.* FUS Interacts with HSP60 to Promote Mitochondrial Damage. *PLoS Genet* **11**, e1005357, doi:10.1371/journal.pgen.1005357 (2015).

74   Magrane, J., Cortez, C., Gan, W. B. & Manfredi, G. Abnormal mitochondrial transport and morphology are common pathological denominators in SOD1 and TDP43 ALS mouse models. *Hum Mol Genet* **23**, 1413-1424, doi:10.1093/hmg/ddt528 (2014).

75   Higgins, C. M., Jung, C. & Xu, Z. ALS-associated mutant SOD1G93A causes mitochondrial vacuolation by expansion of the intermembrane space and by involvement of SOD1 aggregation and peroxisomes. *BMC Neurosci* **4**, 16, doi:10.1186/1471-2202-4-16 (2003).

76   Kausar, S., Wang, F. & Cui, H. The Role of Mitochondria in Reactive Oxygen Species Generation and Its Implications for Neurodegenerative Diseases. *Cells* **7**, doi:10.3390/cells7120274 (2018).

77   Wiedemann, F. R., Manfredi, G., Mawrin, C., Beal, M. F. & Schon, E. A. Mitochondrial DNA and respiratory chain function in spinal cords of ALS patients. *J Neurochem* **80**, 616-625, doi:10.1046/j.0022-3042.2001.00731.x (2002).

78   Youle, R. J. & Narendra, D. P. Mechanisms of mitophagy. *Nat Rev Mol Cell Biol* **12**, 9-14, doi:10.1038/nrm3028 (2011).

79   Moore, A. S. & Holzbaur, E. L. Dynamic recruitment and activation of ALS-associated TBK1 with its target optineurin are required for efficient mitophagy. *Proc Natl Acad Sci U S A* **113**, E3349-3358, doi:10.1073/pnas.1523810113 (2016).

80   Fivenson, E. M. *et al.* Mitophagy in neurodegeneration and aging. *Neurochem Int* **109**, 202-209, doi:10.1016/j.neuint.2017.02.007 (2017).

81   Damiano, M. *et al.* Neural mitochondrial Ca2+ capacity impairment precedes the onset of motor symptoms in G93A Cu/Zn-superoxide dismutase mutant mice. *J Neurochem* **96**,

1349-1361, doi:10.1111/j.1471-4159.2006.03619.x (2006).

82   Yuan, A., Rao, M. V., Veeranna & Nixon, R. A. Neurofilaments and Neurofilament Proteins in Health and Disease. *Cold Spring Harb Perspect Biol* **9**, doi:10.1101/cshperspect.a018309 (2017).

83   Taylor, J. P., Brown, R. H., Jr. & Cleveland, D. W. Decoding ALS: from genes to mechanism. *Nature* **539**, 197-206, doi:10.1038/nature20413 (2016).

84   Prokop, A. Cytoskeletal organization of axons in vertebrates and invertebrates. *J Cell Biol* **219**, doi:10.1083/jcb.201912081 (2020).

85   Fil, D. *et al.* Mutant Profilin1 transgenic mice recapitulate cardinal features of motor neuron disease. *Hum Mol Genet* **26**, 686-701, doi:10.1093/hmg/ddw429 (2017).

86   Wu, C. H. *et al.* Mutations in the profilin 1 gene cause familial amyotrophic lateral sclerosis. *Nature* **488**, 499-503, doi:10.1038/nature11280 (2012).

87   Warita, H., Itoyama, Y. & Abe, K. Selective impairment of fast anterograde axonal transport in the peripheral nerves of asymptomatic transgenic mice with a G93A mutant SOD1 gene. *Brain Res* **819**, 120-131, doi:10.1016/s0006-8993(98)01351-1 (1999).

88   Pasinelli, P. *et al.* Amyotrophic lateral sclerosis-associated SOD1 mutant proteins bind and aggregate with Bcl-2 in spinal cord mitochondria. *Neuron* **43**, 19-30, doi:10.1016/j.neuron.2004.06.021 (2004).

89   Tallon, C., Russell, K. A., Sakhalkar, S., Andrapallayal, N. & Farah, M. H. Length-dependent axo-terminal degeneration at the neuromuscular synapses of type II muscle in SOD1 mice. *Neuroscience* **312**, 179-189, doi:10.1016/j.neuroscience.2015.11.018 (2016).

90   De Vos, K. J. *et al.* Familial amyotrophic lateral sclerosis-linked SOD1 mutants perturb fast axonal transport to reduce axonal mitochondria content. *Hum Mol Genet* **16**, 2720-2728, doi:10.1093/hmg/ddm226 (2007).

91   Pantelidou, M. *et al.* Differential expression of molecular motors in the motor cortex of sporadic ALS. *Neurobiol Dis* **26**, 577-589, doi:10.1016/j.nbd.2007.02.005 (2007).

92   Nicolas, A. *et al.* Genome-wide Analyses Identify KIF5A as a Novel ALS Gene. *Neuron* **97**, 1268-1283 e1266, doi:10.1016/j.neuron.2018.02.027 (2018).

93   Colombrita, C. *et al.* TDP-43 and FUS RNA-binding proteins bind distinct sets of cytoplasmic messenger RNAs and differently regulate their post-transcriptional fate in motoneuron-like cells. *J Biol Chem* **287**, 15635-15647, doi:10.1074/jbc.M111.333450 (2012).

94   Johnson, J. O. *et al.* Mutations in the Matrin 3 gene cause familial amyotrophic lateral sclerosis. *Nat Neurosci* **17**, 664-666, doi:10.1038/nn.3688 (2014).

95   Jutzi, D., Akinyi, M. V., Mechtersheimer, J., Frilander, M. J. & Ruepp, M. D. The emerging role of minor intron splicing in neurological disorders. *Cell Stress* **2**, 40-54, doi:10.15698/cst2018.03.126 (2018).

96   Yang, C. *et al.* Partial loss of TDP-43 function causes phenotypes of amyotrophic lateral sclerosis. *Proc Natl Acad Sci U S A* **111**, E1121-1129, doi:10.1073/pnas.1322641111 (2014).

97   Lagier-Tourenne, C. *et al.* Divergent roles of ALS-linked proteins FUS/TLS and TDP-43 intersect in processing long pre-mRNAs. *Nat Neurosci* **15**, 1488-1497, doi:10.1038/nn.3230 (2012).

98   Rogelj, B. *et al.* Widespread binding of FUS along nascent RNA regulates alternative splicing in the brain. *Sci Rep* **2**, 603, doi:10.1038/srep00603 (2012).

99   Orozco, D. *et al.* Loss of fused in sarcoma (FUS) promotes pathological Tau splicing. *EMBO Rep* **13**, 759-764, doi:10.1038/embor.2012.90 (2012).

100   Balendra, R. & Isaacs, A. M. C9orf72-mediated ALS and FTD: multiple pathways to disease. *Nat Rev Neurol* **14**, 544-558, doi:10.1038/s41582-018-0047-2 (2018).

101   Aladesuyi Arogundade, O. *et al.* Antisense RNA foci are associated with nucleoli and TDP-43 mislocalization in C9orf72-ALS/FTD: a quantitative study. *Acta Neuropathol* **137**, 527-530, doi:10.1007/s00401-018-01955-0 (2019).

102   Mehta, A. R. *et al.* Improved detection of RNA foci in C9orf72 amyotrophic lateral sclerosis post-mortem tissue using BaseScope shows a lack of association with cognitive dysfunction. *Brain Commun* **2**, fcaa009, doi:10.1093/braincomms/fcaa009 (2020).

103   Sama, R. R. *et al.* FUS/TLS assembles into stress granules and is a prosurvival factor during hyperosmolar stress. *J Cell Physiol* **228**, 2222-2231, doi:10.1002/jcp.24395 (2013).

104   Vance, C. *et al.* ALS mutant FUS disrupts nuclear localization and sequesters wild-type FUS within cytoplasmic stress granules. *Hum Mol Genet* **22**, 2676-2688, doi:10.1093/hmg/ddt117 (2013).

105   Purice, M. D. & Taylor, J. P. Linking hnRNP Function to ALS and FTD Pathology. *Front Neurosci* **12**, 326, doi:10.3389/fnins.2018.00326 (2018).

106   Zhang, K. *et al.* Stress Granule Assembly Disrupts Nucleocytoplasmic Transport. *Cell* **173**, 958-971 e917, doi:10.1016/j.cell.2018.03.025 (2018).

107   Kim, H. J. *et al.* Mutations in prion-like domains in hnRNPA2B1 and hnRNPA1 cause multisystem proteinopathy and ALS. *Nature* **495**, 467-473, doi:10.1038/nature11922 (2013).

108   Buchan, J. R., Kolaitis, R. M., Taylor, J. P. & Parker, R. Eukaryotic stress granules are cleared by autophagy and Cdc48/VCP function. *Cell* **153**, 1461-1474, doi:10.1016/j.cell.2013.05.037 (2013).

109   Ferraiuolo, L., Kirby, J., Grierson, A. J., Sendtner, M. & Shaw, P. J. Molecular pathways of motor neuron injury in amyotrophic lateral sclerosis. *Nat Rev Neurol* **7**, 616-630, doi:10.1038/nrneurol.2011.152 (2011).

110   Wang, Y. & Qin, Z. H. Molecular and cellular mechanisms of excitotoxic neuronal death. *Apoptosis* **15**, 1382-1402, doi:10.1007/s10495-010-0481-0 (2010).

111   Netzahualcoyotzi, C. & Tapia, R. Degeneration of spinal motor neurons by chronic AMPA-induced excitotoxicity in vivo and protection by energy substrates. *Acta Neuropathol Commun* **3**, 27, doi:10.1186/s40478-015-0205-3 (2015).

112   Van Den Bosch, L., Van Damme, P., Bogaert, E. & Robberecht, W. The role of excitotoxicity in the pathogenesis of amyotrophic lateral sclerosis. *Biochim Biophys Acta* **1762**, 1068-1082, doi:10.1016/j.bbadis.2006.05.002 (2006).

113   Corona, J. C. & Tapia, R. AMPA receptor activation, but not the accumulation of endogenous extracellular glutamate, induces paralysis and motor neuron death in rat spinal cord in vivo. *J Neurochem* **89**, 988-997, doi:10.1111/j.1471-4159.2004.02383.x (2004).

114   Heath, P. R., Tomkins, J., Ince, P. G. & Shaw, P. J. Quantitative assessment of AMPA receptor mRNA in human spinal motor neurons isolated by laser capture microdissection. *Neuroreport* **13**, 1753-1757, doi:10.1097/00001756-200210070-00012 (2002).

115   Aizawa, H. *et al.* TDP-43 pathology in sporadic ALS occurs in motor neurons lacking the RNA editing enzyme ADAR2. *Acta Neuropathol* **120**, 75-84, doi:10.1007/s00401-010-0678-x (2010).

116   Rothstein, J. D., Van Kammen, M., Levey, A. I., Martin, L. J. & Kuncl, R. W. Selective loss of glial glutamate transporter GLT-1 in amyotrophic lateral sclerosis. *Ann Neurol* **38**, 73-84, doi:10.1002/ana.410380114 (1995).

117   Kong, Q. *et al.* Small-molecule activator of glutamate transporter EAAT2 translation provides neuroprotection. *J Clin Invest* **124**, 1255-1267, doi:10.1172/JCI66163 (2014).

118   Rothstein, J. D. *et al.* Beta-lactam antibiotics offer neuroprotection by increasing glutamate transporter expression. *Nature* **433**, 73-77, doi:10.1038/nature03180 (2005).

119   Van Damme, P. *et al.* Astrocytes regulate GluR2 expression in motor neurons and their vulnerability to excitotoxicity. *Proc Natl Acad Sci U S A* **104**, 14825-14830, doi:10.1073/pnas.0705046104 (2007).

120   Shi, Y. *et al.* Haploinsufficiency leads to neurodegeneration in C9ORF72 ALS/FTD human induced motor neurons. *Nat Med* **24**, 313-325, doi:10.1038/nm.4490 (2018).

121   Thery, C. Exosomes: secreted vesicles and intercellular communications. *F1000 Biol Rep*

3, 15, doi:10.3410/B3-15 (2011).

122 Silverman, J. M. *et al.* CNS-derived extracellular vesicles from superoxide dismutase 1 (SOD1)(G93A) ALS mice originate from astrocytes and neurons and carry misfolded SOD1. *J Biol Chem* **294**, 3744-3759, doi:10.1074/jbc.RA118.004825 (2019).

123 Chen, Y., Xia, K., Chen, L. & Fan, D. Increased Interleukin-6 Levels in the Astrocyte-Derived Exosomes of Sporadic Amyotrophic Lateral Sclerosis Patients. *Front Neurosci* **13**, 574, doi:10.3389/fnins.2019.00574 (2019).

124 Westergard, T. *et al.* Cell-to-Cell Transmission of Dipeptide Repeat Proteins Linked to C9orf72-ALS/FTD. *Cell Rep* **17**, 645-652, doi:10.1016/j.celrep.2016.09.032 (2016).

125 Parkinson, N. *et al.* ALS phenotypes with mutations in CHMP2B (charged multivesicular body protein 2B). *Neurology* **67**, 1074-1077, doi:10.1212/01.wnl.0000231510.89311.8b (2006).

126 Skibinski, G. *et al.* Mutations in the endosomal ESCRTIII-complex subunit CHMP2B in frontotemporal dementia. *Nat Genet* **37**, 806-808, doi:10.1038/ng1609 (2005).

127 Yang, Y. *et al.* The gene encoding alsin, a protein with three guanine-nucleotide exchange factor domains, is mutated in a form of recessive amyotrophic lateral sclerosis. *Nat Genet* **29**, 160-165, doi:10.1038/ng1001-160 (2001).

128 Lai, C. *et al.* Regulation of endosomal motility and degradation by amyotrophic lateral sclerosis 2/alsin. *Mol Brain* **2**, 23, doi:10.1186/1756-6606-2-23 (2009).

129 Buratta, S. *et al.* Lysosomal Exocytosis, Exosome Release and Secretory Autophagy: The Autophagic- and Endo-Lysosomal Systems Go Extracellular. *Int J Mol Sci* **21**, doi:10.3390/ijms21072576 (2020).

130 Bug, M. & Meyer, H. Expanding into new markets--VCP/p97 in endocytosis and autophagy. *J Struct Biol* **179**, 78-82, doi:10.1016/j.jsb.2012.03.003 (2012).

131 Nishimura, A. L. *et al.* A mutation in the vesicle-trafficking protein VAPB causes late-onset spinal muscular atrophy and amyotrophic lateral sclerosis. *Am J Hum Genet* **75**, 822-831,

doi:10.1086/425287 (2004).

132   Blanc, L. & Vidal, M. New insights into the function of Rab GTPases in the context of exosomal secretion. *Small GTPases* **9**, 95-106, doi:10.1080/21541248.2016.1264352 (2018).

133   Neumann, M. *et al.* Ubiquitinated TDP-43 in frontotemporal lobar degeneration and amyotrophic lateral sclerosis. *Science* **314**, 130-133, doi:10.1126/science.1134108 (2006).

134   Winton, M. J. *et al.* A90V TDP-43 variant results in the aberrant localization of TDP-43 in vitro. *FEBS Lett* **582**, 2252-2256, doi:10.1016/j.febslet.2008.05.024 (2008).

135   Duan, W. *et al.* Mutant TAR DNA-binding protein-43 induces oxidative injury in motor neuron-like cell. *Neuroscience* **169**, 1621-1629, doi:10.1016/j.neuroscience.2010.06.018 (2010).

136   Lagier-Tourenne, C. & Cleveland, D. W. Rethinking ALS: the FUS about TDP-43. *Cell* **136**, 1001-1004, doi:10.1016/j.cell.2009.03.006 (2009).

137   Smethurst, P., Sidle, K. C. & Hardy, J. Review: Prion-like mechanisms of transactive response DNA binding protein of 43 kDa (TDP-43) in amyotrophic lateral sclerosis (ALS). *Neuropathol Appl Neurobiol* **41**, 578-597, doi:10.1111/nan.12206 (2015).

138   Polymenidou, M. *et al.* Long pre-mRNA depletion and RNA missplicing contribute to neuronal vulnerability from loss of TDP-43. *Nat Neurosci* **14**, 459-468, doi:10.1038/nn.2779 (2011).

139   Tollervey, J. R. *et al.* Characterizing the RNA targets and position-dependent splicing regulation by TDP-43. *Nat Neurosci* **14**, 452-458, doi:10.1038/nn.2778 (2011).

140   Buratti, E. & Baralle, F. E. Characterization and functional implications of the RNA binding properties of nuclear factor TDP-43, a novel splicing regulator of CFTR exon 9. *J Biol Chem* **276**, 36337-36343, doi:10.1074/jbc.M104236200 (2001).

141   Casafont, I., Bengoechea, R., Tapia, O., Berciano, M. T. & Lafarga, M. TDP-43 localizes in mRNA transcription and processing sites in mammalian neurons. *J Struct Biol* **167**, 235-

241, doi:10.1016/j.jsb.2009.06.006 (2009).

142 Polymenidou, M. *et al.* Misregulated RNA processing in amyotrophic lateral sclerosis. *Brain Res* **1462**, 3-15, doi:10.1016/j.brainres.2012.02.059 (2012).

143 Arnold, E. S. *et al.* ALS-linked TDP-43 mutations produce aberrant RNA splicing and adult-onset motor neuron disease without aggregation or loss of nuclear TDP-43. *Proc Natl Acad Sci U S A* **110**, E736-745, doi:10.1073/pnas.1222809110 (2013).

144 Highley, J. R. *et al.* Loss of nuclear TDP-43 in amyotrophic lateral sclerosis (ALS) causes altered expression of splicing machinery and widespread dysregulation of RNA splicing in motor neurones. *Neuropathol Appl Neurobiol* **40**, 670-685, doi:10.1111/nan.12148 (2014).

145 Volkening, K., Leystra-Lantz, C., Yang, W., Jaffee, H. & Strong, M. J. Tar DNA binding protein of 43 kDa (TDP-43), 14-3-3 proteins and copper/zinc superoxide dismutase (SOD1) interact to modulate NFL mRNA stability. Implications for altered RNA processing in amyotrophic lateral sclerosis (ALS). *Brain Res* **1305**, 168-182, doi:10.1016/j.brainres.2009.09.105 (2009).

146 Ayala, Y. M. *et al.* TDP-43 regulates its mRNA levels through a negative feedback loop. *EMBO J* **30**, 277-288, doi:10.1038/emboj.2010.310 (2011).

147 Alami, N. H. *et al.* Axonal transport of TDP-43 mRNA granules is impaired by ALS-causing mutations. *Neuron* **81**, 536-543, doi:10.1016/j.neuron.2013.12.018 (2014).

148 Wang, I. F., Wu, L. S., Chang, H. Y. & Shen, C. K. TDP-43, the signature protein of FTLD-U, is a neuronal activity-responsive factor. *J Neurochem* **105**, 797-806, doi:10.1111/j.1471-4159.2007.05190.x (2008).

149 Colombrita, C. *et al.* TDP-43 is recruited to stress granules in conditions of oxidative insult. *J Neurochem* **111**, 1051-1061, doi:10.1111/j.1471-4159.2009.06383.x (2009).

150 McDonald, K. K. *et al.* TAR DNA-binding protein 43 (TDP-43) regulates stress granule dynamics via differential regulation of G3BP and TIA-1. *Hum Mol Genet* **20**, 1400-1410, doi:10.1093/hmg/ddr021 (2011).

151   Sampathu, D. M. *et al.* Pathological heterogeneity of frontotemporal lobar degeneration with ubiquitin-positive inclusions delineated by ubiquitin immunohistochemistry and novel monoclonal antibodies. *Am J Pathol* **169**, 1343-1352, doi:10.2353/ajpath.2006.060438 (2006).

152   Kuo, P. H., Doudeva, L. G., Wang, Y. T., Shen, C. K. & Yuan, H. S. Structural insights into TDP-43 in nucleic-acid binding and domain interactions. *Nucleic Acids Res* **37**, 1799-1808, doi:10.1093/nar/gkp013 (2009).

153   Afroz, T. *et al.* Functional and dynamic polymerization of the ALS-linked protein TDP-43 antagonizes its pathologic aggregation. *Nat Commun* **8**, 45, doi:10.1038/s41467-017-00062-0 (2017).

154   Shiina, Y., Arima, K., Tabunoki, H. & Satoh, J. TDP-43 dimerizes in human cells in culture. *Cell Mol Neurobiol* **30**, 641-652, doi:10.1007/s10571-009-9489-9 (2010).

155   Fang, Y. S. *et al.* Full-length TDP-43 forms toxic amyloid oligomers that are present in frontotemporal lobar dementia-TDP patients. *Nat Commun* **5**, 4824, doi:10.1038/ncomms5824 (2014).

156   Johnson, B. S. *et al.* TDP-43 is intrinsically aggregation-prone, and amyotrophic lateral sclerosis-linked mutations accelerate aggregation and increase toxicity. *J Biol Chem* **284**, 20329-20339, doi:10.1074/jbc.M109.010264 (2009).

157   Stallings, N. R., Puttaparthi, K., Luther, C. M., Burns, D. K. & Elliott, J. L. Progressive motor weakness in transgenic mice expressing human TDP-43. *Neurobiol Dis* **40**, 404-414, doi:10.1016/j.nbd.2010.06.017 (2010).

158   Igaz, L. M. *et al.* Dysregulation of the ALS-associated gene TDP-43 leads to neuronal death and degeneration in mice. *J Clin Invest* **121**, 726-738, doi:10.1172/JCI44867 (2011).

159   Bose, J. K., Huang, C. C. & Shen, C. K. Regulation of autophagy by neuropathological protein TDP-43. *J Biol Chem* **286**, 44441-44448, doi:10.1074/jbc.M111.237115 (2011).

160   Xia, Q. *et al.* TDP-43 loss of function increases TFEB activity and blocks autophagosome-

lysosome fusion. *EMBO J* **35**, 121-142, doi:10.15252/embj.201591998 (2016).

161   Filimonenko, M. *et al.* Functional multivesicular bodies are required for autophagic clearance of protein aggregates associated with neurodegenerative disease. *J Cell Biol* **179**, 485-500, doi:10.1083/jcb.200702115 (2007).

162   Liu, G. *et al.* Endocytosis regulates TDP-43 toxicity and turnover. *Nat Commun* **8**, 2092, doi:10.1038/s41467-017-02017-x (2017).

163   Schwenk, B. M. *et al.* TDP-43 loss of function inhibits endosomal trafficking and alters trophic signaling in neurons. *EMBO J* **35**, 2350-2370, doi:10.15252/embj.201694221 (2016).

164   Leibiger, C. *et al.* TDP-43 controls lysosomal pathways thereby determining its own clearance and cytotoxicity. *Hum Mol Genet* **27**, 1593-1607, doi:10.1093/hmg/ddy066 (2018).

165   Braun, R. J. *et al.* Neurotoxic 43-kDa TAR DNA-binding protein (TDP-43) triggers mitochondrion-dependent programmed cell death in yeast. *J Biol Chem* **286**, 19958-19972, doi:10.1074/jbc.M110.194852 (2011).

166   Stribl, C. *et al.* Mitochondrial dysfunction and decrease in body weight of a transgenic knock-in mouse model for TDP-43. *J Biol Chem* **289**, 10769-10784, doi:10.1074/jbc.M113.515940 (2014).

167   Wang, W. *et al.* The ALS disease-associated mutant TDP-43 impairs mitochondrial dynamics and function in motor neurons. *Hum Mol Genet* **22**, 4706-4719, doi:10.1093/hmg/ddt319 (2013).

168   Braun, R. J. Mitochondrion-mediated cell death: dissecting yeast apoptosis for a better understanding of neurodegeneration. *Front Oncol* **2**, 182, doi:10.3389/fonc.2012.00182 (2012).

169   Yu, T. *et al.* The pivotal role of TBK1 in inflammatory responses mediated by macrophages. *Mediators Inflamm* **2012**, 979105, doi:10.1155/2012/979105 (2012).

170   Weidberg, H. & Elazar, Z. TBK1 mediates crosstalk between the innate immune response and autophagy. *Sci Signal* **4**, pe39, doi:10.1126/scisignal.2002355 (2011).

171   Chen, W. *et al.* TBK1 Promote Bladder Cancer Cell Proliferation and Migration via Akt Signaling. *J Cancer* **8**, 1892-1899, doi:10.7150/jca.17638 (2017).

172   Freischmidt, A. *et al.* Haploinsufficiency of TBK1 causes familial ALS and fronto-temporal dementia. *Nat Neurosci* **18**, 631-636, doi:10.1038/nn.4000 (2015).

173   Gijselinck, I. *et al.* Loss of TBK1 is a frequent cause of frontotemporal dementia in a Belgian cohort. *Neurology* **85**, 2116-2125, doi:10.1212/WNL.0000000000002220 (2015).

174   Le Ber, I. *et al.* TBK1 mutation frequencies in French frontotemporal dementia and amyotrophic lateral sclerosis cohorts. *Neurobiol Aging* **36**, 3116 e3115-3116 e3118, doi:10.1016/j.neurobiolaging.2015.08.009 (2015).

175   Pottier, C. *et al.* Whole-genome sequencing reveals important role for TBK1 and OPTN mutations in frontotemporal lobar degeneration without motor neuron disease. *Acta Neuropathol* **130**, 77-92, doi:10.1007/s00401-015-1436-x (2015).

176   Williams, K. L. *et al.* Novel TBK1 truncating mutation in a familial amyotrophic lateral sclerosis patient of Chinese origin. *Neurobiol Aging* **36**, 3334 e3331-3334 e3335, doi:10.1016/j.neurobiolaging.2015.08.013 (2015).

177   Tsai, P. C. *et al.* Mutational analysis of TBK1 in Taiwanese patients with amyotrophic lateral sclerosis. *Neurobiol Aging* **40**, 191 e111-191 e116, doi:10.1016/j.neurobiolaging.2015.12.022 (2016).

178   Klionsky, D. J. Autophagy: from phenomenology to molecular understanding in less than a decade. *Nat Rev Mol Cell Biol* **8**, 931-937, doi:10.1038/nrm2245 (2007).

179   Korac, J. *et al.* Ubiquitin-independent function of optineurin in autophagic clearance of protein aggregates. *J Cell Sci* **126**, 580-592, doi:10.1242/jcs.114926 (2013).

180   Thurston, T. L., Ryzhakov, G., Bloor, S., von Muhlinen, N. & Randow, F. The TBK1 adaptor and autophagy receptor NDP52 restricts the proliferation of ubiquitin-coated bacteria. *Nat*

Immunol **10**, 1215-1221, doi:10.1038/ni.1800 (2009).

181   Wild, P. *et al.* Phosphorylation of the autophagy receptor optineurin restricts Salmonella growth. *Science* **333**, 228-233, doi:10.1126/science.1205405 (2011).

182   Pilli, M. *et al.* TBK-1 promotes autophagy-mediated antimicrobial defense by controlling autophagosome maturation. *Immunity* **37**, 223-234, doi:10.1016/j.immuni.2012.04.015 (2012).

183   Tojima, Y. *et al.* NAK is an IkappaB kinase-activating kinase. *Nature* **404**, 778-782, doi:10.1038/35008109 (2000).

184   Chau, T. L. *et al.* Are the IKKs and IKK-related kinases TBK1 and IKK-epsilon similarly activated? *Trends Biochem Sci* **33**, 171-180, doi:10.1016/j.tibs.2008.01.002 (2008).

185   Sharma, S. *et al.* Triggering the interferon antiviral response through an IKK-related pathway. *Science* **300**, 1148-1151, doi:10.1126/science.1081315 (2003).

186   Yamamoto, M. *et al.* Role of adaptor TRIF in the MyD88-independent toll-like receptor signaling pathway. *Science* **301**, 640-643, doi:10.1126/science.1087262 (2003).

187   Liang, Q. *et al.* Crosstalk between the cGAS DNA sensor and Beclin-1 autophagy protein shapes innate antimicrobial immune responses. *Cell Host Microbe* **15**, 228-238, doi:10.1016/j.chom.2014.01.009 (2014).

188   Watson, R. O. *et al.* The Cytosolic Sensor cGAS Detects Mycobacterium tuberculosis DNA to Induce Type I Interferons and Activate Autophagy. *Cell Host Microbe* **17**, 811-819, doi:10.1016/j.chom.2015.05.004 (2015).

189   Xu, D. *et al.* TBK1 Suppresses RIPK1-Driven Apoptosis and Inflammation during Development and in Aging. *Cell* **174**, 1477-1491 e1419, doi:10.1016/j.cell.2018.07.041 (2018).

190   Gerbino, V. *et al.* The Loss of TBK1 Kinase Activity in Motor Neurons or in All Cell Types Differentially Impacts ALS Disease Progression in SOD1 Mice. *Neuron* **106**, 789-805 e785, doi:10.1016/j.neuron.2020.03.005 (2020).

191 Brenner, D. *et al.* Heterozygous Tbk1 loss has opposing effects in early and late stages of ALS in mice. *J Exp Med* **216**, 267-278, doi:10.1084/jem.20180729 (2019).

192 Nguyen, D. K. H., Thombre, R. & Wang, J. Autophagy as a common pathway in amyotrophic lateral sclerosis. *Neurosci Lett* **697**, 34-48, doi:10.1016/j.neulet.2018.04.006 (2019).

193 Van Mossevelde, S. *et al.* Clinical features of TBK1 carriers compared with C9orf72, GRN and non-mutation carriers in a Belgian cohort. *Brain* **139**, 452-467, doi:10.1093/brain/awv358 (2016).

CHAPTER 2: Generation of a human stem cell model with loss-of-function mutations of TBK1 by gene editing

2.1 Abstract

Recent exome sequencing data suggested that loss-of-function mutations in the gene encoding TBK1 are associated with neurodegenerative disorders of ALS and FTD. Previous studies have identified the role of TBK1 in regulating multiple cellular pathways, including inflammation, innate immunity, and autophagy. However, how the loss of TBK1 function contributes to the increased susceptibility to ALS remains elusive. In addition, most recent studies focused on the non-cell-autonomous role of TBK1 in affecting astrocytes and microglia, raising the question of whether cell-autonomous contributions of TBK1 in human motor neurons, which are known to degenerate in ALS patients, are central to disease pathology. To demonstrate the mechanisms of TBK1 deficiency in human motor neuron physiology, we generated loss-of-function mutations of TBK1 in human embryonic stem cells (hESCs) based on gene editing. TBK1 deficiency triggered impaired autophagic flux and p62 accumulations in hESCs. Meanwhile, in differentiated human motor neurons, TBK1 deficiency is sufficient to cause mislocalization of TDP-43 and its insoluble accumulations, a hallmark of ALS pathology. Finally, we performed assays to test the physiological functions of motor neurons, like electrophysiological properties and axonal repairability, in TBK1 deficient models. Therefore, our loss-of-function model of TBK1 in human motor neurons recapitulated key disease pathologies and showed disrupted homeostatic functions that have been found in ALS patients.

2.2 Introduction

Amyotrophic lateral sclerosis (ALS) is a neurodegenerative disease characterized by progressive degeneration of motor neurons, resulting in paralysis and death [1]. About 10% of ALS cases are inherited from families, almost always a dominant trait with high penetrance [2]. Recently, next-generation sequencing techniques have discovered that loss-of-function mutations in the gene encoding TBK1 are associated with neurodegenerative disorders of ALS and frontotemporal dementia (FTD) [3,4]. Additional *TBK1* (OMIM 604834) variants have also been found in patients with ALS or FTD, making *TBK1* mutations the third or fourth most frequent cause of the diseases in the studied populations [5-9]. Like many ALS and FTD-associated genes, *TBK1* variants have been related to the full phenotypic spectrum of ALS and FTD syndromes even within the same family [4,5].

TBK1 is an IKK family kinase previously identified for a central role in controlling type-I interferon production in response to viral infection. It is also involved in regulating multiple cellular pathways, including inflammation [10], immune response [11], and cell proliferation [12]. Because TBK1 is a multifunctional kinase involved in many biological pathways, determining which specific downstream functions of TBK1 absence contribute to the development of ALS and FTD remains unresolved. A previous study has shown that the reduced Tbk1 expression synergizes with aging mediated RIPK1 inhibition to promote neuroinflammation and neurodegeneration in mouse models [13]. In this study, heterozygous *Tbk1* mutations might function as a genetic risk factor that predisposes neuroinflammation and neurodegeneration under specific environmental or physiological stresses. Additional studies also reported that loss-of-function mutations of *Tbk1* in mouse motor neurons do not display any neurodegeneration phenotype, but TBK1 might contribute to the onset of disease in SOD1^{G93A} mouse models [14,15]. These studies suggested that loss of TBK1 activity contributed to mouse motor neuron pathology but might affect disease progression in a non-cell-autonomous manner. A recent study using induced pluripotent stem cell

(iPSC)-derived TBK1 patient human motor neurons showed decreased cell viability due to disrupted autophagic flux [16], raising the question of whether cell-autonomous contributions of TBK1 in human motor neurons, which are known to degenerate in ALS patients, are central to disease pathology.

Resolving the cell-autonomous functions of TBK1 in human motor neurons remains critical for three reasons. First, it could provide insights into whether the reduction of TBK1 protein found in patients directly contribute to motor neuron pathology. Second, efforts are being made to develop therapeutics targeting autophagy [17], a prevailing disease mechanism for *TBK1* mutation-related ALS/FTD. Therefore, determining whether loss of autophagy activity downstream of *TBK1* mutations is the crucial disease-causing mechanism, specifically in human motor neurons, could be therapeutically beneficial. Third, TDP-43 pathology has been observed in the spinal cord of patients with *TBK1* mutations [18], but not in *Tbk1* mutant mice [14]. Thus, it is necessary to systematically evaluate the effects of loss-of-function mutations of *TBK1* in human cell models.

Here, we generated human embryonic stem cells (ESCs) harboring loss-of-function mutations of *TBK1* by CRISPR/Cas9. We found that TBK1$^{-/-}$ cells showed impaired autophagic flux in human cellular models and increased cytoplasmic and insoluble TDP-43 in TBK1$^{-/-}$ human motor neurons. Functional analysis using MEA and axotomy also validated the roles of TBK1 in early-stage disease progression. Our results also show that our loss-of-function model of TBK1 recapitulated key disease pathologies and disrupted homeostatic functions that have been found in ALS patients.

2.3 Results

2.3.1 Generating loss-of-function mutations of TBK1 by CRISPR/Cas9

To generate the loss-of-function mutation model of *TBK1*, we aimed to disrupt the protein expression without introducing a massive trunk into the genome. Therefore, the critical first step

is to define the target site of *TBK1*. Recent structural studies have provided valuable insights [19-22]. The N terminus of TBK1 protein contains a kinase domain (KD), a ubiquitin-like domain (ULD), a substrate dimerization domain (SDD), and a C-terminal domain (CTD). The SDDs comprise the entire dimerization interface, and mutations at this site lead to structural disruption [23,24]. To investigate whether the loss of TBK1 protein activity is relevant to ALS pathology, we used CRISPR/Cas9-mediated genome editing to introduce mutations at the SDD (or CCD1 domain) in the human embryonic stem cell (hESC) line HUES3 Hb9::GFP (Figure 2.1) [25]. After isolating and expanding single clones upon puromycin selection, 25 mutant clones were selected and sequenced. Among them, 21 out of 25 clones were successfully edited by CRISPR/Cas9, with 3 of them having frameshift mutations, 8 of them having in-frame deletions, and 14 of them being mixed mutations (Figure 2.2 a). Two potential TBK1$^{-/-}$ clones with the highest efficiency were validated in cells by Sanger sequencing, and Tide analysis confirmed the mutation types (Figure 2.2 b,c).
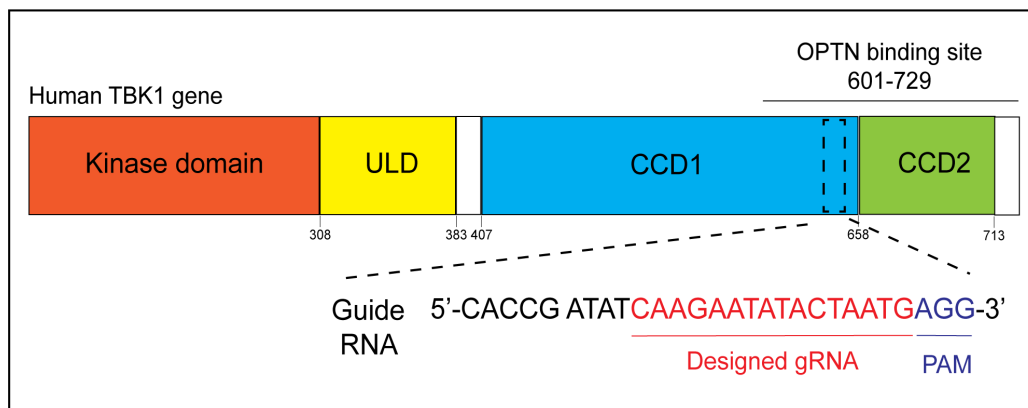

Figure 2.1 Design of sgRNA targeting at TBK1.

The schematic of gene-editing strategy and targeting locus of sgRNA for human TBK1 gene in HUES3 HB9::GFP ESCs. To facilitate the loss-of-function mutations of TBK1, the sgRNA was designed to target the CCD1 domain, which had been reported to affect TBK1 dimerization and protein stability.
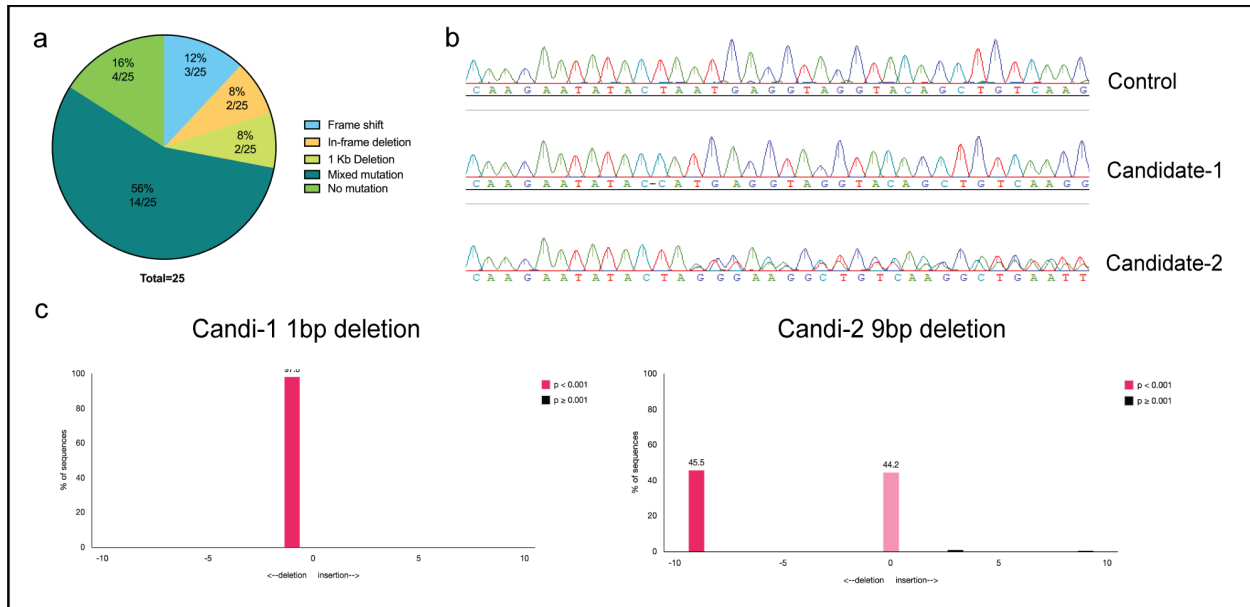
Figure 2.2 Validation of TBK1 mutant clones by Sanger sequencing.

Sanger sequencing was used to validate the mutations introduced by gene editing. (a) The summary of mutation types selected from isolated mutant clones. (b) Sanger sequencing of control and two candidate mutant clones. (c) TIDE analysis of indels percentage of the two candidate clones based on the sequencing data. Deletions were shown on the left X-axis, and insertions were shown on the right based on the number of deleted or inserted base pairs.
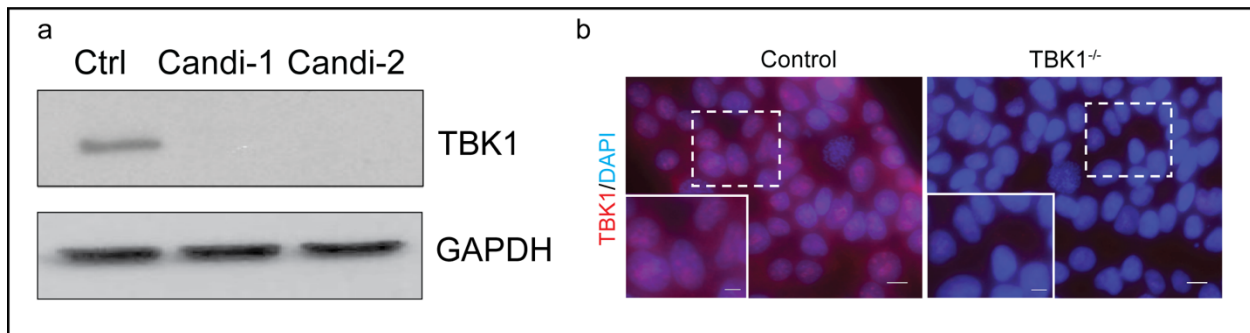

Figure 2.3 Validation of TBK1 expression by immunoblot and immunocytochemistry.

(a) Validation of TBK1 protein expression for two candidate mutant clones by western blot. (b) Immunostaining of TBK1 for hESC cultures of control and TBK1$^{-/-}$ cells. Scale bar, 20 μm.

Western blot and immunocytochemistry (ICC) analysis also confirmed the loss of TBK1 expression. TBK1 proteins were disrupted in both clones and could not be detected (Figure 2.3 a,b). Previous research has reported the link between TBK1 mutations and autophagy activity [26]. To confirm the functionality of our loss-of-function model, we assayed the activity of autophagic flux in control and TBK1$^{-/-}$ clones. Increased levels of SQSTM1/p62 were detected in the two candidate clones (p<0.01) (Figure 2.4 a,b). The elevated p62 level indicated impaired autophagic flux, as TBK1 could mediate autophagic flux and cargo selection by phosphorylating autophagic receptors like p62. For clarification, we used candidate 1, which has a frameshift mutation at the desired mutant location, for future experiments. We next tested how the loss of TBK1 activity affected autophagic flux and confirmed the role of TBK1 in autophagosomal maturation as measured by LC3 immunoblotting (Figure 2.4 c,d). While control cells showed increased LC3-II (an early autophagic organelle marker) upon lysosomal inhibitor bafilomycin A1 (Baf A1) treatment, TBK1$^{-/-}$ hESCs accumulated LC3-II in the basal level but failed to further increase upon Baf A1 treatment. This indicates a deficiency in autophagosome maturation in the TBK1$^{-/-}$ cells, consistent with a previous report [27].

Next, we sought to determine whether the clearance of p62 puncta, which was reported as an ALS pathological hallmark, would be affected by TBK1 deficiency. We performed ICC and quantitative imaging analysis and detected significantly increased p62 puncta in TBK1$^{-/-}$ cells (p<0.0001) (Figure 2.5 a,b), consistent with previous protein blot analysis (Figure 2.4 a,b). Therefore, p62 puncta cannot be cleared when TBK1 is deficient. In addition, the accumulated p62 puncta at the peri-nuclear sites indicated blocked autophagic degradative pathways, which has been reported in *TBK1* mutant and other sporadic ALS patients [18,28]. Next, we sought to determine whether loss of TBK1 activity leads to mislocalization of TDP-43, another critical pathological hallmark for ALS, in hESC models. We deployed immunocytochemistry analysis using endogenous TDP-43 antibody (Figure 2.5 c) and compared the correlation coefficient of

TDP-43 with nuclear staining DAPI (Figure 2.5 d). However, we detected no mislocalized TDP-43 in TBK1$^{-/-}$ cells compared to the control cells (p=0.7161). Protein blot analysis using subcellular fractionation confirmed that TBK1$^{-/-}$ cells did not show any aberrant TDP-43 localizations (Figure 2.6). Thus, we generated a human stem cell model with loss-of-function mutations of *TBK1* and loss of TBK1 activity-induced p62, but not TDP-43 pathology, in human stem cell models.
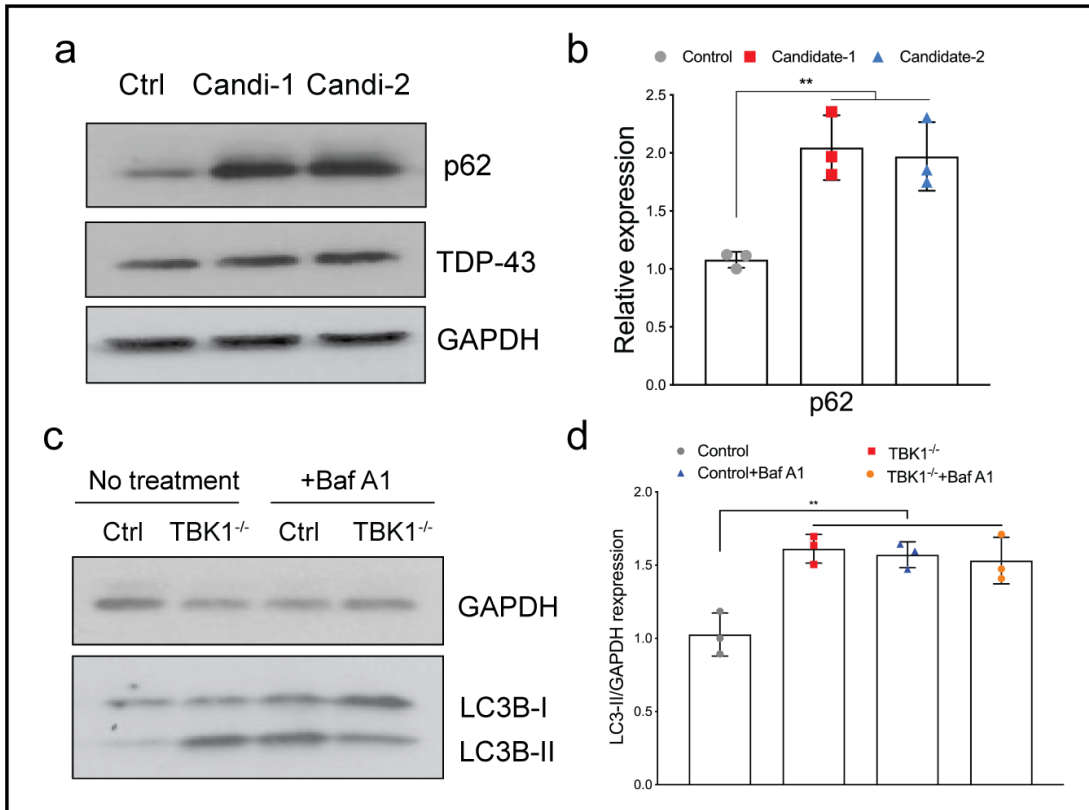

Figure 2.4 Loss of TBK1 leads to impaired autophagic flux.

(a) Validation of P62 and TDP-43 protein expression for two candidate mutant clones by western blot. (b) Quantifications of the protein levels in (a) from 3 independent experiments are shown. (c) Effects of TBK-1 on LC3-II levels and degradation during autophagic maturation. Control and TBK1$^{-/-}$ cells are treated or not treated with bafilomycin A1 (BafA1) to inhibit autophagic degradation of LC3-II. (d) Quantification of LC3-II level is shown from 3 independent experiments. Levels of LC3-II expression are normalized to GAPDH.
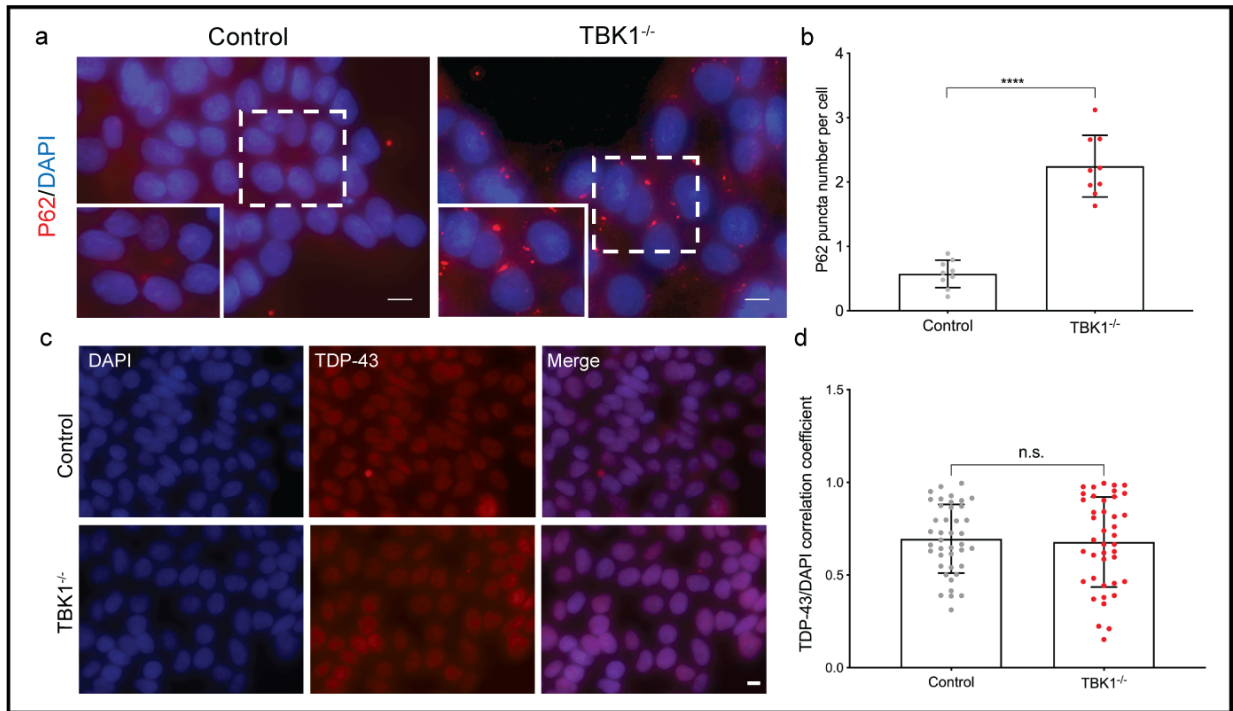
Figure 2.5 Loss of TBK1 leads to p62 accumulations does not affect TDP-43 in hESCs.

(a) Immunostaining of p62 for hESC cultures of control and TBK1$^{-/-}$ cells. Scale bar, 20 μm. (b) Quantifications of p62 puncta numbers are shown. (c) Immunostaining of TDP-43 for hESC cultures of control and TBK1$^{-/-}$ cells. Scale bar, 20 μm. (d) Quantifications of the TDP-43/DAPI correlation coefficient are shown.
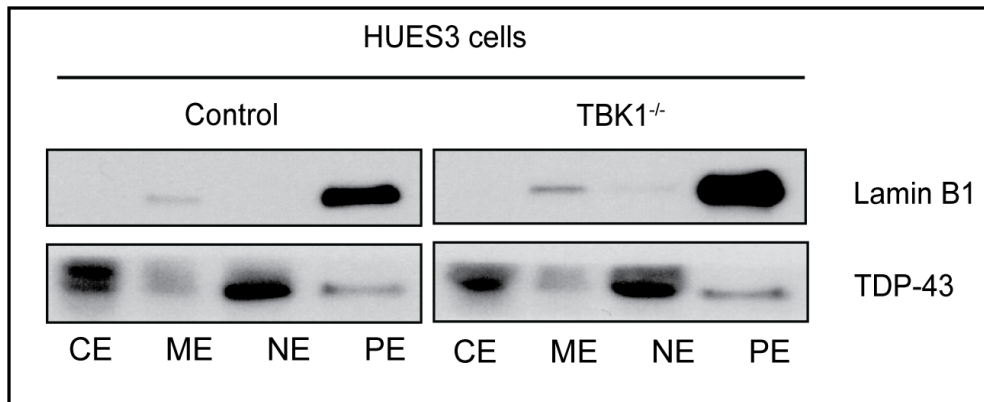

Figure 2.6 Subcellular fractionation of TDP-43 in control and TBK1 mutant hESCs.

Subcellular fractionation analysis of Lamin B1 (pellet control) and TDP-43 levels in different fractions of control and TBK1$^{-/-}$ hESCs. Representative blots show TDP-43 levels in cytosol extract (CE), membrane extract (ME), nuclear extract (NE), and pellet extract (PE).

2.3.2 TBK1 deficiency leads to TDP-43 pathology in human motor neurons

To investigate the functional consequences of TBK1 mutation in human motor neurons, the most ALS-relevant cell type, we differentiated the control and TBK1$^{-/-}$ hESCs transfected by NGN2 into motor neurons using the NGN2 overexpression method adapted from previous protocols (Figure 2.7 a) [29]. Over 90% of cells showed Hb9::GFP positive signals during motor neuron patterning (Figure 2.7 b). To determine the efficiency of motor neuron differentiation in both control and TBK1$^{-/-}$ cells, we used ICC to quantify the percentage of ISL-1 positive cells and found that TBK1 deficiency did not affect the differentiation efficiency (p=0.9757) (Figure 2.8 a,b).
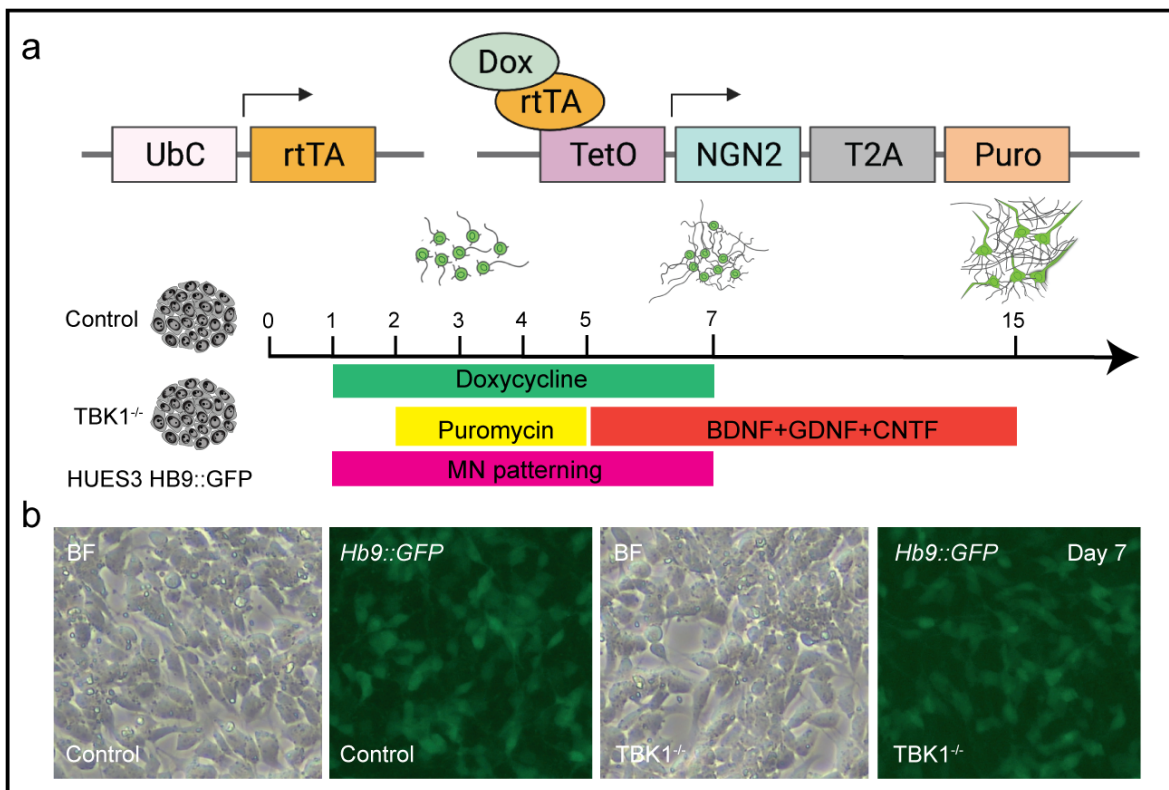

Figure 2.7 Motor neuron differentiation by NGN2 programming.

(a) Design of lentiviral vectors for NGN2-induced motor neuron differentiation through Dox-inducible promotor (TetO) mediated expression. Cells were transduced with the two viruses and selected with puromycin. The induction of motor neuron differentiation was based on NGN2 expression and motor neuron patterning. (b) Representative images showing the Hb9::GFP positive cells in control and TBK1$^{-/-}$ cells on Day 7.
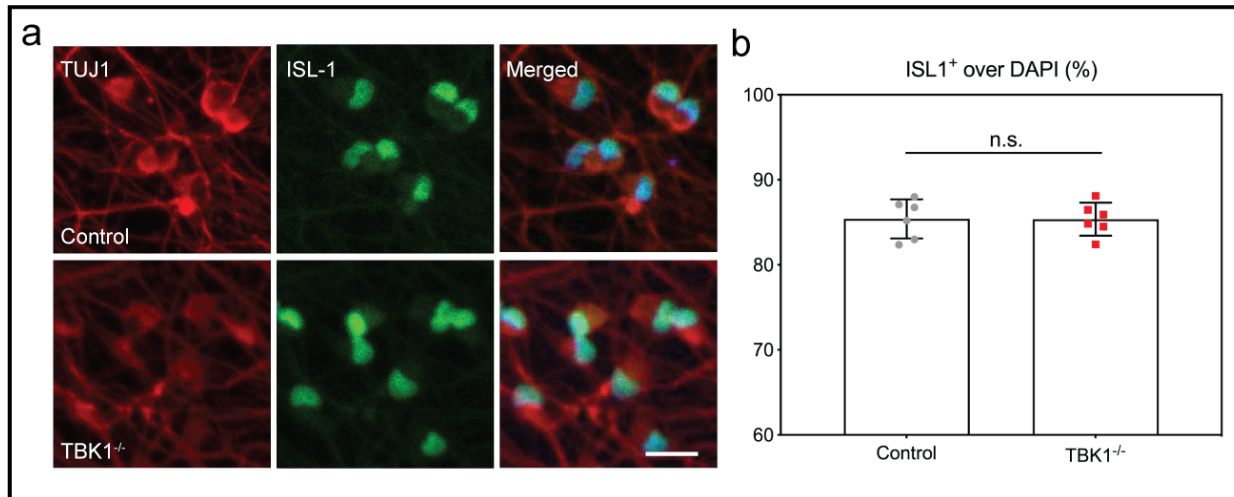
Figure 2.8 Loss of TBK1 has no effects on motor neuron differentiation efficiency.

(a) Immunostaining of motor neuron marker, ISL-1, in control and TBK1$^{-/-}$ cells. All cells are stained by DAPI and neuronal marker TUJ1. Scale bar, 20 μm. (b) Quantifications of the percentage of cells expressing ISL-1 are shown.

To determine whether loss of TBK1 activity in human motor neurons had a similar effect on crucial ALS protein expression as in hESCs, we first performed protein blot analysis to confirm the increased expression of p62 ($p<0.0001$) and TDP-43 (candidate-1: $p=0.9987$, candidate-2: $p=0.7270$) in human motor neurons, which is consistent with the previous result in hESCs (Figure 2.9 a,b). Although TDP-43 pathology was not detected in TBK1$^{-/-}$ hESCs, it is intriguing to investigate this effect in human motor neurons, which have been reported to display TDP-43 proteinopathies in ALS patients with reduced TBK1 expressions [18]. To determine whether TBK1 activity affects TDP-43 homeostasis in human motor neurons, we performed ICC and immunoblot analysis using differentiated human motor neurons on day 7 after plating. Interestingly, TBK1 deficiency in human motor neurons led to increased cytoplasmic localization of TDP-43, a key feature of TDP-43 proteinopathies in ALS/FTD [30,31] (Figure 2.10 a). The correlation coefficient analysis of TDP-43 with nuclear staining DAPI confirmed the decreased overlapping of TDP-43 with the nucleus in TBK1$^{-/-}$ human motor neurons ($p<0.0001$) (Figure 2.10 b). To further determine

the subcellular localization of TDP-43 in TBK1$^{-/-}$ motor neurons, we performed subcellular fractionation followed by immunoblotting (Figure 2.10 c). TDP-43 was primarily localized in the nucleus in the control motor neurons, while loss of TBK1 activity led to a dominant localization of TDP-43 in the pellet fraction (Figure 2.10 d,e). Our results indicate that loss of TBK1 activity is sufficient to cause cytoplasmic TDP-43 and their insoluble accumulations in human motor neurons.
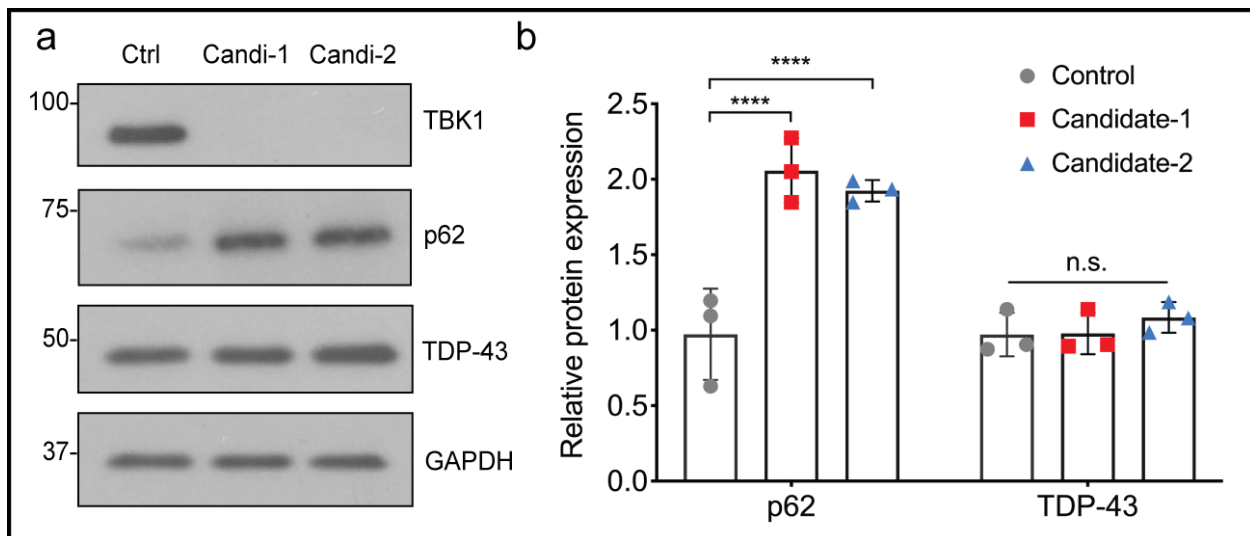

Figure 2.9 Loss of TBK1 causes increased p62, but not TDP-43, in human motor neurons.

(a) Immunoblot analysis of TBK1, P62, and TDP-43 protein expression for two candidate mutant clones. (b) Quantifications of the protein levels from 3 independent experiments are shown. GAPDH was used as an internal control.
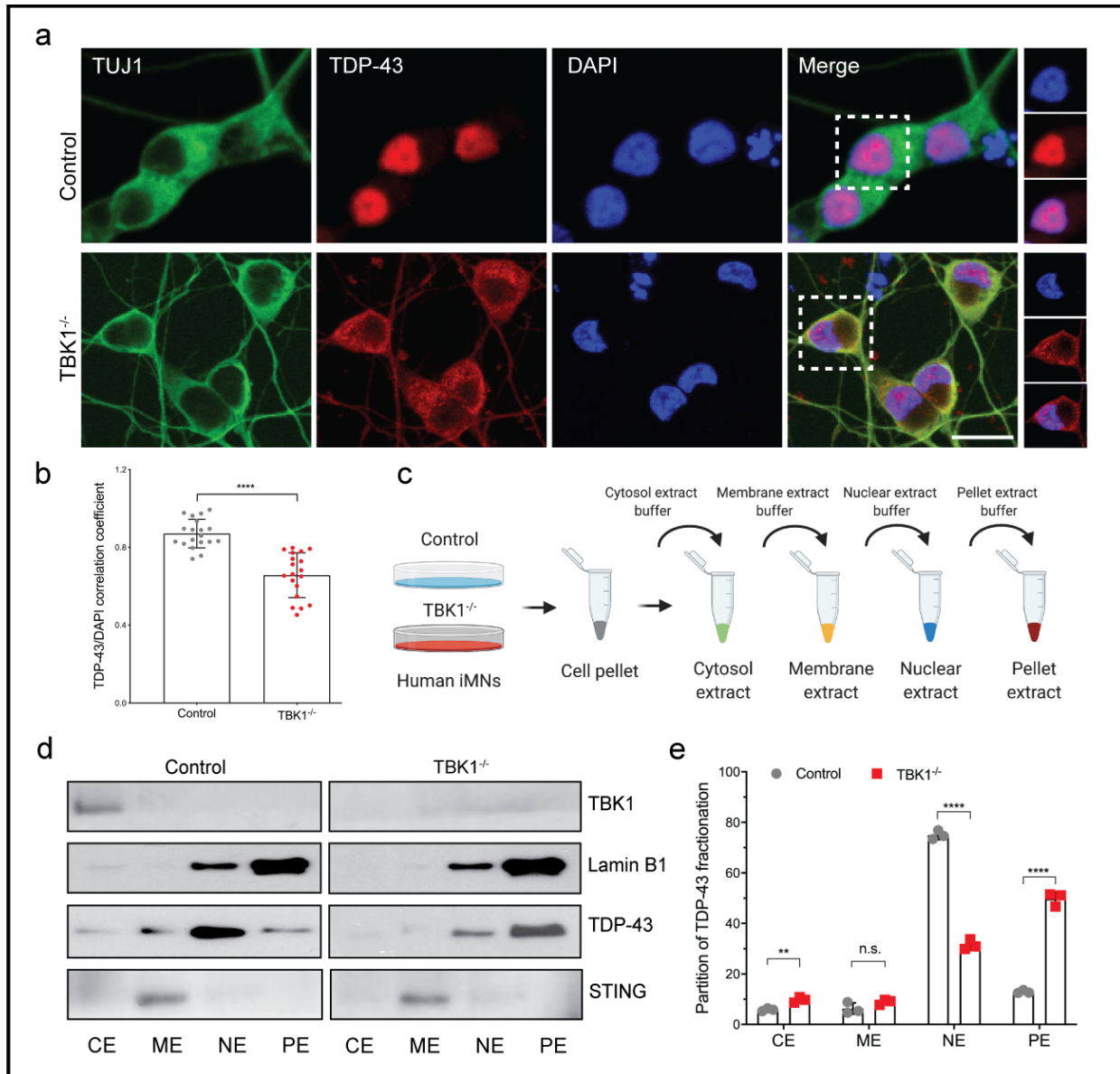
Figure 2.10 TBK1 deficiency leads to mislocalization of TDP-43 and its insoluble accumulations.

(a) Representative images of Day 7 motor neurons for quantification of TDP-43 localization. All cells are stained by DAPI, TDP-43, and neuronal marker TUJ1. Scale bar, 20 μm. (b) Quantifications of the TDP-43/DAPI correlation coefficient from (a) are shown. (c) Schematic of subcellular fractionation experiment for control and TBK1$^{-/-}$ motor neurons. Sequential extracts of cytosol, membrane, nuclear, and pellet fractions are performed. (d) Subcellular fractionation analysis of TBK1 (cytosol control), Lamin B1 (nuclear and pellet control), STING (membrane control), and TDP-43 levels in different fractions of control and TBK1$^{-/-}$ motor neurons. Representative blots show TDP-43 levels in cytosol extract (CE), membrane extract (ME),

nuclear extract (NE), and pellet extract (PE). (e) Quantifications of the partition of TDP-43 in each cellular fraction for control and TBK1$^{-/-}$ human motor neurons are shown.

2.3.3 Loss of TBK1 causes increased neuronal activity and impaired axonal repair in human motor neurons

As loss-of-function mutations of *TBK1* caused TDP-43 proteinopathies in human motor neurons, we proceeded to ask if TBK1$^{-/-}$ could disrupt neuronal homeostatic functions. Survival of control and TBK1$^{-/-}$ human motor neurons was measured on Days 14 and 28 compared to Day 2 (Figure 2.11 a,b). With the culture of human motor neurons, about 60% of control and TBK1$^{-/-}$ neurons survived on Day 14 (p=0.8281), and about 43% of them survived on Day 28 (p=0.9759) (Figure 2.11 c). Therefore, loss of TBK1 activity did not affect human motor neuron survival in culture.

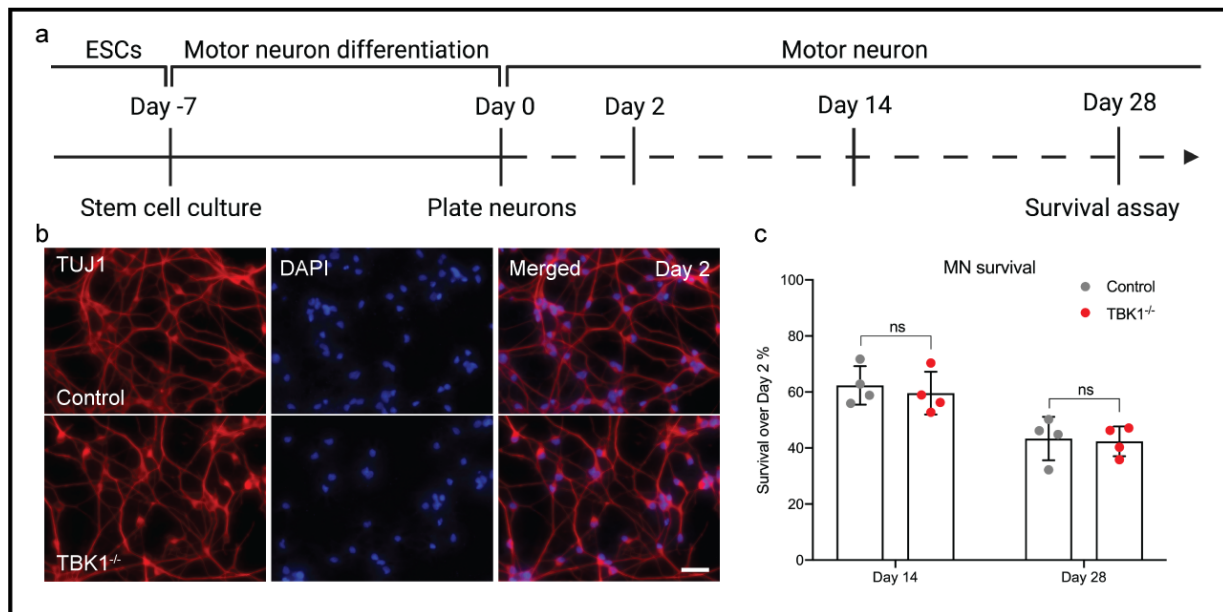**Figure 2.11 Loss of TBK1 does not affect human motor neuron survival in cultures.**

(a) Experimental outline of motor neuron survival assay in human motor neurons. Motor neurons were differentiated and plated on Day 0. Cell survival assay was performed on Day 2, Day 14, and Day 28. (b) Immunostaining of TUJ1 and DAPI in control and TBK1$^{-/-}$ human motor neurons on Day 2 before the survival

assay. (c) The survival rate of control and TBK1$^{-/-}$ human motor neurons on Day 14 and Day 28 compared to Day 2.

Although *TBK1* mutation in human motor neurons did not cause neuronal death, we sought to examine whether loss of TBK1 could lead to early-stage neurodegenerative phenotypes. Physiological analyses had demonstrated alterations in the functional properties of motor neurons at very early stages in transgenic mouse models of ALS. Subsequent studies had revealed pre-symptomatic hyperexcitability in ALS motor neurons [32,33]. Therefore, perturbations of the intrinsic biological properties might lead to abnormal electrophysiological activities of motor neurons, and these activities could reflect and contribute to the earliest events that caused neurodegeneration in ALS motor neurons. To determine if TBK1 ablation in human motor neurons caused any electrophysiological phenotype, we recorded the spontaneous firing of control and TBK1$^{-/-}$ motor neurons using extracellular multielectrode arrays (MEAs) on Day 21 and 28 in culture (Figure 2.12 a,b & Figure 2.13 a). We plated an equal number of Hb9::GFP positive control and TBK1$^{-/-}$ motor neurons and carefully monitored their attachment to the plate throughout the experiments (Figure 2.13 b). After four weeks of culture, the control and TBK1$^{-/-}$ motor showed a similar number of active electrodes on MEA plates (p=0.9585) (Figure 2.12 c). Intriguingly, TBK1$^{-/-}$ motor neurons exhibited a significantly greater number of spikes and a higher spontaneous firing rate (p<0.0001) (Figure 2.13 c). Furthermore, TBK1$^{-/-}$ motor neurons consistently showed increased bursting (p<0.0001) and network bursting frequency (p<0.01) than control motor neurons (Figure 2.13 c). Next, to confirm if the signals detected from TBK1$^{-/-}$ motor neurons were real neuronal signals, we sought to determine if retigabine, a specific activator of subthreshold Kv7 currents, could inhibit the spontaneous firing of TBK1$^{-/-}$ motor neurons. Consistent with our previous report using SOD1 ALS motor neurons [33], retigabine also stopped the spontaneous firing of TBK1$^{-/-}$ motor neurons in a dose-dependent manner (Figure 2.12 d).
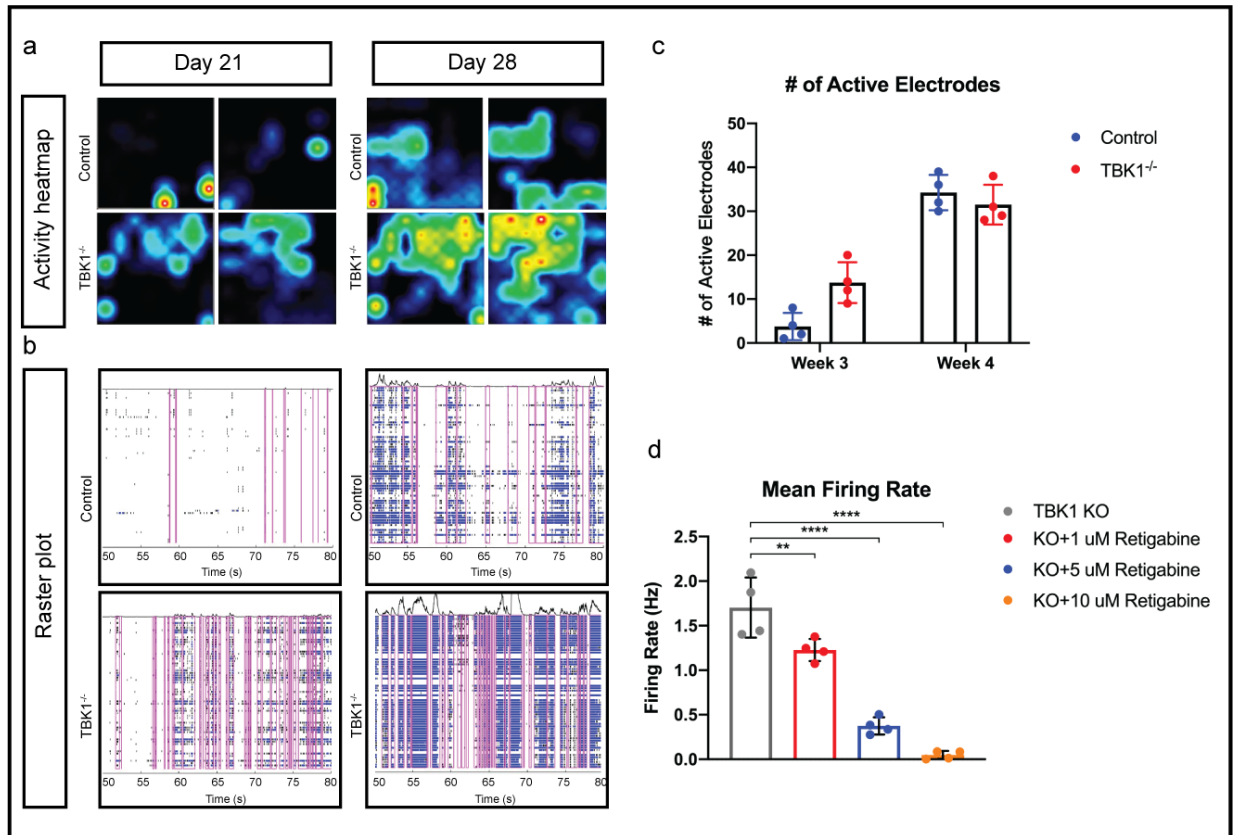
Figure 2.12 The electrophysiological properties of control and TBK1$^{-/-}$ motor neurons.

(a) Heatmaps of spontaneous electrophysiological activity of control and TBK1$^{-/-}$ motor neurons on MEA recorded at the indicated time points. (b) Raster plots of MEA activity across 64 electrodes (rows) in a single well over 30 seconds. Tick marks indicate single spike activity. Blue ticks show bursting events closely spaced. Pink boxes indicate spontaneous synchronous activity across many electrodes. (c) The number of active electrodes in control and TBK1$^{-/-}$ human motor neurons cultured on MEA plates. Analysis was performed at week 3 and week 4. (d) Analysis of MEA recordings for mean firing rate in TBK1$^{-/-}$ human motor neurons treated with different doses of retigabine at week 4.
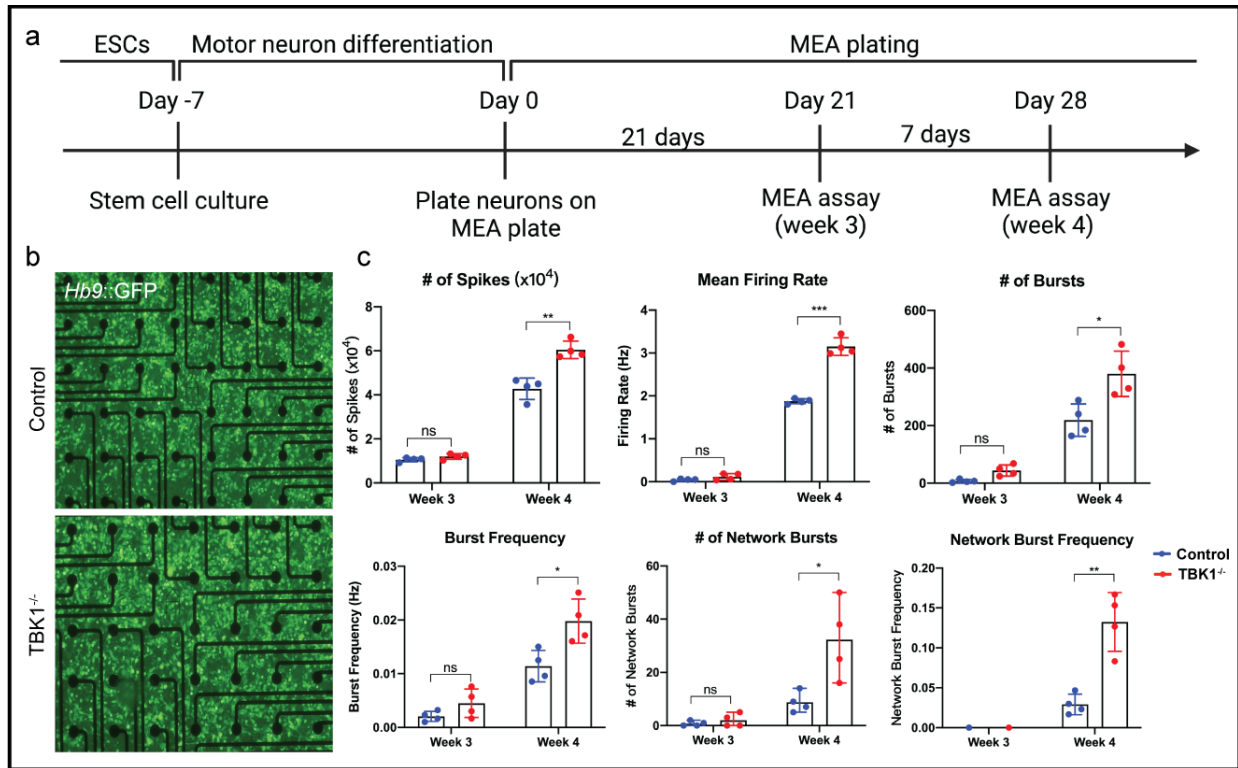
Figure 2.13 TBK1 deficiency leads to increase neuronal firing activity in human motor neurons.

(a) Experimental outline of MEA assay in human motor neurons. Motor neurons are differentiated and replated on MEA plates. Electrophysiological properties of control and TBK1$^{-/-}$ motor neurons are measured on Day 21 and Day 28 after replating. (b) Representative images at ×4 magnification of Hb9::GFP-fluorescing control and TBK1$^{-/-}$ motor neurons plated on MEA wells on day 14 in culture. Scale bar: 400 μm. (c) Analysis of MEA recordings from days 21 to 28 in culture from four independent replicates. TBK1$^{-/-}$ motor neurons show increased spike numbers and mean firing rate compared to control motor neurons, and the number of bursts, network bursts, and burst frequency are elevated.

In addition to hyperexcitability, distal motor axons could often degenerate from the neuromuscular junctions (NMJs) in ALS [34-36]. Therefore, the ability for motor axons to regrow or reconnect to NMJs is also a marker of early-stage ALS phenotype. To determine if loss-of-function mutations of TBK1 impaired motor axonal repair after injury, we seeded human motor neurons in microfluidic devices that allowed motor axons to sprout from the neuronal cell body chamber to a

separate axonal chamber (Figure 2.14 a,b). Motor neurons were plated for seven days on the soma side, and axons sprouted into the axon side through the microchannels of the device (Figure 2.14 b). Motor axons were severed after seven days of culture on the device, and axonal regeneration was measured at 0 hr and 24 hr after the axotomy (Figure 2.14 c). As shown in the 0 hr group, axotomy severed most axons in the axon chamber (Figure 2.14 c middle panel). After 24 hr, while control neurons showed axonal re-growth, TBK1$^{-/-}$ motor neurons showed significantly reduced axonal length after injury (p<0.0001) (Figure 2.14 d). Our results indicated that loss of TBK1 activity caused hyperexcitability and deficient axonal repair in human motor neurons, two key disease phenotypes found in ALS.
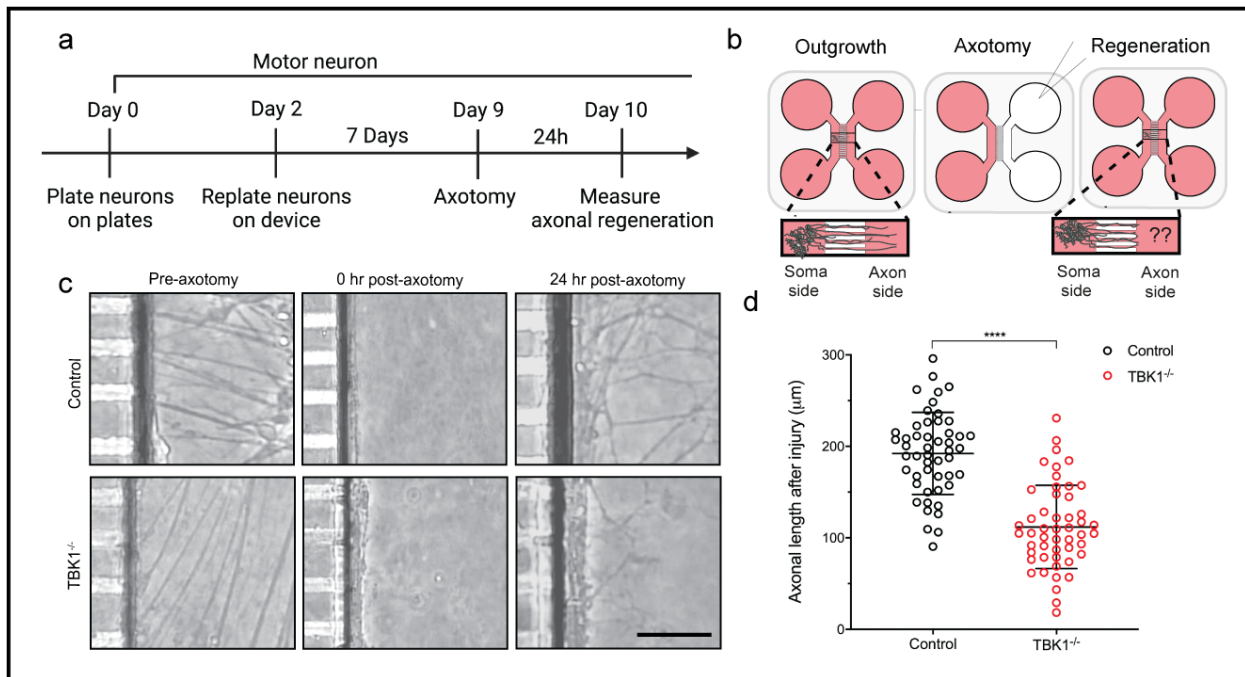
Figure 2.14 Loss of TBK1 leads to impaired axonal repair in human motor neurons.

(a) Experimental outline of axotomy assay in human motor neurons. Control and TBK1$^{-/-}$ motor neurons are plated on the axotomy device. Axotomy is performed on Day 9, and measurement of axonal regrowth is conducted on Day 10. (b) Schematic of axonal regrowth experiment upon injury. The motor neurons are plated on the left chamber (soma side) of the device, and axons sprout into the right chamber (axon side) through the channels connecting both sides. Axotomy is performed by washing out the axon side to cut the

sprouted axons. The ability of axonal repair is measured by the length of re-sprouted axons. (c) Representative images of axonal sprouting in control and TBK1^{-/-} motor neurons from pre- and post-axotomy conditions. Scale bar: 500 μm. (d) Quantifications of axonal regrowth length for control and TBK1^{-/-} motor neurons are shown.

2.4 Discussion and implications

The advance of next-generation sequencing techniques has led to the discovery of multiple new ALS genes [3], and the heterozygous loss-of-function mutations of *TBK1* have been reported to associate with ALS and FTD [4]. However, evaluation of the loss-of-function mutations of *TBK1* is halted by the incomplete understanding of TBK1 related pathology in human motor neurons, which prevents the development of more targeted therapeutics [37].

Here we generated a human stem cell model with homozygous loss-of-function mutations of TBK1. Loss of TBK1 led to aberrant autophagic flux and p62 accumulations, which is consistent with previous study [16]. Intriguingly, TBK1 deficiency was sufficient to cause mislocalization of TDP-43 and its insoluble accumulations, a hallmark found in more than 90% of ALS patients [38-40]. Notably, the TDP-43 pathology was only found in human motor neurons but not in stem cell models, suggesting the cell type-specific role of TBK1 in TDP-43 pathology.

Next, we investigated the functional consequences of loss of TBK1 activity in human motor neurons. In ALS, motor neuron degeneration is the characteristic phenotype that leads to paralysis and death of the patient [41]. However, in differentiated human motor neurons, loss of TBK1 activity did not trigger motor neuron death in culture. This could be explained in several theories. First, TBK1 is an important kinase involved in many biological pathways and events, and homozygous mutations of *TBK1* are embryonic lethal. Therefore, in the cell culture system, ablation of TBK1 could be compensated in many downstream mechanisms. Second, most neurodegeneration diseases are aging-related, meaning that most patients have their disease

onset at the age of 60s [42], suggesting the more critical role of environmental factors in disease onset and progression. Although functional motor neurons could be generated in this way in the cell culture and differentiation system, these motor neurons were not considered sufficiently "mature". Therefore, the TBK1 deficient motor neuron model may not recapitulate the late-stage disease phenotype, like motor neuron death.

Although we did not observe the late-stage disease phenotype in our TBK1 deficiency model, we examined early-stage disease phenotypes implicated in ALS using our model. Previous studies had demonstrated alterations in the functional properties of motor neurons at early stages in transgenic mouse models of ALS and human patients. Subsequent studies had revealed pre-symptomatic hyperexcitability in ALS motor neurons [32,33]. Therefore, loss of TBK1 might trigger aberrant electrophysiological activities of motor neurons, and these activities could reflect and contribute to the earliest events in ALS motor neurons. Our data suggested that TBK1 deficiency increased the neuronal activity, and a Kv7 current activator, retigabine, could reduce such increased activity. The fact that TBK1 deficiency was associated with hyperexcitability in motor neurons indicated the role of TBK1 mutation as an ALS risk factor.

Distal motor axon degeneration was another early-stage disease phenotype in ALS. In fact, the ability for motor axons to regrow and reconnect to NMJs determined disease progression. We found that TBK1 deficient motor neurons showed reduced ability to regrow their axons after injury. In addition, Lys05 treatment also caused reduced axonal regeneration after injury in control hMNs, suggesting that the reduced axonal repair might be a phenotypic consequence of lysosomal dysfunction induced TDP-43 pathology.

In closing, our data suggested that loss of TBK1 in human motor neurons could lead to early-stage disease phenotypes, including hyperexcitability and reduced axonal regeneration. The detailed mechanisms of how the loss of TBK1 contributed to these phenotypes were not discussed in this project. However, previous research suggested that both phenotypes could be

the consequence of TDP-43 pathology, which was found in our TBK1 deficient model. Therefore, our cell model of TBK1 deficiency recapitulated the key disease hallmark of TDP-43 pathology in human motor neurons and caused early-stage disease phenotypes that were relevant to ALS.

2.5 Experimental procedures

Human pluripotent stem cell lines

The HUES3 Hb9::GFP used in this study was previously approved by the institutional review boards of Harvard University. Specific point mutations were confirmed by PCR amplification followed by Sanger sequencing. Our lab screens for mycoplasma contamination weekly using the MycoAlert kit (Lonza), with no cell lines used in this study testing positive. The use of these cells at Harvard was further approved and determined not to constitute Human Subjects Research by the Committee on the Use of Human Subjects in Research at Harvard University.

Cell Culture and differentiation

Pluripotent stem cells were cultured with mTeSR plus medium (Stem Cell Technologies) on Matrigel (BD Biosciences) coated tissue culture dishes. Stem cells were maintained in 5% CO_2 incubators at 37 °C and passaged as small aggregates after 1mM EDTA treatment. After dissociation, 10 µM ROCK inhibitor (Sigma, Y-27632) was added to cell culture for 24 hr to prevent cell death, and then incubated with lentiviruses (FUW-M2rtTA, TetO-Ngn2-Puro). The HUES3 Hb9::GFP cell line has been previously described [43]. Motor neurons were differentiated using a modified protocol based on previous strategies [29,44]. This protocol relies on neural induction through NGN2 programming, SMAD inhibition through small molecules, and motor neuron patterning through retinoic activation and Sonic Hedgehog signaling. In brief, hESCs were dissociated into single cells using accutase (Stem Cell Technologies), and then plated on Matrigel-

coated culture dish at a density of 80,000 cells per cm^2 with mTeSR plus medium (Stem Cell Technologies) supplemented with 10 µM ROCK inhibitors (Sigma, Y-27632). When cells reached confluency, medium was changed to N2 medium (DMEM-F12 (Life Technologies) supplemented with ×1 Gibco GlutaMAX (Life Technologies), ×1 N-2 supplement (Gibco), × 0.3% Glucose) on Day 1-3. For small molecule treatment, 10 µM SB431542 (Custom Synthesis), 100 nM LDN-193189 (Custom Synthesis), 1 µM retinoic acid (Sigma), 1 µM SAG (Custom Synthesis) were added on Day 1-3. For NGN2 induction and neuron selection, 20 mg/ml Doxycycline and 10 mg/ml puromycin were added on Day 2-3. On Day 4-7, the N2 medium was changed to Neurobasal (Neurobasal (Life Technologies) supplemented with ×1 N-2 supplement (Gibco), ×1 B-27 supplement (Gibco), ×1 Gibco GlutaMAX (Life Technologies) and 100 µM non-essential amino-acids: NEAA) along with 1 µM retinoic acid, 1 µM SAG, 20 mg/ml Doxycycline, 10 mg/ml puromycin, and 10 ng/ml of neurotrophic factors: glial cell-derived neurotrophic factor (GDNF), ciliary neurotrophic factor (CNTF) and brain-derived neurotrophic factor (BDNF) (R&D). For post-mitotic cell selection, 10 mM 5-Fluoro-2'-deoxyuridine thymidylate synthase inhibitor (FUDR, Sigma) was added on Day 5-7. From Day 8, media was changed to the motor neuron maintenance media containing Neurobasal (Neurobasal (Life Technologies) supplemented with ×1 N-2 supplement (Gibco), ×1 B-27 supplement (Gibco), ×1 Gibco GlutaMAX (Life Technologies) and 100 µM non-essential amino-acids: NEAA) supplemented with 10 ng/ml of neurotrophic factors (GDNF, CNTF, and BDNF) and 10 mM FUDR. Half of the maintenance media was changed every two days.

Cell viability assay

Motor neuron viability assay was performed based on the CellTiter-Glo luminescent for each sample according to the manufacturer's recommendations (Promega G7570). In brief, motor neurons were plated in triplicate onto 96-well plates. After treatment incubation, motor neurons were incubated for 10 min with CellTiter-Glo reagent at room temperature, and luminescence was

measured using the Cytation imaging reader (BioTek). Background luminescence was measured using medium without cells and then subtracted from experimental values.

CRISPR/Cas9 genome editing

TBK1 mutant cell lines were generated using CRISPR/Cas9-mediated genome editing as previously described [45,46]. To generate loss-of-function alleles of TBK1, control hESCs were transfected with guide RNAs targeting the desired location of human TBK1 gene. TBK1 gRNAs were designed using a web tool: CHOPCHOP (https://chopchop.rc.fas.harvard.edu) [47]. Guides were cloned into a vector with the human U6 promotor (custom synthesis, Broad Institute), with a BbsI cleavage site. The modified TBK1 gRNA sequences were used for Cas9 nuclease genome editing guide 1: 5'-CACCG CAAGAATATACTAATGAGGT-3', guide 2: 5'-CACCGATATCAAGAATATACTAATG-3'. After annealing and ligation, vectors were cloned in OneShot Top10 (ThermoFisher Scientific) cells and isolated using Qiagen MIDI-prep kit (Qiagen). After verification by sequencing, 1 μg of each vector containing the guide and 1.5 μg of the pSpCas9n(BB)−2A-Puro (PX462) V2.0 (Addgene) were added to cells for transfection using the Neon Transfection System (ThermoFisher Scientific). Colonies were picked on day 10 after transfection and genotyped by PCR amplification and sequencing. The TBK1 amplification and sequencing primers used were as followed: TBK1_Forward: 5' GTCAGAAGAATGGATAAGGTGAG 3', TBK1_Reverse: 5' CAGATCTGACATCAAGTGTTACAG 3', and TBK1_Sequencing: 5' ATGCTTCACTAGACTGCATATC 3'. Loss-of-function mutations of TBK1 were further confirmed using immunoblot analysis.

Immunocytochemistry and imaging

For immunocytochemistry, cells were fixed with 4% PFA for 20 min, and were subject to permeabilization with 0.25% Triton-X in PBS for 40 min. After that, cells were blocked using 10% donkey serum supplemented with 0.1% Triton-X in PBS (blocking buffer) for 1 hr at room

temperature. Primary antibody diluted in blocking buffer was used for cell incubation overnight at 4 °C. At least three washes (5 min incubation each) with PBS were carried out, before incubating the cells with secondary antibodies (diluted in blocking buffer) for 1 hr at room temperature. Nuclei was stained with DAPI. The following antibodies were used in this study: TBK1 (1:200, Abcam ab109735), SQSTM1 / p62 (1:200, Abcam ab56416), TDP-43 (1:200, Proteintech Group 10782 & Cell Signaling Technology 3448S), Islet1 (1:500, Abcam ab20670), TUJ1 (1:1,000, R&D Systems MAB NL493), Secondary antibodies used (488, 555, and 647) were AlexaFluor (1:1,000, Life Technologies). Images were acquired using a Zeiss LSM 880 confocal microscope or a Nikon Eclipse Ti microscope. Images were analyzed using ImageJ or NIS- Elements (Nikon).

Western blot assays

For protein extraction, cells were lysed using 1% SDS lysis buffer (PhosphoSolutions, 100-LYS) with a brief sonication. For insoluble protein extraction, cells were lysed using RIPA buffer (Life Technology, 89900) with protease inhibitors (Life Technology, 78425) for 20 min on ice. After centrifuge, the supernatant was collected as soluble fraction, and the insoluble fraction was collected from the pellet using 8M urea with 4% CHAPS, 40 mM Tris, and 0.2% Bio-Lyte 3/10 ampholyte (Bio-Rad, 1632103). For subcellular fractionation, cells were subject to sequential extract using the subcellular fractionation kit for cultured cell (Thermo Scientific, 78840) according to manufacturer instructions. After sample preparation, equivalent amount of 5-10 µg protein from each ample were subjected to electrophoresis using 4–20% SDS-PAGE (Bio-Rad, 4561096) and then transferred to a PVDF membrane (Thermo Fisher, 88518). The membrane was blocked with 3% Bovine Serum Albumin (Sigma, A9647) for 1 hr at room temperature, and incubated with primary antibodies overnight at 4°C. The next day, membrane was washed in TBST X3, 10 min each, and then incubated with HRP-conjugated secondary antibodies for 1 hr at room temperature. After that, membrane was washed in TBST X3, 10 min each, and then developed using ECL Western Blotting Detection System (VWR, 95038) and blotting films (Genesee Scientific, 30-810).

TDP-43 localization assay

For analysis of correlation coefficient of TDP-43 and nuclei, motor neurons were stained for TDP-43 (Cell Signaling Technology), TUJ1 (R&D Systems), and counterstained with DAPI. TUJ1 staining was used to determine the neuronal cell body, and the Pearson's correlation coefficient was calculated using NIS-Elements (Nikon) for TDP-43 and DAPI with at least 50 neurons being analyzed. Cells were segmented into the nuclear (DAPI positive) and cytoplasmic (DAPI negative) regions by NIS. The TDP-43 intensity in these two regions were used to determine the nuclear to cytoplasmic ratio (correlation coefficient) for TDP-43 fluorescent intensity.

Multi-electrode array (MEA) recordings

Recordings from 64 extracellular electrodes were made using a Maestro (Axion BioSystems) MEA recording amplifier with a head stage that maintained a temperature of 37 °C. In brief, 12-well MEA plates (Axion Biosystems, M768-GL1-30Pt200) were coated with PDL and laminin. Motor neurons were seeded at a density of 500,000 cells per well and were fed with the motor neuron maintenance media supplemented with 10 ng/ml of neurotrophic factors (GDNF, CNTF, and BDNF) 2-3 times per week. Neuronal activity was measured weekly for 5 min using the Maestro 12-well 64 electrodes per well micro-electrode array (MEA) plate system (Axion Biosystems, Atlanta, GA). Data were sampled at 12.5 kHz, digitized, and analyzed using the Axion Integrated Studio software (Axion Biosystems) with a 200 Hz high pass and 2.5 kHz low pass filter and an adaptive spike detection threshold set at 5.5 times the SD for each electrode with 1 s binning. For each data point presented, four replicates were used for one experiment with 5 minutes recording. These standard settings were maintained for all Axion MEA recording and analysis. We confirmed that we obtained similar results across a wide range of action potential threshold and cluster similarity radius settings. Data was analyzed using the Axion Integrated Studio 2.4.2 and the Neural Metric Tool (Axion Biosystems). For retigabine dose-response experiment, 1 min of recording in each concentration of retigabine were performed. Mean firing

rate were detected using the Axion Integrated Studio 2.4.2 with the default settings and analyzed with the Neural Metric Tool.

Axotomy

Standard neuron microfluidic devices (SND150, XONA Microfluidics) were mounted on glass coverslips coated with 0.1 mg/ml poly-L-ornithine (Sigma-Aldrich) and 5 µg/ml laminin (Invitrogen). Motor neurons were cultured on the devices at a concentration of around 250,000 cells per device for 7 days. Axotomy was performed by repeated vacuum aspiration and reperfusion using PBS in the axonal side of the device until all axons were diminished without disturbing the soma side cells. For the experiment, two independent replicates were performed with at least 20 neurites measured.

Data presentation and statistical analysis.

Comparisons were made between control and TBK1$^{-/-}$ motor neurons using t tests (two-tailed, unpaired)/ANOVA for continuous data and rank tests for nonparametric data. For multiple comparisons, one-way ANOVA to normalize variance and post hoc Tukey tests were used. In all figure elements, bars and lines represent the median with error bars representing standard deviation. The box and whisker plots display the minimum to maximum. Data distribution was assumed to be normal, but this was not formally tested. Significance was assumed at $P < 0.05$. Error bars represent the SD unless otherwise stated. Analysis was performed with the statistical software package Prism 8 (Graph Pad).

References:

1   Rowland, L. P. & Shneider, N. A. Amyotrophic lateral sclerosis. *N Engl J Med* **344**, 1688-1700, doi:10.1056/NEJM200105313442207 (2001).

2   Brown, R. H. & Al-Chalabi, A. Amyotrophic Lateral Sclerosis. *N Engl J Med* **377**, 162-172,

doi:10.1056/NEJMra1603471 (2017).

3   Cirulli, E. T. *et al.* Exome sequencing in amyotrophic lateral sclerosis identifies risk genes and pathways. *Science* **347**, 1436-1441, doi:10.1126/science.aaa3650 (2015).

4   Freischmidt, A. *et al.* Haploinsufficiency of TBK1 causes familial ALS and fronto-temporal dementia. *Nat Neurosci* **18**, 631-636, doi:10.1038/nn.4000 (2015).

5   Gijselinck, I. *et al.* Loss of TBK1 is a frequent cause of frontotemporal dementia in a Belgian cohort. *Neurology* **85**, 2116-2125, doi:10.1212/WNL.0000000000002220 (2015).

6   Le Ber, I. *et al.* TBK1 mutation frequencies in French frontotemporal dementia and amyotrophic lateral sclerosis cohorts. *Neurobiol Aging* **36**, 3116 e3115-3116 e3118, doi:10.1016/j.neurobiolaging.2015.08.009 (2015).

7   Pottier, C. *et al.* Whole-genome sequencing reveals important role for TBK1 and OPTN mutations in frontotemporal lobar degeneration without motor neuron disease. *Acta Neuropathol* **130**, 77-92, doi:10.1007/s00401-015-1436-x (2015).

8   Williams, K. L. *et al.* Novel TBK1 truncating mutation in a familial amyotrophic lateral sclerosis patient of Chinese origin. *Neurobiol Aging* **36**, 3334 e3331-3334 e3335, doi:10.1016/j.neurobiolaging.2015.08.013 (2015).

9   Tsai, P. C. *et al.* Mutational analysis of TBK1 in Taiwanese patients with amyotrophic lateral sclerosis. *Neurobiol Aging* **40**, 191 e111-191 e116, doi:10.1016/j.neurobiolaging.2015.12.022 (2016).

10   Yu, T. *et al.* The pivotal role of TBK1 in inflammatory responses mediated by macrophages. *Mediators Inflamm* **2012**, 979105, doi:10.1155/2012/979105 (2012).

11   Weidberg, H. & Elazar, Z. TBK1 mediates crosstalk between the innate immune response and autophagy. *Sci Signal* **4**, pe39, doi:10.1126/scisignal.2002355 (2011).

12   Chen, W. *et al.* TBK1 Promote Bladder Cancer Cell Proliferation and Migration via Akt Signaling. *J Cancer* **8**, 1892-1899, doi:10.7150/jca.17638 (2017).

13   Xu, D. *et al.* TBK1 Suppresses RIPK1-Driven Apoptosis and Inflammation during

Development and in Aging. *Cell* **174**, 1477-1491 e1419, doi:10.1016/j.cell.2018.07.041 (2018).

14   Gerbino, V. *et al.* The Loss of TBK1 Kinase Activity in Motor Neurons or in All Cell Types Differentially Impacts ALS Disease Progression in SOD1 Mice. *Neuron* **106**, 789-805 e785, doi:10.1016/j.neuron.2020.03.005 (2020).

15   Brenner, D. *et al.* Heterozygous Tbk1 loss has opposing effects in early and late stages of ALS in mice. *J Exp Med* **216**, 267-278, doi:10.1084/jem.20180729 (2019).

16   Catanese, A. *et al.* Retinoic acid worsens ATG10-dependent autophagy impairment in TBK1-mutant hiPSC-derived motoneurons through SQSTM1/p62 accumulation. *Autophagy* **15**, 1719-1737, doi:10.1080/15548627.2019.1589257 (2019).

17   Nguyen, D. K. H., Thombre, R. & Wang, J. Autophagy as a common pathway in amyotrophic lateral sclerosis. *Neurosci Lett* **697**, 34-48, doi:10.1016/j.neulet.2018.04.006 (2019).

18   Van Mossevelde, S. *et al.* Clinical features of TBK1 carriers compared with C9orf72, GRN and non-mutation carriers in a Belgian cohort. *Brain* **139**, 452-467, doi:10.1093/brain/awv358 (2016).

19   Larabi, A. *et al.* Crystal structure and mechanism of activation of TANK-binding kinase 1. *Cell Rep* **3**, 734-746, doi:10.1016/j.celrep.2013.01.034 (2013).

20   Tu, D. *et al.* Structure and ubiquitination-dependent activation of TANK-binding kinase 1. *Cell Rep* **3**, 747-758, doi:10.1016/j.celrep.2013.01.033 (2013).

21   Ma, X. *et al.* Molecular basis of Tank-binding kinase 1 activation by transautophosphorylation. *Proc Natl Acad Sci U S A* **109**, 9378-9383, doi:10.1073/pnas.1121552109 (2012).

22   Shu, C. *et al.* Structural insights into the functions of TBK1 in innate antimicrobial immunity. *Structure* **21**, 1137-1148, doi:10.1016/j.str.2013.04.025 (2013).

23   Xu, G. *et al.* Crystal structure of inhibitor of kappaB kinase beta. *Nature* **472**, 325-330, doi:10.1038/nature09853 (2011).

24   Ye, J. *et al.* Effects of ALS-associated TANK binding kinase 1 mutations on protein-protein

interactions and kinase activity. *Proc Natl Acad Sci U S A* **116**, 24517-24526, doi:10.1073/pnas.1915732116 (2019).

25   Di Giorgio, F. P., Boulting, G. L., Bobrowicz, S. & Eggan, K. C. Human embryonic stem cell-derived motor neurons are sensitive to the toxic effect of glial cells carrying an ALS-causing mutation. *Cell Stem Cell* **3**, 637-648, doi:10.1016/j.stem.2008.09.017 (2008).

26   Oakes, J. A., Davies, M. C. & Collins, M. O. TBK1: a new player in ALS linking autophagy and neuroinflammation. *Mol Brain* **10**, 5, doi:10.1186/s13041-017-0287-x (2017).

27   Pilli, M. *et al.* TBK-1 promotes autophagy-mediated antimicrobial defense by controlling autophagosome maturation. *Immunity* **37**, 223-234, doi:10.1016/j.immuni.2012.04.015 (2012).

28   Mizuno, Y. *et al.* Immunoreactivities of p62, an ubiqutin-binding protein, in the spinal anterior horn cells of patients with amyotrophic lateral sclerosis. *J Neurol Sci* **249**, 13-18, doi:10.1016/j.jns.2006.05.060 (2006).

29   Nehme, R. *et al.* Combining NGN2 Programming with Developmental Patterning Generates Human Excitatory Neurons with NMDAR-Mediated Synaptic Transmission. *Cell Rep* **23**, 2509-2523, doi:10.1016/j.celrep.2018.04.066 (2018).

30   Suk, T. R. & Rousseaux, M. W. C. The role of TDP-43 mislocalization in amyotrophic lateral sclerosis. *Mol Neurodegener* **15**, 45, doi:10.1186/s13024-020-00397-1 (2020).

31   Barmada, S. J. *et al.* Cytoplasmic mislocalization of TDP-43 is toxic to neurons and enhanced by a mutation associated with familial amyotrophic lateral sclerosis. *J Neurosci* **30**, 639-649, doi:10.1523/JNEUROSCI.4988-09.2010 (2010).

32   Zona, C., Pieri, M. & Carunchio, I. Voltage-dependent sodium channels in spinal cord motor neurons display rapid recovery from fast inactivation in a mouse model of amyotrophic lateral sclerosis. *J Neurophysiol* **96**, 3314-3322, doi:10.1152/jn.00566.2006 (2006).

33   Wainger, B. J. *et al.* Intrinsic membrane hyperexcitability of amyotrophic lateral sclerosis patient-derived motor neurons. *Cell Rep* **7**, 1-11, doi:10.1016/j.celrep.2014.03.019 (2014).

34   Jawhar, S., Trawicka, A., Jenneckens, C., Bayer, T. A. & Wirths, O. Motor deficits, neuron

loss, and reduced anxiety coinciding with axonal degeneration and intraneuronal Abeta aggregation in the 5XFAD mouse model of Alzheimer's disease. *Neurobiol Aging* **33**, 196 e129-140, doi:10.1016/j.neurobiolaging.2010.05.027 (2012).

35   Fischer, L. R. & Glass, J. D. Axonal degeneration in motor neuron disease. *Neurodegener Dis* **4**, 431-442, doi:10.1159/000107704 (2007).

36   Carrasco, D. I., Rich, M. M., Wang, Q., Cope, T. C. & Pinter, M. J. Activity-driven synaptic and axonal degeneration in canine motor neuron disease. *J Neurophysiol* **92**, 1175-1181, doi:10.1152/jn.00157.2004 (2004).

37   Freischmidt, A., Muller, K., Ludolph, A. C., Weishaupt, J. H. & Andersen, P. M. Association of Mutations in TBK1 With Sporadic and Familial Amyotrophic Lateral Sclerosis and Frontotemporal Dementia. *JAMA Neurol* **74**, 110-113, doi:10.1001/jamaneurol.2016.3712 (2017).

38   Neumann, M. *et al.* Ubiquitinated TDP-43 in frontotemporal lobar degeneration and amyotrophic lateral sclerosis. *Science* **314**, 130-133, doi:10.1126/science.1134108 (2006).

39   Mackenzie, I. R. *et al.* Pathological TDP-43 distinguishes sporadic amyotrophic lateral sclerosis from amyotrophic lateral sclerosis with SOD1 mutations. *Ann Neurol* **61**, 427-434, doi:10.1002/ana.21147 (2007).

40   Jo, M. *et al.* The role of TDP-43 propagation in neurodegenerative diseases: integrating insights from clinical and experimental studies. *Exp Mol Med* **52**, 1652-1662, doi:10.1038/s12276-020-00513-7 (2020).

41   Ragagnin, A. M. G., Shadfar, S., Vidal, M., Jamali, M. S. & Atkin, J. D. Motor Neuron Susceptibility in ALS/FTD. *Front Neurosci* **13**, 532, doi:10.3389/fnins.2019.00532 (2019).

42   Hou, Y. *et al.* Ageing as a risk factor for neurodegenerative disease. *Nat Rev Neurol* **15**, 565-581, doi:10.1038/s41582-019-0244-7 (2019).

43   Han, S. S., Williams, L. A. & Eggan, K. C. Constructing and deconstructing stem cell models of neurological disease. *Neuron* **70**, 626-644, doi:10.1016/j.neuron.2011.05.003 (2011).

44   Amoroso, M. W. *et al.* Accelerated high-yield generation of limb-innervating motor neurons

from human stem cells. *J Neurosci* **33**, 574-586, doi:10.1523/JNEUROSCI.0906-12.2013 (2013).

45   Cong, L. & Zhang, F. Genome engineering using CRISPR-Cas9 system. *Methods Mol Biol* **1239**, 197-217, doi:10.1007/978-1-4939-1862-1_10 (2015).

46   Klim, J. R. *et al.* ALS-implicated protein TDP-43 sustains levels of STMN2, a mediator of motor neuron growth and repair. *Nat Neurosci* **22**, 167-179, doi:10.1038/s41593-018-0300-4 (2019).

47   Labun, K., Montague, T. G., Gagnon, J. A., Thyme, S. B. & Valen, E. CHOPCHOP v2: a web tool for the next generation of CRISPR genome engineering. *Nucleic Acids Res* **44**, W272-276, doi:10.1093/nar/gkw398 (2016).

CHAPTER 3: Exploring the mechanisms of TDP-43 pathology induced by loss of TBK1 activity in human motor neurons

3.1 Abstract

In the previous chapter, we successfully generated the human stem cell model of TBK1 deficiency. When induced into motor neurons, TBK1 deficiency leads to mislocalization of TDP-43 and its insoluble accumulations and impaired physiological functionalities. However, the mechanism of the TDP-43 pathology induced by loss of TBK1 activity remains elusive. One intriguing hypothesis is that TBK1 is a crucial regulator of autophagy activity, which plays an important role in ALS progression. In this chapter, we first blocked autophagy induction by knocking down ATG7 by shRNA, and we found that blocking autophagosome formation failed to induce TDP-43 pathology in human motor neurons. To explore the downstream mechanism of TBK1 deficiency, we performed phospho-proteomics to identify impaired pathways by their phosphorylation state. Interestingly, the phosphorylation of proteins involved in endosomal trafficking was reduced when TBK1 was deficient in human motor neurons. Endosomal trafficking is an intriguing pathway for protein degradation, and the activity of the endo-lysosomal pathway was significantly inhibited in TBK1 deficient motor neurons. Therefore, we hypothesized that impaired endo-lysosomal activity could be the primary cause of TDP-43 pathology in TBK1 deficient cells. To test our hypothesis, we used lysosomal inhibitors, Lys05, to block the lysosomal acidification. Lys05 treatment increased insoluble TDP-43 accumulations, suggesting the critical role of lysosomal activity in TDP-43 aggregate degradation.

3.2 Introduction

Like other neurodegenerative diseases, a key hallmark of ALS is the mislocalization of proteins and their cytoplasmic aggregates in affected cells, suggesting the defective machinery of protein quality control [1]. In eukaryotic cells, there are two major protein degradation systems: the autophagy-lysosome pathway and the ubiquitin proteasome system (UPS). The UPS is the major proteolytic pathway that degrades short-lived, soluble proteins, while autophagy mediates the degradation of relatively long-lived, cytoplasmic misfolded proteins [2].

In ALS, a key pathological hallmark is the misfolded cytoplasmic proteins and the accumulations of insoluble protein aggregates in motor neurons and surrounding cells [3,4]. These insoluble protein aggregates are naturally formed by misfolded proteins in the cells with aberrant conformations. Under normal conditions, this process is a physiological phenomenon with cells employing the protein quality control systems to either clear the formed aggregated or degrade the misfolded proteins at the early stage to avoid aggregate formation. In pathological conditions, like diseased neurons, the persistence of protein aggregates indicates the impaired mechanisms of misfolded protein turnover and clearance. These protein aggregates may contribute to cytotoxicity by two mechanisms: 1) disrupting cellular functions by sequestering normal proteins within aggregates, and 2) triggering aberrant interactions between proteins. As the abnormal protein aggregates are a hallmark of ALS, suggesting that disruption of autophagy is essential in ALS pathology [5].

The physiological autophagy process consists of several critical steps. In response to the signaling of ULK1-ATG13-FIP200 phosphorylation, autophagy begins with the formation of immature membrane structures called phagophores [6]. This process can be inhibited by mTORC1, which can, in turn, be inhibited by AMPK [7,8]. The phosphorylation of the ULK1 complex mediates the movement of beclin1 and PI3K CIII complex towards the phagophores, which induces the elongation of the phagophore membrane as a double-membrane structure and the engulfment of

proteins for degradation. The formation of these double-membrane structures, named autophagosomes, is mediated by two interlinked control systems: the LC3 1A/1B system and the Atg5-Atg12 conjugation system [9,10]. The autophagosome is transported along microtubules to a lysosome-rich area, followed by maturation and fusion with the lysosome for degradation [5].

TBK1 is a key mediator of autophagy involved in phosphorylating several autophagy adaptors, including p62, OPTN, and NDP52 [11], increasing their ability to bind to LC3-II and ubiquitinated cargoes [7]. Several TBK1 mutations have been found with decreased mRNA and protein levels, which may lead to reduced autophagy adaptor activation. The reduced activity of autophagy adaptors can trigger impaired autophagy activity and accumulations of protein aggregates. TBK1 has also been implicated in autophagosome maturation [12], which requires the transport of autophagosomes to lysosomes through the action of the motor protein dynein [13]. TBK1 has been found to regulate microtubule dynamics and the level of cytoplasmic dynein [14]. Therefore, loss of TBK1 could contribute to ALS by impaired autophagosomal maturation due to microtubule transport disruption. Previous studies have shown that ALS patients carrying a *TBK1* mutation show both TDP-43 positive and p62 positive inclusions in the cortex [15]. These findings with p62 and ubiquitin-positive inclusions suggest that *TBK1* mutations may contribute to ALS through impaired autophagy mechanisms. However, which detailed mechanism in autophagy contributes to TDP-43 pathology in human motor neurons remains unknown. In this chapter, we used our TBK1 loss-of-function model to identify the specific downstream mechanism that contributed to TDP-43 pathology. In addition, we compared our TBK1 model with the shATG7 model to specify which autophagy mechanism was the primary contributor to disease pathology, which was therapeutically beneficial and could guide future clinical trials.

3.3 Results

3.3.1 Impaired autophagosome formation fails to induce TDP-43 pathology

As shown in Chapter 1, loss-of-function mutations of TBK1 caused impaired autophagic flux, and the autophagy pathways were considered a key mechanism for ALS progression. To investigate if loss of TBK1 contributed to pathological TDP-43 accumulations through the autophagy induction pathway, we compromised autophagy and measured the amount of insoluble TDP-43 accumulation in human motor neurons. Specifically, we treated motor neurons with DMSO (vehicle control) or 100 nM Baf A1 for 24 hr (Figure 3.1 a). The treatment of Baf A1 did not significantly affect the amount of soluble and insoluble TDP-43 in control motor neurons (Figure 3.1 b,c), indicating that insoluble TDP-43 accumulation was not initiated by autophagosome formation. By contrast, TBK1$^{-/-}$ motor neurons accumulated about 2-fold more insoluble TDP-43 ($p<0.0001$) (Figure 3.1 b,c). In addition, when we compromised the proteasome activity proteasome inhibitor MG132, fractions of soluble TDP-43 were reduced in control human motor neurons ($p=0.03$), while insoluble forms of TDP-43 were not substantially altered in both control and TBK1$^{-/-}$ motor neurons ($p>0.99$) (Figure 3.2 a,b).
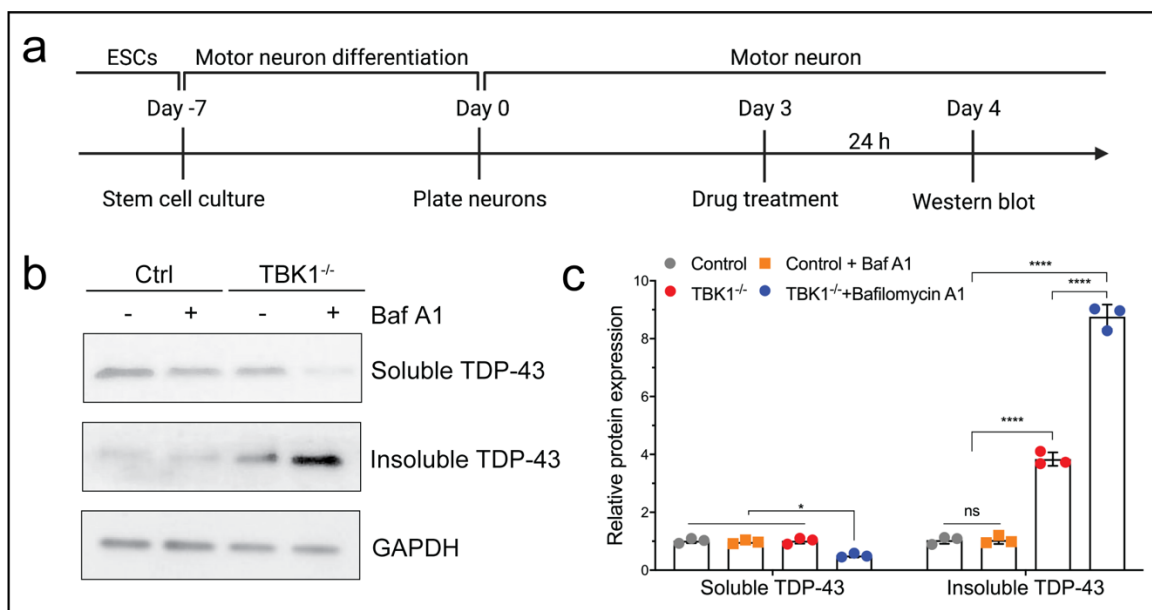
Figure 3.1 Baf A1 fails to induce insoluble TDP-43 accumulations.

(a) Experimental outline of western blot analysis for insoluble TDP-43. Control and TBK1$^{-/-}$ motor neurons are treated with DMSO or 100 nM Baf A1 for 24 hr on Day 3. Western blot analysis is performed on Day 4. (b) Western blot analysis of control and TBK1$^{-/-}$ motor neurons treated with DMSO or Baf A1. Accumulations of TDP-43 proteins are shown in the soluble (RIPA) and insoluble (urea) fractions. (c) Quantification of TDP-43 expression between DMSO and Baf A1 treated human motor neurons. GAPDH in the soluble fraction is used as the loading control for normalization.
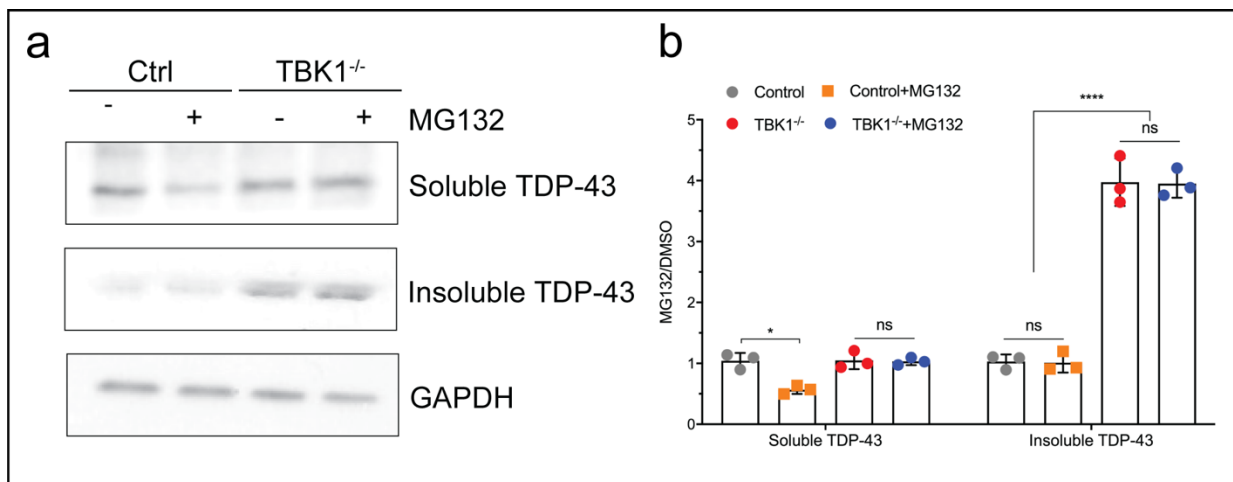

Figure 3.2 Proteasome inhibition fails to induce insoluble TDP-43 accumulations.

(a) Western blot analysis of control and TBK1$^{-/-}$ motor neurons treated with DMSO or MG132. Accumulations of TDP-43 proteins are shown in the soluble (RIPA) and insoluble (urea) fractions. (b) Quantification of TDP-43 expression between DMSO and MG132 treated human motor neurons was shown. GAPDH in the soluble fraction is used as the loading control for normalization.

Next, to evaluate if the increased level of insoluble TDP-43 affected the survival of control and TBK1$^{-/-}$ motor neurons, Day 2 motor neurons were treated with different concentrations of MG132 or Baf A1 for 48 hr for subsequent survival assay (Figure 3.3 a). Compared to control motor neurons, treatment of MG132 did not affect the survival of TBK1$^{-/-}$ motor neurons, while Baf

A1 treated TBK1$^{-/-}$ motor neurons showed significantly reduced survival in a variety of concentrations (p<0.0001) (Figure 3.3 b). Therefore, the treatment of Baf A1 could prevent TBK1$^{-/-}$ motor neurons from degrading pathological TDP-43 proteins, increasing insoluble TDP-43 accumulations, and hindering motor neuron survival to treatment.

The autophagy pathway contains several critical steps, including autophagosome formation and maturation. Considering the multifaced function of Baf A1, which could also block autophagosome-lysosome fusion and inhibit endosomal acidification, we investigated the role of autophagosome formation inhibition in regulating TDP-43 homeostasis by shRNA knockdown of ATG7. We generated cells stably expressing non-targeting control (shNTC) and ATG7 shRNA (shATG7) hairpin. Immunoblotting confirmed that ATG7 was deficient in shATG7 motor neurons, and ATG7 deficiency caused increased levels of p62 and impaired autophagic flux (Figure 3.4 a,b). After motor neuron differentiation, the shATG7 did not affect the percentage of cells expressing the motor neuron marker, ISL-1, compared to the shNTC control (p=0.4417) (Figure 3.5 a,b). Interestingly, we found that inhibition of ATG7 did not alter the localization of TDP-43, as it stayed mainly in the nucleus (Figure 3.4 c,d). To determine if ATG7 inhibition affected the localization of TDP-43 expression, we performed subcellular fractionation and immunoblotting. We found that ATG7-deficient human motor neurons showed similar levels of TDP-43 in different fractions compared to control human motor neurons (NE: p=0.9983, PE: p=0.9885) (Figure 3.4 e,f). These data suggest that defective autophagosome formation is unlikely to be the primary cause of TDP-43 pathology in human motor neurons, and TBK1 deficiency might initiate TDP-43 pathology independent of autophagosome formation pathways.

Figure 3.3 Motor neuron survival is not affected by Baf A1 or MG132.
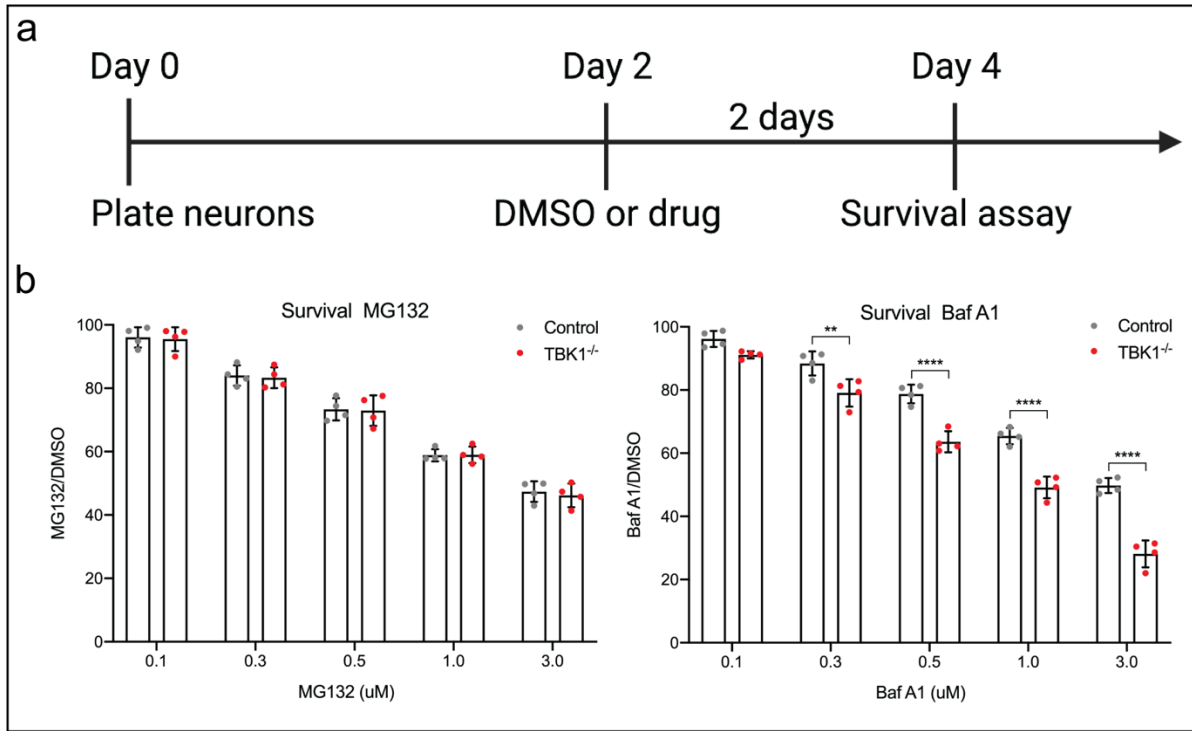
(a) Experimental outline of motor neuron survival assay. Motor neurons were differentiated and plated and were treated with DMSO or drug on Day 2 for 48 hr before the assay. (b) The survival rate of control and TBK1 [-/-] motor neurons in response to different concentrations of MG132 and Baf A1. The relative survival rate was compared to that of DMSO control.
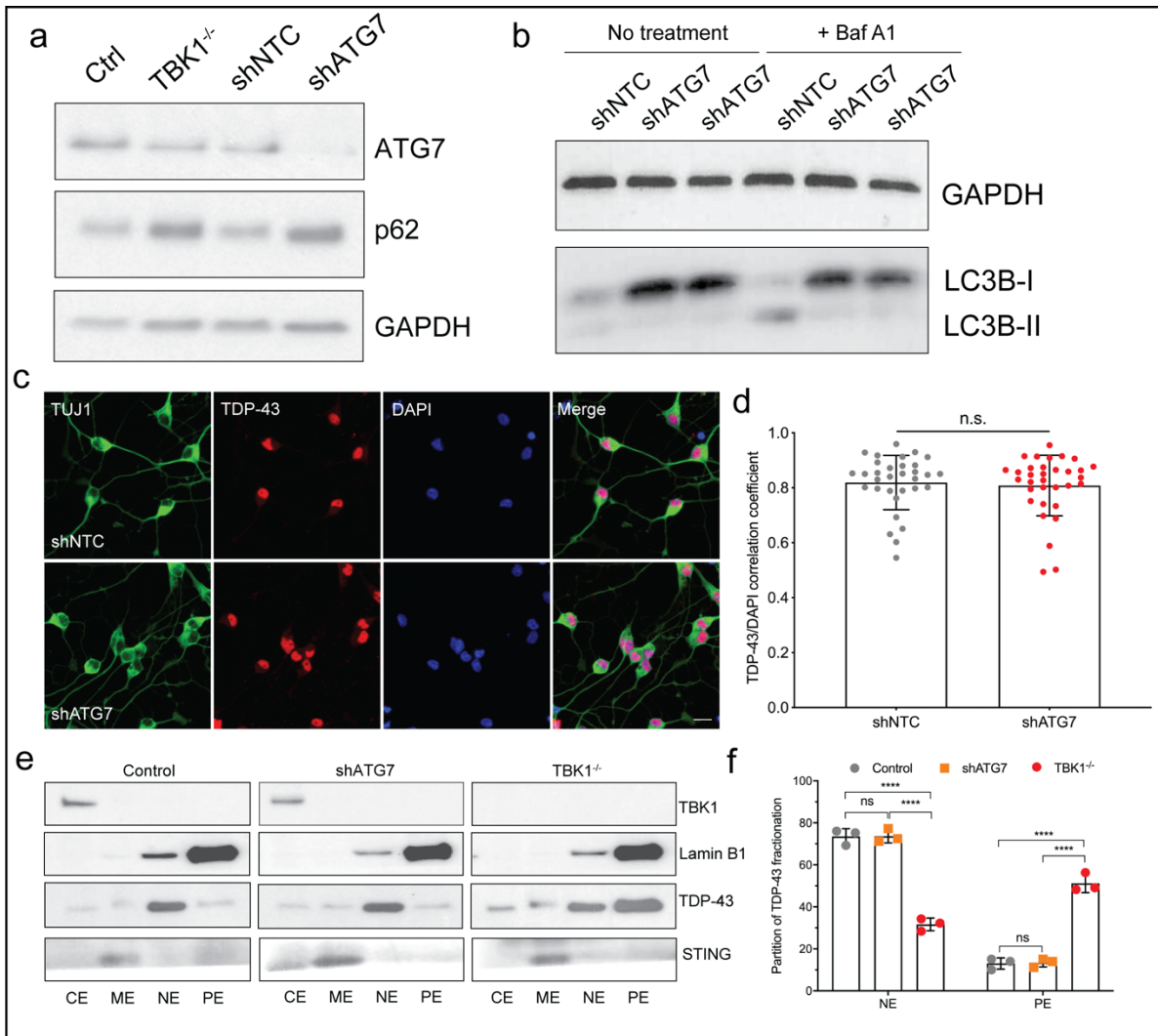
Figure 3.4 Inhibition of autophagy induction by shATG7 fails to induce TDP-43 pathology.

(a) Western blot analysis of human motor neurons stably expressing non-targeting control (shNTC) or shATG7 hairpin. The expression of ATG7 and p62 is normalized to GAPDH (loading control). (b) Effects of shATG7 on LC3-II levels and degradation during autophagic maturation. The shNTC control and shATG7 human motor neurons are treated or not treated with BafA1 to inhibit autophagic degradation of LC3-II. (c) Representative images of shNTC and shATG7 motor neurons for quantification of TDP-43 localization. All cells are stained by DAPI, TDP-43, and neuronal marker TUJ1. Scale bar, 20 μm. (d) Quantifications of the TDP-43/DAPI correlation coefficient from (c) are shown. (e) Subcellular fractionation analysis of TBK1

(cytosol control), Lamin B1 (nuclear and pellet control), STING (membrane control), and TDP-43 levels in different fractions of control, TBK1$^{-/-}$, and shATG7 motor neurons. (f) Quantifications of the partition of TDP-43 in each cellular fraction for control, TBK1$^{-/-}$, and shATG7 motor neurons are shown.
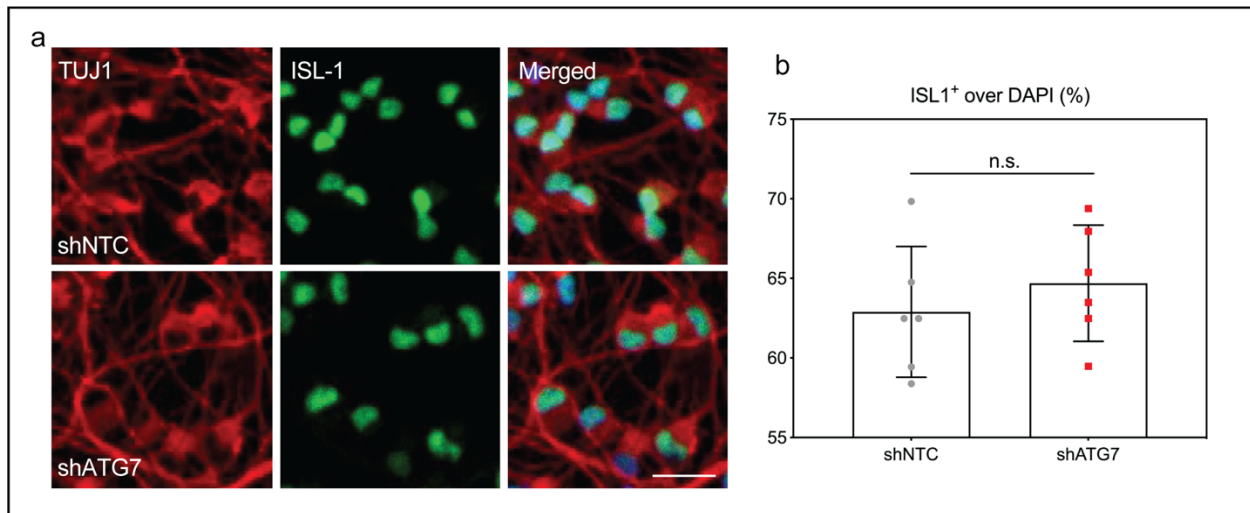

Figure 3.5 Motor neuron differentiation is not affected by shATG7.

(a) Immunostaining of ISL-1 in shNTC and shATG7 human motor neurons. All cells are stained by DAPI and neuronal marker TUJ1. Scale bar, 20 μm. (b) Quantifications of the percentage of cells expressing ISL-1 are shown.

3.3.2 TBK1 deficiency impairs endosomal maturation and lysosomal functions

Determining the functional pathway in which TBK1 acts may be beneficial for designing therapeutics treating ALS. To better understand the mechanisms of TBK1$^{-/-}$ induced TDP-43 pathology and neurodegeneration, we performed phosphoproteome analysis for control, shATG7, and TBK1$^{-/-}$ motor neurons using TMT labeling (Figure 3.6 a). Compared to control motor neurons, TBK1$^{-/-}$, but not shATG7 motor neurons, showed markedly reduced phosphorylation levels of proteins involved in nuclear transport and endosomal transport signaling pathways (Figure 3.6

b,c). Previous reports also showed that TBK1 was required for early endosomal targeting, and TBK1 might modulate RAB GTPase activity [12,16,17]. To determine whether loss of TBK1 caused changes in endosomal transport in human motor neurons, we evaluated the expression of markers for early endosomes (EEA1, RAB5) and late endosomes (RAB7) in control and TBK1^{-/-} motor neurons by ICC. We identified an increased number of EEA1-positive and RAB5-positive vesicles but reduced RAB7-positive vesicles in TBK1^{-/-} motor neurons using confocal microscopy (p<0.0001) (Figure 3.6 d-g). Our results suggested that TBK1 might mediate the maturation of early endosomes to late endosomes, and reduced RAB7 level caused by loss of TBK1 might indicate the impaired maturation and fusion of late endosomes with lysosomes (Figure 3.7 a).
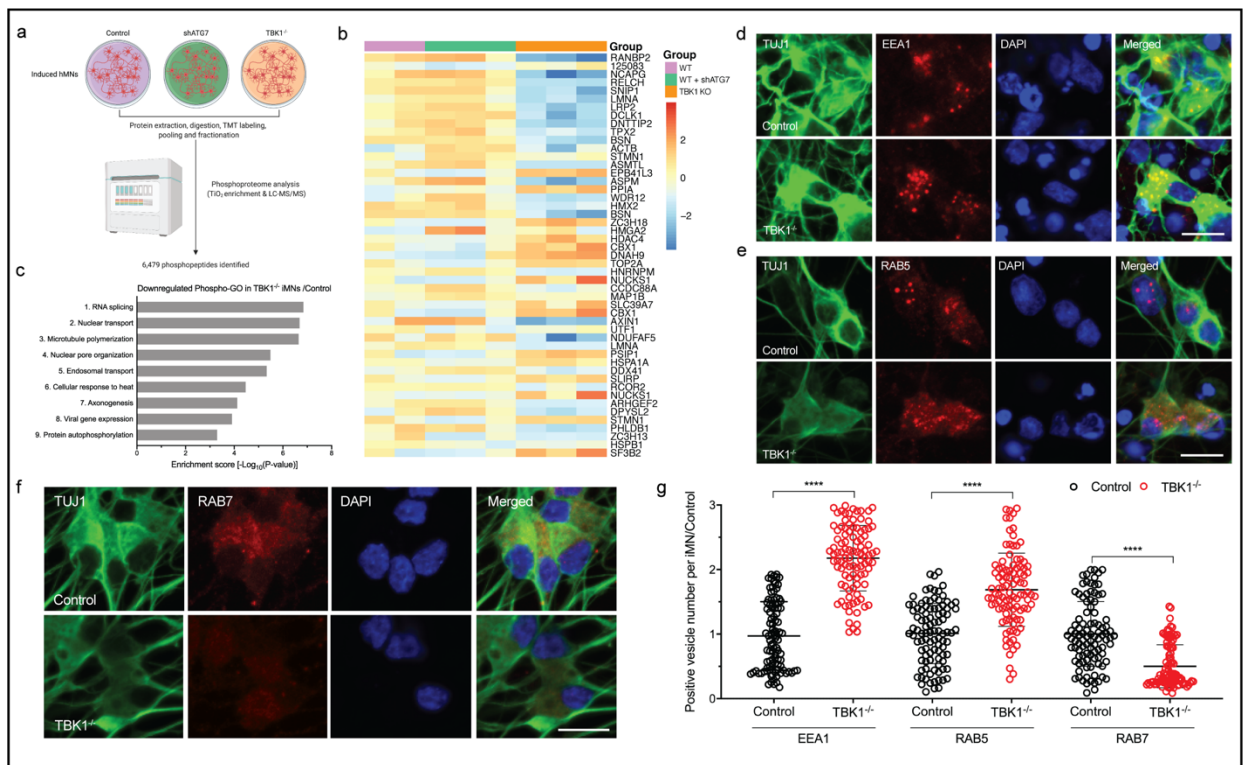

Figure 3.6 Impaired endosomal trafficking in TBK1^{-/-} motor neurons identified by phospho-proteomics

(a) Schematic of experimental design for phospho-proteomic analysis from control, TBK1^{-/-}, and shATG7

human motor neurons. (b) Heatmap of the 50 most significant differentially expressed phosphoproteins (log2 expression). (c) GO analysis of down phosphorylated proteins in TBK1$^{-/-}$ compared to control motor neurons. (d-g) Representative images of control and TBK1$^{-/-}$ motor neurons for vesicle number quantification of EEA1 (d), RAB5 (e), and RAB7 (f). All cells are stained by DAPI and neuronal marker TUJ1. Scale bar, 20 µm. Quantifications of the positive vesicle numbers in TBK1$^{-/-}$ motor neurons from (d-f) are shown. All quantifications are normalized to control human motor neurons (g).
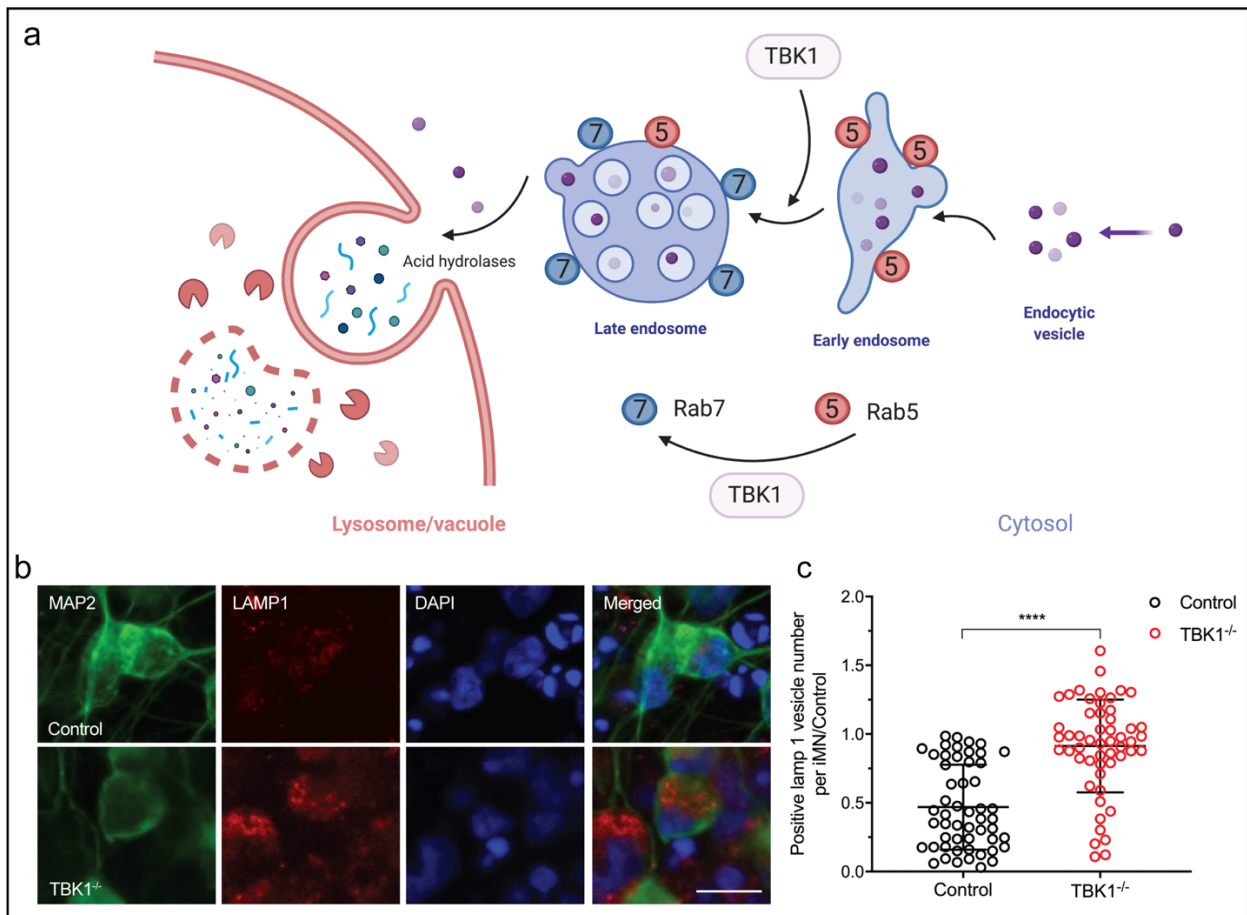
Figure 3.7 Loss of TBK1 induces impaired endosomal trafficking and accumulated LAMP1^{+} vesicles.

(a) Schematic illustration showing the potential function of TBK1 in endosomal maturation. TBK1 promotes the maturation of early endosomes into late endosomes by converting RAB5 to RAB7. (b) Representative images of control and TBK1$^{-/-}$ motor neurons for vesicle number quantification of LAMP1. All cells are stained by DAPI and neuronal marker MAP2. Scale bar, 20 µm. (c) Quantifications of the positive LAMP1

vesicle numbers in TBK1^{-/-} motor neurons from (b) are shown. All quantifications are normalized to control motor neurons.

To determine the functional consequences of impaired endosomal pathway and its link with TDP-43 pathology, we sought to examine the lysosomal function, which is downstream of the endosomal pathway, in TBK1^{-/-} motor neurons. Our study demonstrated that TBK1 mediates autophagosomes and endosomes maturation, thereby preventing their fusion with lysosomes. A previous report shows that the functional activation of lysosomes is regulated by the lysosomal fusion process [18]. To determine if loss of TBK1 affected lysosomal biogenesis, we analyzed the number of LAMP1-positive vesicles in control and TBK1^{-/-} motor neurons by ICC (Figure 3.7 b,c). TBK1^{-/-} motor neurons showed an increased number of LAMP1-positive vesicles than control motor neurons ($p<0.0001$), indicating that TBK1 deletion in motor neurons might lead to accumulations of lysosomes. The other critical function of lysosomes is being acidic, mediated by the degradation of lysosomal-substrates [19]. To assess whether these LAMP1-positive vesicles were acidic, a functional indicator of lysosomes, motor neurons were labeled with LysoTracker red, an acidic organelle staining dye. Surprisingly, we found that LysoTracker-positive vesicles were reduced in TBK1^{-/-} motor neurons ($p<0.0001$), and Baf A1, a lysosomal acidification inhibitor, diminished the LysoTracker staining in motor neurons (Figure 3.8 a,b). Next, we quantified the LysoTracker Red fluorescence intensity in motor neurons using flow cytometry. Consistent with LysoTracker staining data, total LysoTracker intensity was markedly reduced in TBK1^{-/-} motor neurons ($p<0.05$) (Figure 3.9 a-c), suggesting that lysosomes were less acidic in TBK1^{-/-} motor neurons. Subsequently, we used the self-quenched enzymatic substrates, which would be targeted to the lysosomes by endocytosis and turn fluorescent upon the enzymatic activity to quantify endo-lysosomal activities [20]. Consistent with the impaired endosomal maturation and deficient lysosomal enzyme activities observed in TBK1^{-/-} motor neurons, fluorescent endocytic

cargos upon endo-lysosomal transport and lysosomal enzymatic activity were reduced by ~60% relative to control cells (p<0.0001) (Figure 3.8 c,d). Together, our results suggest that loss of TBK1 impairs endosomal maturation and leads to deficient lysosomal enzymatic activities with reduced acidifications.
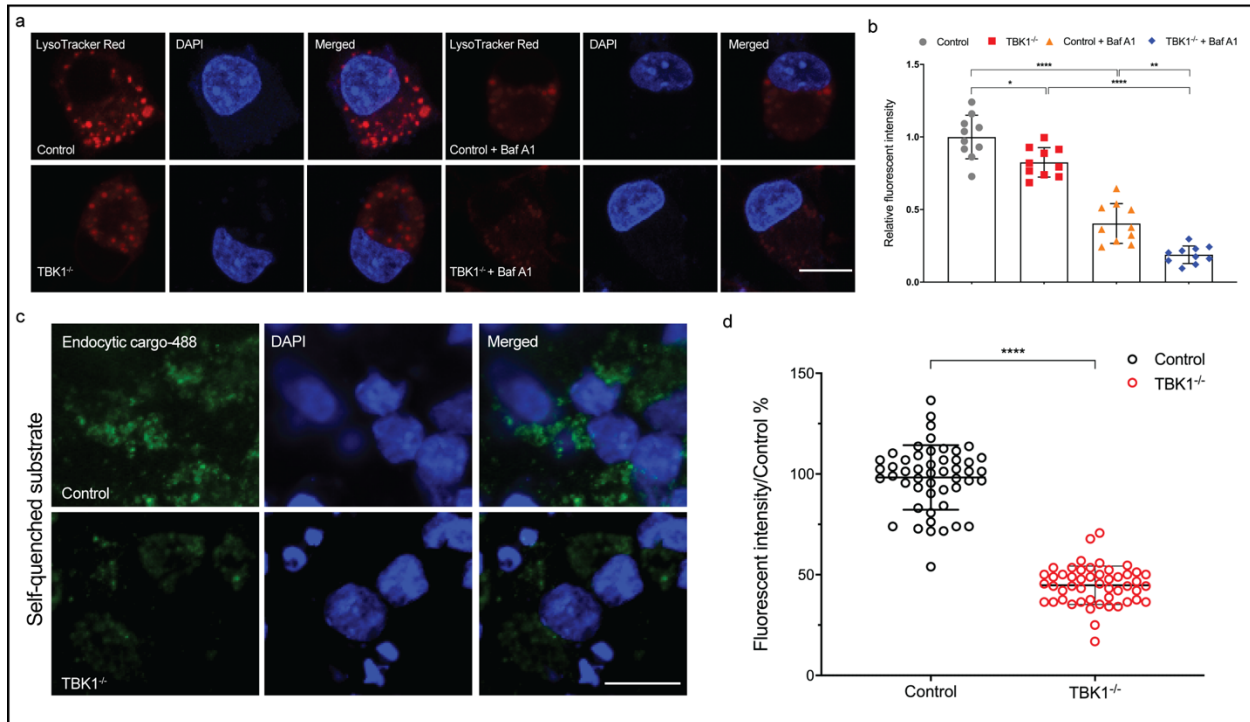
Figure 3.8 Loss of TBK1 leads to defective lysosomal acidification and enzymatic functions.

(a) LysoTracker Red staining of control and TBK1^{-/-} human motor neurons. The control cells show bright puncta, while the TBK1^{-/-} cells have much dimmer and fewer puncta. Baf A1 is used as a positive control as the acidification inhibitor. (b) Quantification of LysoTracker relative intensity from (a) is shown. (c) Lysosome enzyme activity assay in control and TBK1^{-/-} motor neurons. The self-quenched substrate is used as endocytic cargo, and the fluorescence signal generated by lysosomal degradation is proportional to the intracellular lysosomal activity. (d) Quantifications of the relative fluorescent intensity from (c) are shown.
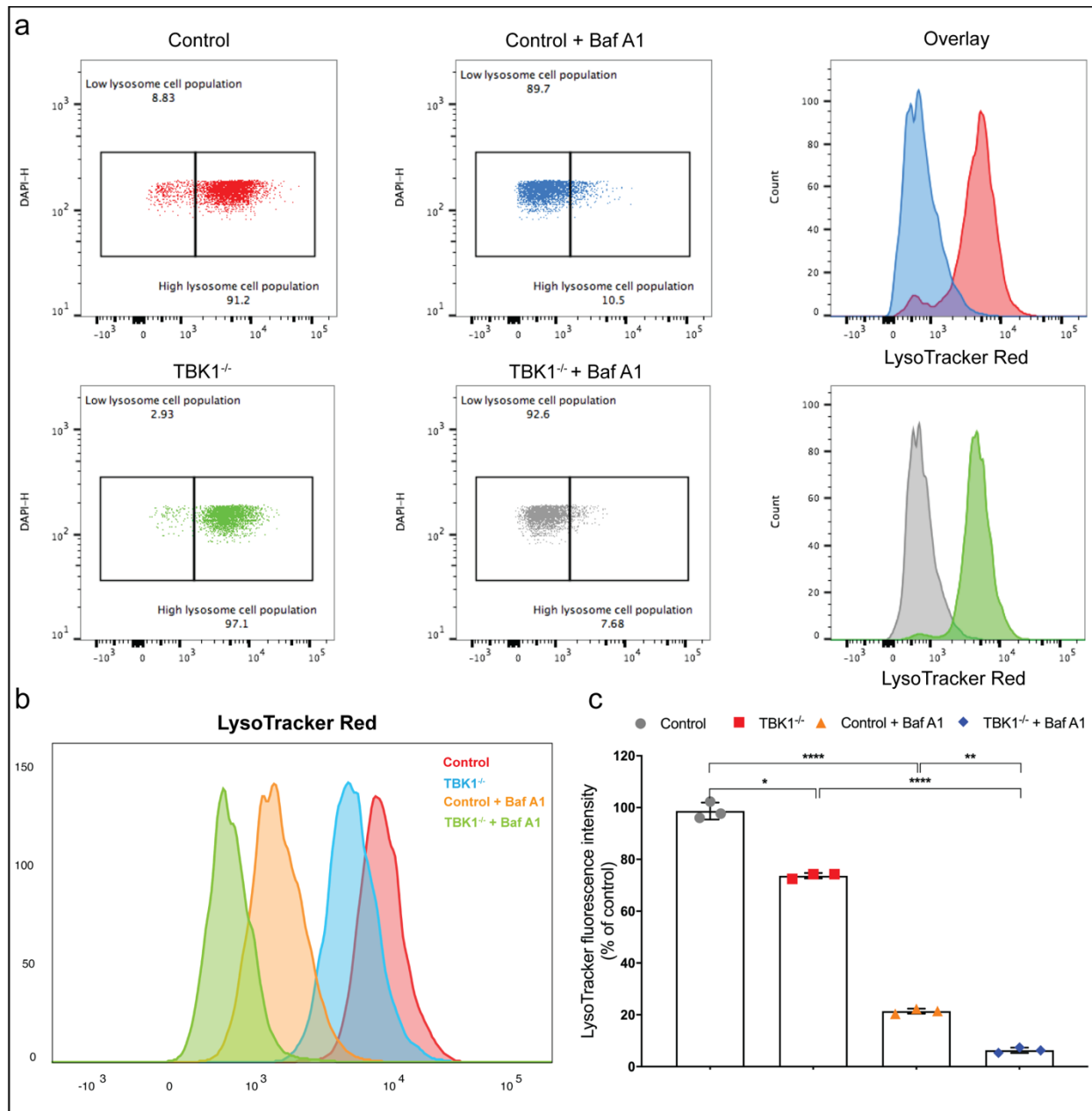
Figure 3.9 TBK1 deficiency leads to reduced lysosomal acidification identified by flow cytometry.

(a) Flow cytometry analysis of LysoTracker Red staining in control and TBK1$^{-/-}$ motor neurons. Baf A1 is added as a positive control and shows decreased LysoTracker Red staining. (b) The intensity of LysoTracker Red in control, TBK1$^{-/-}$, control + Baf A1, and TBK1$^{-/-}$ + Baf A1 motor neurons are compared. (c) Quantifications of LysoTracker Red fluorescent intensity are shown.

3.3.3 Inhibiting lysosomal acidification triggers TDP-43 pathology

Our data suggest that TBK1^{-/-} motor neurons accumulate cytoplasmic and insoluble TDP-43 as well as impaired endosomal maturation and subsequent lysosomal dysfunction. To establish the link between TDP-43 pathology and the lysosomes, motor neurons were treated with Lys05, which blocks lysosomal enzymatic activity by neutralizing lysosomal pH [21] (Figure 3.10 a). To validate the role of TBK1 in the endo-lysosomal pathway, we co-stained active phosphorylated TBK1 (p-TBK1) with key markers of early endosomes under lysosomal stress. Consistent with a previous study [16], p-TBK1 stained positively with EEA1 vesicles when lysosomal activity was inhibited (Figure 3.10 b,c), suggesting that TBK1 activity lies upstream of endo-lysosomal pathways. The fact that p-TBK1 interacts with early endosomal marker EEA1 is consistent with our previous data that loss of TBK1 caused impaired lysosomal function and suggests a potential link between TDP-43 pathology and the endo-lysosomal pathway.

To further validate the link connecting TBK1^{-/-} induced TDP-43 pathology and the impairment of the endo-lysosomal pathway, we asked whether the inhibited lysosomal activity is sufficient to cause TDP-43 pathology in human motor neurons. To this end, we treated control and TBK1^{-/-} motor neurons with 1 µM Lys05 for 4-5 days to inhibit the lysosomal activity and tested the level of insoluble TDP-43 accumulation. Lysosomal inhibition in control motor neurons showed increased insoluble TDP-43 levels (p<0.0001), supporting the notion that the TBK1^{-/-} induced TDP-43 pathology might be caused by deficient lysosomal activity (Figure 3.10 d,e). Interestingly, the level of insoluble TDP-43 in control motor neurons treated with Lys05 was comparable to that of TBK1^{-/-} motor neurons (Figure 3.10 d,e), highlighting the central role of lysosomal activity in the clearance of insoluble TDP-43. The subcellular fractionation experiment also confirmed an increased pellet fraction of TDP-43 in control motor neurons when treated with Lys05 (Figure 3.10 f). In addition, increased cytoplasmic TDP-43 was observed in control cells treated with Lys05 (p<0.0001) (Figure 3.10 g,h), suggesting that lysosomal activity is linked to cytoplasmic TDP-43 proteins and their insoluble accumulations. Thus, our data validate the strong link between TDP-

43 pathology and the activity of the endo-lysosomal pathway, and TBK1 is an important mediator of these processes.
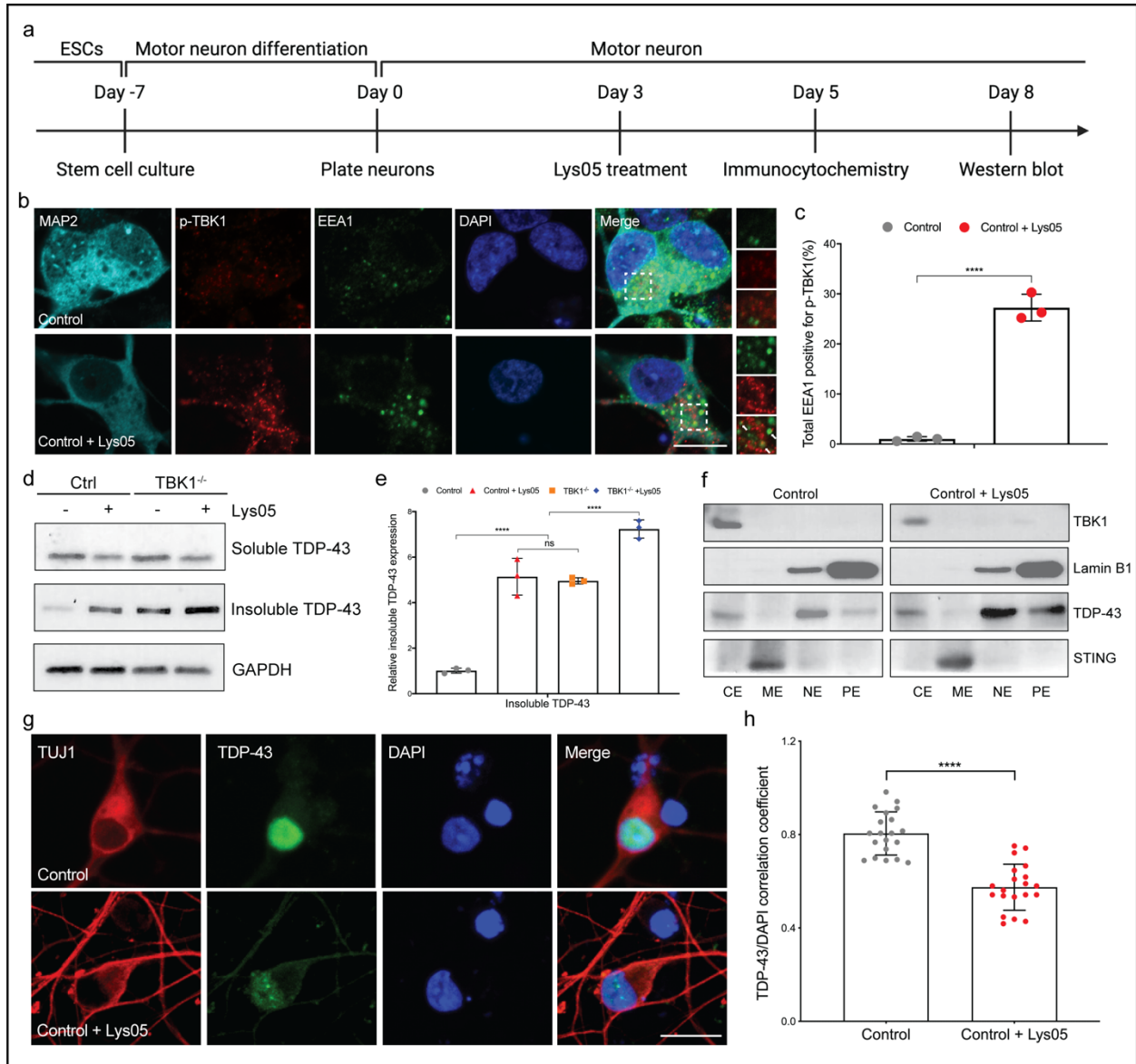
Figure 3.10 Lysosomal function defects trigger TDP-43 pathology in human motor neurons.

(a) Schematic of experimental outline for lysosomal inhibitor treatment in human motor neurons. (b) Representative images of control motor neurons treated with and without Lys05 for staining against EEA1 and pTBK1. All cells are stained by DAPI, EEA1, pTBK1, and neuronal marker MAP2. Scale bar, 20 μm. (c) Quantifications of the percentage of total EEA1 vesicles showed positive for pTBK1. (d) Western blot

analysis of control and TBK1$^{-/-}$ motor neurons treated with DMSO or Lys05. Accumulations of TDP-43 proteins are shown in the soluble (RIPA) and insoluble (urea) fractions. (e) Quantification of TDP-43 expression between DMSO and Lys05 treated human motor neurons. GAPDH in the soluble fraction is used as the loading control for normalization. (f) Subcellular fractionation analysis of TBK1 (cytosol control), Lamin B1 (nuclear and pellet control), STING (membrane control), and TDP-43 levels in different fractions of control motor neurons treated with and without Lys05. Representative blots show TDP-43 levels in cytosol extract (CE), membrane extract (ME), nuclear extract (NE), and pellet extract (PE). (g) Representative images of control motor neurons treated with and without Lys05 for staining against TDP-43. All cells are stained by DAPI, TDP-43, and neuronal marker TUJ1. Scale bar, 20 μm. (h) Quantifications of the TDP-43/DAPI correlation coefficient from (g) are shown.

3.4 Discussion and implications

In this chapter, we explored the detailed mechanism of TBK1 deficiency-induced TDP-43 pathology. TDP-43 pathology is a universal hallmark and a prominent feature of ALS. Previous studies have led to the proposal that cytosolic and insoluble accumulations of TDP-43 were initiated by autophagy or proteasome activity inhibition [22,23]. However, our data using human motor neurons suggests that although proteasome inhibition reduces the soluble fraction of TDP-43, it has little effect on its insoluble accumulations. In addition, autophagosome formation inhibition by ATG7 deletion does not trigger insoluble TDP-43 accumulations or TDP-43 mislocalization, suggesting pathways independent of autophagosome formation and proteasome activity in TBK1$^{-/-}$ induced TDP-43 pathology. Therefore, in contrast to the previous recognition that autophagy inhibition is a disease-causing mechanism of TBK1 mutations [24,25], our data provide the first evidence that defective autophagosome formation cannot initiate TDP-43 pathology, a key disease-relevant phenotype, in human motor neurons. Notably, our results show that increased cytoplasmic TDP-43 protein and its insoluble accumulations are found in TBK1$^{-/-}$ motor neurons but not in hESCs. This suggests that TDP-43 pathology may be a motor neuron- or neuron-

specific phenotype, at least in the scenario of TBK1 deficiency.

To better understand the downstream functions of TBK1 in maintaining motor neuron homeostasis, we identified the differential phospho-proteome expression map of TBK1$^{-/-}$ motor neurons for the first time. The phospho-proteome data establishes a mechanistic link between TDP-43 pathology and the impaired endosomal pathways. Our results show impaired endosomal maturation with a reduced number of late endosomes and accumulated early endosomes in TBK1$^{-/-}$ motor neurons, possibly through insufficient phosphorylation of RAB GTPase controlling this process [17]. A recent study has linked increased TDP-43 aggregation with impaired endocytosis, while enhanced endocytosis reversed TDP-43 toxicity and motor neuron dysfunctions [26]. In an independent study, reduced TDP-43 expression decreased the number and motility of recycling endosomes, specifically in human iPSC-derived neurons, while overexpression of TDP-43 showed opposite effects [27]. Consistent with previous results [28], we show that endosomal pathways dominate the clearance of pathological TDP-43, while autophagy contributes to the clearance of TDP-43 only when the endosomal pathway is dysfunctional. In addition, the observation that loss-of-function mutations of other ALS genes also encode components of endosomal pathways, e.g., CHMP2B, highlighted the importance of the endosomal pathway in TDP-43 pathology [28].

To determine the functional consequences of impaired endosomal maturation, we evaluated the function of lysosomes by acidification levels in TBK1$^{-/-}$ motor neurons. Previous studies have shown that the formation of lysosomes is accomplished by the fusion of transport vesicles from the *trans* Golgi network with endosomes and/or autophagosomes [19]. During endosomal maturation, the late endosomes target acid hydrolases to the lysosomal lumen [29]. Therefore, our data validated that impaired endosomal fusion could result in insufficient lysosomal acidifications, which would cause subsequent lysosomal dysfunction. Notably, our data bridges the link between TDP-43 pathology and lysosomal dysfunction. The small molecule inhibition of lysosomal activity is sufficient to cause cytosolic and insoluble TDP-43 accumulations in human

93

motor neurons. Interestingly, the reduced expression of C9ORF72 in human motor neurons has also been reported to show perturbation of vesicle trafficking and reduced lysosomal biogenesis, resulting in lysosomal dysfunctions [30]. Previous studies also implicate several ALS or FTD mutations linked to lysosomal dysfunction, e.g., C9ORF72, TARDBP, CHMP2B, OPTN, VCP, and SQSTM1/p62 [31]. Although mechanistically divergent, our findings highlight a phenotypic convergence of TBK1 with a large portion of other genetic causes of ALS or FTD, providing evidence for potential broad-spectrum therapeutics for ALS/FTD.

3.5 Experimental procedures

Human pluripotent stem cell lines

The HUES3 Hb9::GFP used in this study was previously approved by the institutional review boards of Harvard University. Specific point mutations were confirmed by PCR amplification followed by Sanger sequencing. Our lab screens for mycoplasma contamination weekly using the MycoAlert kit (Lonza) with no cell lines used in this study testing positive. The use of these cells at Harvard was further approved and determined not to constitute Human Subjects Research by the Committee on the Use of Human Subjects in Research at Harvard University.

Cell Culture and differentiation

Pluripotent stem cells were cultured with mTeSR plus medium (Stem Cell Technologies) on Matrigel (BD Biosciences) coated tissue culture dishes. Stem cells were maintained in 5% CO_2 incubators at 37 °C and passaged as small aggregates after 1mM EDTA treatment. After dissociation, 10 µM ROCK inhibitor (Sigma, Y-27632) was added to cell culture for 24 hr to prevent cell death, and then incubated with lentiviruses (FUW-M2rtTA, TetO-Ngn2-Puro). The HUES3 Hb9::GFP cell line has been previously described [32]. Motor neurons were differentiated using a

modified protocol based on previous strategies [33,34]. This protocol relies on neural induction through NGN2 programming, SMAD inhibition through small molecules, and motor neuron patterning through retinoic activation and Sonic Hedgehog signaling. In brief, hESCs were dissociated into single cells using accutase (Stem Cell Technologies), and then plated on Matrigel-coated culture dish at a density of 80,000 cells per cm^2 with mTeSR plus medium (Stem Cell Technologies) supplemented with 10 µM ROCK inhibitors (Sigma, Y-27632). When cells reached confluency, medium was changed to N2 medium (DMEM-F12 (Life Technologies) supplemented with ×1 Gibco GlutaMAX (Life Technologies), ×1 N-2 supplement (Gibco), × 0.3% Glucose) on Day 1-3. For small molecule treatment, 10 µM SB431542 (Custom Synthesis), 100 nM LDN-193189 (Custom Synthesis), 1 µM retinoic acid (Sigma), 1 µM SAG (Custom Synthesis) were added on Day 1-3. For NGN2 induction and neuron selection, 20 mg/ml Doxycycline and 10 mg/ml puromycin were added on Day 2-3. On Day 4-7, the N2 medium was changed to Neurobasal (Neurobasal (Life Technologies) supplemented with ×1 N-2 supplement (Gibco), ×1 B-27 supplement (Gibco), ×1 Gibco GlutaMAX (Life Technologies) and 100 µM non-essential amino-acids: NEAA) along with 1 µM retinoic acid, 1 µM SAG, 20 mg/ml Doxycycline, 10 mg/ml puromycin, and 10 ng/ml of neurotrophic factors: glial cell-derived neurotrophic factor (GDNF), ciliary neurotrophic factor (CNTF) and brain-derived neurotrophic factor (BDNF) (R&D). For post-mitotic cell selection, 10 mM 5-Fluoro-2'-deoxyuridine thymidylate synthase inhibitor (FUDR, Sigma) was added on Day 5-7. From Day 8, media was changed to the motor neuron maintenance media containing Neurobasal (Neurobasal (Life Technologies) supplemented with ×1 N-2 supplement (Gibco), ×1 B-27 supplement (Gibco), ×1 Gibco GlutaMAX (Life Technologies) and 100 µM non-essential amino-acids: NEAA) supplemented with 10 ng/ml of neurotrophic factors (GDNF, CNTF, and BDNF) and 10 mM FUDR. Half of the maintenance media was changed every two days.

Cell viability assay

Motor neuron viability assay was performed based on the CellTiter-Glo luminescent for each sample according to the manufacturer's recommendations (Promega G7570). In brief, motor neurons were plated in triplicate onto 96-well plates. After treatment incubation, motor neurons were incubated for 10 min with CellTiter-Glo reagent at room temperature, and luminescence was measured using the Cytation imaging reader (BioTek). Background luminescence was measured using medium without cells and then subtracted from experimental values.

Immunocytochemistry and imaging

For immunocytochemistry, cells were fixed with 4% PFA for 20 min, and were subject to permeabilization with 0.25% Triton-X in PBS for 40 min. After that, cells were blocked using 10% donkey serum supplemented with 0.1% Triton-X in PBS (blocking buffer) for 1 hr at room temperature. Primary antibody diluted in blocking buffer was used for cell incubation overnight at 4 °C. At least three washes (5 min incubation each) with PBS were carried out, before incubating the cells with secondary antibodies (diluted in blocking buffer) for 1 hr at room temperature. Nuclei was stained with DAPI. The following antibodies were used in this study: TBK1 (1:200, Abcam ab109735), SQSTM1 / p62 (1:200, Abcam ab56416), TDP-43 (1:200, Proteintech Group 10782 & Cell Signaling Technology 3448S), Islet1 (1:500, Abcam ab20670), MAP2 (1:10,000, Abcam ab5392), TUJ1 (1:1,000, R&D Systems MAB NL493), EEA1 (1:100, Cell Signaling Technology 3288 & BD Biosciences 610456), RAB5 (1:100, Cell Signaling Technology 46449S), RAB7 (1:100, Cell Signaling Technology 9367S), LAMP1 (1:100, Abcam ab25630), phospho-TBK1 (1:200, Cell Signaling Technology 13498S). Secondary antibodies used (488, 555, and 647) were AlexaFluor (1:1,000, Life Technologies). Images were acquired using a Zeiss LSM 880 confocal microscope or a Nikon Eclipse Ti microscope. Images were analyzed using ImageJ or NIS- Elements (Nikon).

Western blot assays

For protein extraction, cells were lysed using 1% SDS lysis buffer (PhosphoSolutions, 100-

LYS) with a brief sonication. For insoluble protein extraction, cells were lysed using RIPA buffer (Life Technology, 89900) with protease inhibitors (Life Technology, 78425) for 20 min on ice. After centrifuge, the supernatant was collected as soluble fraction, and the insoluble fraction was collected from the pellet using 8M urea with 4% CHAPS, 40 mM Tris, and 0.2% Bio-Lyte 3/10 ampholyte (Bio-Rad, 1632103). For subcellular fractionation, cells were subject to sequential extract using the subcellular fractionation kit for cultured cell (Thermo Scientific, 78840) according to manufacturer instructions. After sample preparation, equivalent amount of 5-10 µg protein from each ample were subjected to electrophoresis using 4–20% SDS-PAGE (Bio-Rad, 4561096) and then transferred to a PVDF membrane (Thermo Fisher, 88518). The membrane was blocked with 3% Bovine Serum Albumin (Sigma, A9647) for 1 hr at room temperature, and incubated with primary antibodies overnight at 4°C. The next day, membrane was washed in TBST X3, 10 min each, and then incubated with HRP-conjugated secondary antibodies for 1 hr at room temperature. After that, membrane was washed in TBST X3, 10 min each, and then developed using ECL Western Blotting Detection System (VWR, 95038) and blotting films (Genesee Scientific, 30-810).

TDP-43 localization assay

For analysis of correlation coefficient of TDP-43 and nuclei, motor neurons were stained for TDP-43 (Cell Signaling Technology), TUJ1 (R&D Systems), and counterstained with DAPI. TUJ1 staining was used to determine the neuronal cell body, and the Pearson's correlation coefficient was calculated using NIS-Elements (Nikon) for TDP-43 and DAPI with at least 50 neurons being analyzed. Cells were segmented into the nuclear (DAPI positive) and cytoplasmic (DAPI negative) regions by NIS. The TDP-43 intensity in these two regions were used to determine the nuclear to cytoplasmic ratio (correlation coefficient) for TDP-43 fluorescent intensity.

Molecular cloning and viral production

Stable cell lines expressing inducible shATG7 were made by lentivirus infection. shATG7

hairpin sequence GGAGTCACAGCTCTTCCTTAC was cloned into Tet-pLKO-puro 'all-in-one' tetracycline-inducible vector, as described previously [35]. Viruses were produced as follows. HEK293 cells were transfected with viral vectors containing genes of interest and viral packaging plasmids (pPAX2 and VSVG) with lipofectamine 3000 (Invitrogen) in Opti-MEM (Gibco). The medium was changed 24 hr, and viruses were harvested at 48 hr and 72 hr after transfection. The supernatants were filtered with 0.45 µM filters, incubated with Lenti-X concentrator (Clontech) for 24 hr, and centrifuged at 1,500 g at 4 °C for 45 min. The pellets were resuspended in 300 µl DMEM supplemented with 10% FBS and stored at −80 °C.

Lysosomal enzyme activity assay

Control and TBK1$^{-/-}$ motor neurons were incubated with Self-Quenched Substrate (Abcam Cat No. ab234622) following manufacturer's instructions. Briefly, cells were incubated with the substrate for 1hr and fixed with 4% PFA at room temperature for 20 min. After washing with PBS, cells were stained with DAPI and then mounted for imaging with Zeiss LSM880 Confocal Laser Scanning microscope. Images were analyzed using ImageJ. Mean fluorescence intensity was quantified in control and TBK1$^{-/-}$ motor neurons.

Mass spectrometry

The phospho-proteomics was performed at Harvard Center for Mass Spectrometry (HCMS). Cell pellets were prepared using DF Covaris duffer and undergo protein extraction procedure for 120 s with 10% power in Covaris S220 focused ultrasound instrument (Woburn). Samples were resolubilized in 50 mM TEAB (try-ethyl ammonia bicarbonate) buffer for reduction and alkylation, further digested in buffer trypsin (Promega) for 5 hours. The digested samples were enriched by High-Select™ TiO2 Phosphopeptide Enrichment Kit (Thermo-Fisher) according to the vendor's instructions. Enriched phosphopeptides were labeled with TMT16plexPRO (Thermo-Fisher) according to manufacturer protocol. Sample fraction was submitted for single

LC-MS/MS experiment that was performed on a Lumos Tribrid (Thermo) equipped with 3000 Ultima Dual nanoHPLC pump (Thermo). The Lumos Orbitrap was operated in data-dependent mode for the mass spectrometry methods. The mass spectrometry survey scan was performed in the Orbitrap in the range of 400 –1,800 m/z at a resolution of 6 × 104, followed by the selection of the twenty most intense ions (TOP20) for CID-MS2 fragmentation in the Ion trap using a precursor isolation width window of 2 m/z, AGC setting of 10,000, and a maximum ion accumulation of 50 ms. Ions in a 10 ppm m/z window around ions selected for MS2 were excluded from further selection. The same TOP20 ions were subjected to HCD MS2 event in Orbitrap part of the equipment. The fragmentation isolation width was 0.8 m/z, AGC was 50,000, the maximum ion time was 150 ms, normalized collision energy was 38V and an activation time of 1 ms for each HCD MS2 scan was set.

Mass spectrometry analysis

Raw data were analyzed in Proteome Discoverer 2.4 (Thermo Scientific) software with Byonic 3.5 node and ptmRS node. Assignment of MS/MS spectra was performed using the Sequest HT algorithm by searching the data against a protein sequence database including all entries from the Human Uniprot database. A MS2 spectra assignment false discovery rate (FDR) of 1% on protein level was achieved by applying the target-decoy database search. Filtering was performed using a Percolator (64bit version) [36]. For quantification, a 0.02 m/z window centered on the theoretical m/z value of each the six reporter ions and the intensity of the signal closest to the theoretical m/z value was recorded. Reporter ion intensities were exported in result file of Proteome Discoverer 2.4 search engine as an excel tables. The exact place of phosphor moiety was analyzed by ptmRS program [37]. Differentially expressed proteins between sample groups were analyzed using R script programs based on Bioconductor (https://www.bioconductor.org/), Statistical analysis for differentially expressed proteins was based on peptide level to find changes that are statistically significant between two sets.

Data presentation and statistical analysis.

Comparisons were made between control and TBK1$^{-/-}$ motor neurons using t tests (two-tailed, unpaired)/ANOVA for continuous data and rank tests for nonparametric data. For multiple comparisons, one-way ANOVA to normalize variance and post hoc Tukey tests were used. In all figure elements, bars and lines represent the median with error bars representing standard deviation. The box and whisker plots display the minimum to maximum. Data distribution was assumed to be normal, but this was not formally tested. Significance was assumed at $P < 0.05$. Error bars represent the SD unless otherwise stated. Analysis was performed with the statistical software package Prism 8 (Graph Pad).

References:

1   Shahheydari, H. *et al.* Protein Quality Control and the Amyotrophic Lateral Sclerosis/Frontotemporal Dementia Continuum. *Front Mol Neurosci* **10**, 119, doi:10.3389/fnmol.2017.00119 (2017).

2   Lilienbaum, A. Relationship between the proteasomal system and autophagy. *Int J Biochem Mol Biol* **4**, 1-26 (2013).

3   Balch, W. E., Morimoto, R. I., Dillin, A. & Kelly, J. W. Adapting proteostasis for disease intervention. *Science* **319**, 916-919, doi:10.1126/science.1141448 (2008).

4   Peters, O. M., Ghasemi, M. & Brown, R. H., Jr. Emerging mechanisms of molecular pathology in ALS. *J Clin Invest* **125**, 1767-1779, doi:10.1172/JCI71601 (2015).

5   Lee, J. K., Shin, J. H., Lee, J. E. & Choi, E. J. Role of autophagy in the pathogenesis of amyotrophic lateral sclerosis. *Biochim Biophys Acta* **1852**, 2517-2524, doi:10.1016/j.bbadis.2015.08.005 (2015).

6   Jung, C. H. *et al.* ULK-Atg13-FIP200 complexes mediate mTOR signaling to the autophagy machinery. *Mol Biol Cell* **20**, 1992-2003, doi:10.1091/mbc.E08-12-1249 (2009).

7   Kiriyama, Y. & Nochi, H. The Function of Autophagy in Neurodegenerative Diseases. *Int J Mol Sci* **16**, 26797-26812, doi:10.3390/ijms161125990 (2015).

8   Rui, Y. N. & Le, W. Selective role of autophagy in neuronal function and neurodegenerative diseases. *Neurosci Bull* **31**, 379-381, doi:10.1007/s12264-015-1551-7 (2015).

9   Mizushima, N. *et al.* A protein conjugation system essential for autophagy. *Nature* **395**, 395-398, doi:10.1038/26506 (1998).

10   Ichimura, Y. *et al.* A ubiquitin-like system mediates protein lipidation. *Nature* **408**, 488-492, doi:10.1038/35044114 (2000).

11   Heo, J. M., Ordureau, A., Paulo, J. A., Rinehart, J. & Harper, J. W. The PINK1-PARKIN Mitochondrial Ubiquitylation Pathway Drives a Program of OPTN/NDP52 Recruitment and TBK1 Activation to Promote Mitophagy. *Mol Cell* **60**, 7-20, doi:10.1016/j.molcel.2015.08.016 (2015).

12   Pilli, M. *et al.* TBK-1 promotes autophagy-mediated antimicrobial defense by controlling autophagosome maturation. *Immunity* **37**, 223-234, doi:10.1016/j.immuni.2012.04.015 (2012).

13   Kimura, S., Noda, T. & Yoshimori, T. Dynein-dependent movement of autophagosomes mediates efficient encounters with lysosomes. *Cell Struct Funct* **33**, 109-122, doi:10.1247/csf.08005 (2008).

14   Pillai, S. *et al.* Tank binding kinase 1 is a centrosome-associated kinase necessary for microtubule dynamics and mitosis. *Nat Commun* **6**, 10072, doi:10.1038/ncomms10072 (2015).

15   Van Mossevelde, S. *et al.* Clinical features of TBK1 carriers compared with C9orf72, GRN and non-mutation carriers in a Belgian cohort. *Brain* **139**, 452-467, doi:10.1093/brain/awv358 (2016).

16   Fraser, J. *et al.* Targeting of early endosomes by autophagy facilitates EGFR recycling and signalling. *EMBO Rep* **20**, e47734, doi:10.15252/embr.201947734 (2019).

17   Heo, J. M. *et al.* RAB7A phosphorylation by TBK1 promotes mitophagy via the PINK-PARKIN pathway. *Sci Adv* **4**, eaav0443, doi:10.1126/sciadv.aav0443 (2018).

18   Zhou, J. *et al.* Activation of lysosomal function in the course of autophagy via mTORC1

suppression and autophagosome-lysosome fusion. *Cell Res* **23**, 508-523, doi:10.1038/cr.2013.11 (2013).

19   Hu, Y. B., Dammer, E. B., Ren, R. J. & Wang, G. The endosomal-lysosomal system: from acidification and cargo sorting to neurodegeneration. *Transl Neurodegener* **4**, 18, doi:10.1186/s40035-015-0041-1 (2015).

20   Humphries, W. H. t. & Payne, C. K. Imaging lysosomal enzyme activity in live cells using self-quenched substrates. *Anal Biochem* **424**, 178-183, doi:10.1016/j.ab.2012.02.033 (2012).

21   Amaravadi, R. K. & Winkler, J. D. Lys05: a new lysosomal autophagy inhibitor. *Autophagy* **8**, 1383-1384, doi:10.4161/auto.20958 (2012).

22   Bose, J. K., Huang, C. C. & Shen, C. K. Regulation of autophagy by neuropathological protein TDP-43. *J Biol Chem* **286**, 44441-44448, doi:10.1074/jbc.M111.237115 (2011).

23   Scotter, E. L. *et al.* Differential roles of the ubiquitin proteasome system and autophagy in the clearance of soluble and aggregated TDP-43 species. *J Cell Sci* **127**, 1263-1278, doi:10.1242/jcs.140087 (2014).

24   Oakes, J. A., Davies, M. C. & Collins, M. O. TBK1: a new player in ALS linking autophagy and neuroinflammation. *Mol Brain* **10**, 5, doi:10.1186/s13041-017-0287-x (2017).

25   Catanese, A. *et al.* Retinoic acid worsens ATG10-dependent autophagy impairment in TBK1-mutant hiPSC-derived motoneurons through SQSTM1/p62 accumulation. *Autophagy* **15**, 1719-1737, doi:10.1080/15548627.2019.1589257 (2019).

26   Liu, G. *et al.* Endocytosis regulates TDP-43 toxicity and turnover. *Nat Commun* **8**, 2092, doi:10.1038/s41467-017-02017-x (2017).

27   Schwenk, B. M. *et al.* TDP-43 loss of function inhibits endosomal trafficking and alters trophic signaling in neurons. *EMBO J* **35**, 2350-2370, doi:10.15252/embj.201694221 (2016).

28   Leibiger, C. *et al.* TDP-43 controls lysosomal pathways thereby determining its own clearance and cytotoxicity. *Hum Mol Genet* **27**, 1593-1607, doi:10.1093/hmg/ddy066 (2018).

29   Pillay, C. S., Elliott, E. & Dennison, C. Endolysosomal proteolysis and its regulation.

Biochem J **363**, 417-429, doi:10.1042/0264-6021:3630417 (2002).

30   Shi, Y. *et al.* Haploinsufficiency leads to neurodegeneration in C9ORF72 ALS/FTD human induced motor neurons. *Nat Med* **24**, 313-325, doi:10.1038/nm.4490 (2018).

31   Root, J., Merino, P., Nuckols, A., Johnson, M. & Kukar, T. Lysosome dysfunction as a cause of neurodegenerative diseases: Lessons from frontotemporal dementia and amyotrophic lateral sclerosis. *Neurobiol Dis* **154**, 105360, doi:10.1016/j.nbd.2021.105360 (2021).

32   Han, S. S., Williams, L. A. & Eggan, K. C. Constructing and deconstructing stem cell models of neurological disease. *Neuron* **70**, 626-644, doi:10.1016/j.neuron.2011.05.003 (2011).

33   Nehme, R. *et al.* Combining NGN2 Programming with Developmental Patterning Generates Human Excitatory Neurons with NMDAR-Mediated Synaptic Transmission. *Cell Rep* **23**, 2509-2523, doi:10.1016/j.celrep.2018.04.066 (2018).

34   Amoroso, M. W. *et al.* Accelerated high-yield generation of limb-innervating motor neurons from human stem cells. *J Neurosci* **33**, 574-586, doi:10.1523/JNEUROSCI.0906-12.2013 (2013).

35   Dou, Z. *et al.* Autophagy mediates degradation of nuclear lamina. *Nature* **527**, 105-109, doi:10.1038/nature15548

nature15548 [pii] (2015).

36   Kall, L., Storey, J. D. & Noble, W. S. Non-parametric estimation of posterior error probabilities associated with peptides identified by tandem mass spectrometry. *Bioinformatics* **24**, i42-48, doi:10.1093/bioinformatics/btn294 (2008).

37   Taus, T. *et al.* Universal and confident phosphorylation site localization using phosphoRS. *J Proteome Res* **10**, 5354-5362, doi:10.1021/pr200611n (2011).

CHAPTER 4: TBK1 deficiency induced pathology could be rescued by TBK1 restoration and PYKFYVE inhibition

4.1 Abstract

In Chapter 3, we identified the mechanisms of TDP-43 pathology induced by TBK1 deficiency. Using phospho-proteomics data, we found that loss of TBK1 led to impaired endosomal trafficking and lysosomal functions. In addition, blocking lysosomal acidification was sufficient to trigger insoluble TDP-43 accumulations in human motor neurons. In this chapter, we first restored TBK1 expression in the loss-of-function cell model with the TRE3G inducible system. Restoration of TBK1 re-sustained endo-lysosomal function and rescued TDP-43 pathology in motor neurons. In addition, restoration of TBK1 reversed the functional defects found in TBK1 deficient motor neurons, including electrophysiological properties and the ability of axonal regeneration, suggesting that the disease pathology is reversible. Furthermore, we derived two induced pluripotent stem cell (iPSC) lines from ALS patients with TBK1 mutations. Haploinsufficiency of TBK1 failed to trigger TDP-43 pathology in cultured motor neurons. However, TBK1 mutations sensitized motor neurons to lysosomal stress, indicating the critical role of the endo-lysosomal pathway in maintaining TBK1 mutant motor neuron homeostasis. Notably, apilimod, a PYKFYVE inhibitor and RAB5 effector, could rescue neurodegeneration by promoting endosomal maturation. Rapamycin, an autophagy inducer, failed to rescue the TDP-43 pathology in TBK1 mutant motor neurons under stress. Our results further suggest that TBK1 induced TDP-43 pathology could be a consequence of impaired endo-lysosomal pathways rather than autophagy induction mechanisms.

4.2 Introduction

In neurons, when TDP-43 becomes abnormal by misfolding and aggregation, cells possess several clearance pathways to dispose of it. The most studied pathways regarding the clearance of pathological TDP-43 have been autophagy, the UPS system, and the endo-lysosomal pathway [1]. Many efforts have been made to manipulate these pathways to clear the pathological TDP-43 in ALS models. In addition, there are several ongoing clinical trials using autophagy inducers, like rapamycin and lithium, for ALS patients [2,3]. In chapter 3, we identified that TBK1 deficiency-induced TDP-43 pathology has mainly resulted from the impaired endo-lysosomal pathway rather than the autophagy induction mechanism. Therefore, it remains critical to elucidate the therapeutic effect of the endo-lysosomal pathway in TDP-43 pathology and other neurodegenerative phenotypes in the scenario of TBK1 mutations.

In mammalian cells, autophagy is accountable for the clearance of large protein aggregates and dysfunctional organelles [4]. TDP-43 has also been reported to regulate autophagy by increasing the mRNA stability of ATG7, a critical mediator of autophagosome formation [5]. In addition, several ALS-associated genes have been identified to involve in autophagy, including *SQSTM1, OPTN, C9orf72, VCP, FIG4, UBQLN2*, and *TBK1*. Previous research has reported the accumulation of 25-KDa C-terminal fragment of TDP-43 upon autophagy inhibition [6]. These findings support the theory that pathological TDP-43 aggregation could be related to impaired autophagy activity, and autophagy induction could counteract this effect. However, some reports challenged the therapeutic potential of certain autophagy inducers. Previous research showed that rapamycin did not affect the pathological TDP-43 clearance in HEK293 cells [7]. In addition, rapamycin was reported to have detrimental effects in yeast when TDP-43 was overexpressed. Therefore, it remains unclear whether autophagy would be a potential therapeutic target against TDP-43 pathology.

In the previous chapter, we showed that the inhibition of lysosomal function, rather than

autophagy induction, could recapitulate the insoluble TDP-43 accumulations in human motor neurons. We found the impaired endo-lysosomal pathway in TBK1 deficient motor neurons, suggesting an attractive therapeutic target for the clearance of pathological TDP-43. In this chapter, we sought to explore the promising therapeutic targets for the loss or reduction of TBK1 activity in human motor neurons. In addition, we derived two iPSC lines from ALS patients with TBK1 mutations and found that TBK1 patient-derived motor neurons had TDP-43 pathology under lysosomal stress, further confirming the endo-lysosomal mechanism of TDP-43 pathology. Furthermore, we compared the effect of autophagy inducer and RAB5 activator on TDP-43 pathology and motor neuron survival in TBK1 mutant motor neurons. Our results provided therapeutic insights on manipulating the endo-lysosomal pathway to clear pathological TDP-43 and might guide future clinical trials using autophagy inducers for ALS patients with TBK1 mutations or TDP-43 pathology.

4.3 Results

4.3.1 TBK1 restoration re-sustained TDP-43 and motor neuron homeostasis

Our results thus far suggest that eliminating TBK1 expression in human motor neurons disrupted TDP-43 homeostasis and the endo-lysosomal pathway and caused impaired homeostatic functions. To reassure these phenotypes were the functional results of TBK1 ablation and if the detrimental effects were reversible, we restored TBK1 expression by introducing the inducible TRE3G vector system containing the full-length TBK1 cDNA into the TBK1$^{-/-}$ cells [8] (Figure 4.1 a). Upon doxycycline (dox) induction, we found that TBK1 and p-TBK1 expression was partially restored (about 50%), with p62 levels reduced in TBK1$^{-/-}$ motor neurons by protein blot analysis (Figure 4.1 b-d). To determine whether TBK1 restoration could restore lysosomal function, we performed flow cytometry to quantify lysosomal acidification levels using LysoTracker Red (Figure 4.2 a). TBK1 restoration ultimately rescued the acidification level of lysosomes

(Figure 4.2 b), highlighting the critical role of TBK1 in maintaining lysosomal functions in motor neurons. In addition, we examined the number of RAB5-positive vesicles, which we found to be accumulated in TBK1$^{-/-}$ motor neurons upon TBK1 restoration (Fig. 7f). Restoration of TBK1 decreased RAB5 vesicle numbers and increased lysosomal enzymatic activity (Fig. 7g and Supplementary Fig. 7d,e), suggesting the impaired endosomal maturation and endo-lysosomal pathway have been reversed by TBK1 restoration.
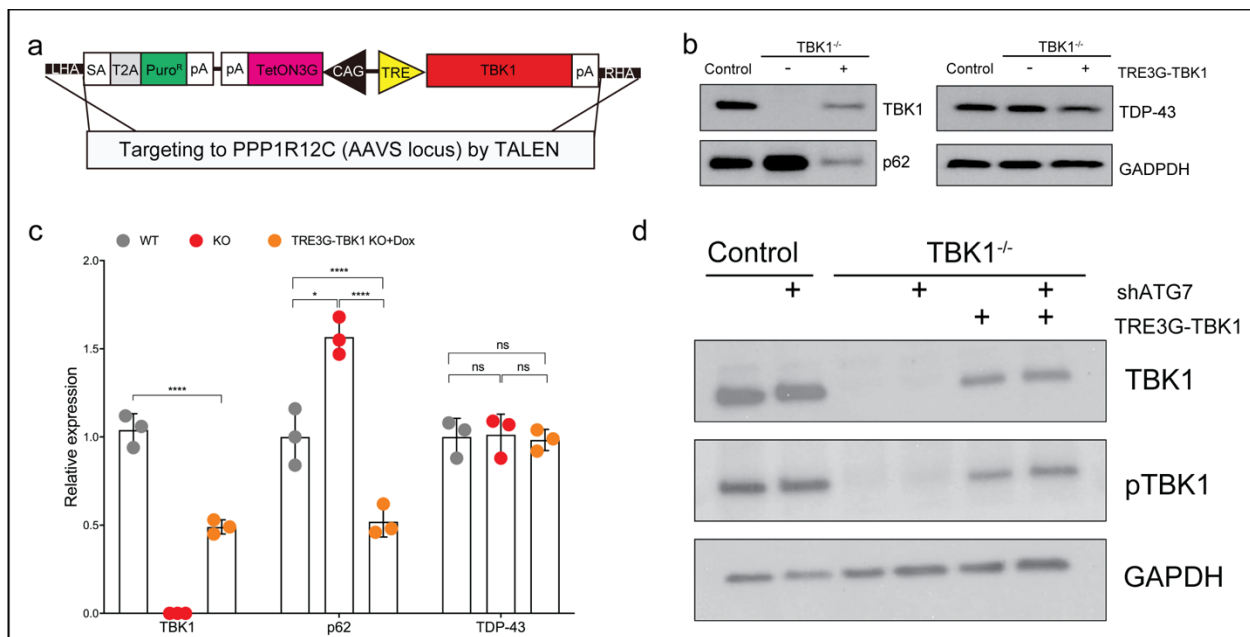

Figure 4.1 Restoration of TBK1 by TRE3G inducible system in TBK1 deficient cells.

(a) Strategy used to insert full-length WT-TBK1 gene at the AAVs locus by TALEN. The TRE-TetON3G (TRE3G) system is used for doxycycline-inducible TBK1 expression. (b) Western blot analysis of TBK1, p62, and TDP-43 expression in control, TBK1$^{-/-}$, and TBK1$^{-/-}$ + TRE3G-TBK1 motor neurons. (c) Quantifications of TBK1, p62, and TDP-43 levels from (b) are shown. GAPDH is used as the loading control for normalization. (d) Immunoblot analysis of TBK1 and pTBK1 expression in control and TBK1-/- motor neurons with and without TBK1 restoration.
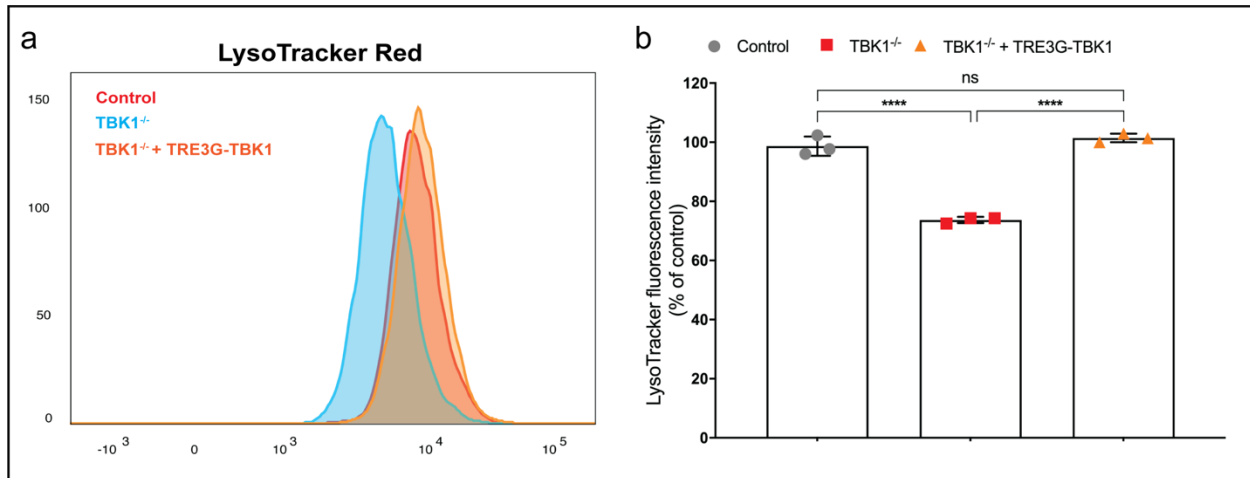
Figure 4.2 TBK1 restoration restored lysosomal acidification in TBK1 deficient motor neurons.

(a) Flow cytometry analysis of LysoTracker Red staining in control, TBK1$^{-/-}$, and TBK1$^{-/-}$ + TRE3G-TBK1 motor neurons. (b) Quantifications of the intensity of LysoTracker Red in control, TBK1$^{-/-}$, and TBK1$^{-/-}$ + TRE3G-TBK1 motor neurons from (a) are shown.
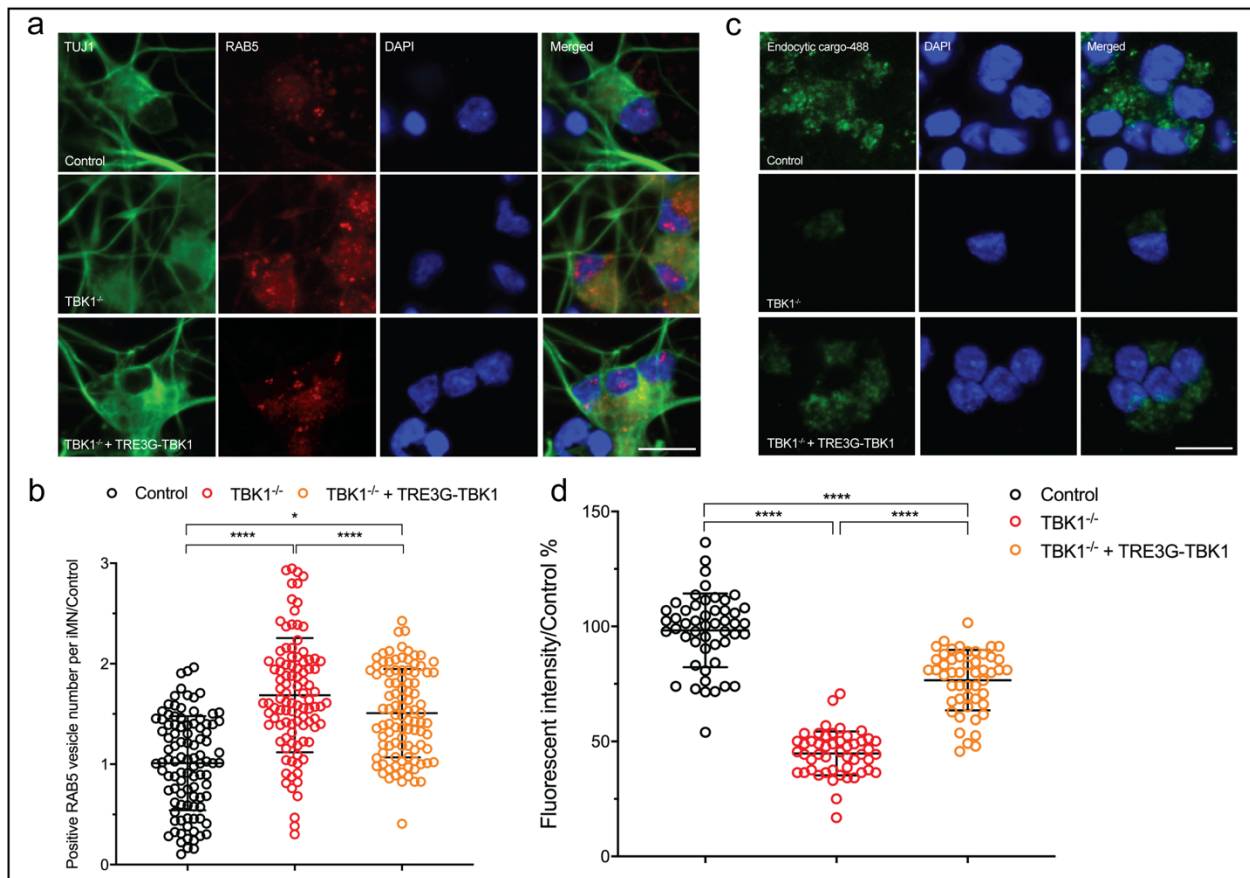
Figure 4.3 TBK1 restoration restored endo-lysosomal pathways in TBK1 deficient motor neurons.

(a) Representative images of control, TBK1$^{-/-}$, and TBK1$^{-/-}$ + TRE3G-TBK1 motor neurons for RAB5$^+$ vesicles. All cells are stained by DAPI and neuronal marker TUJ1. Scale bar, 20 μm. (b) Quantifications of the positive vesicle numbers in TBK1$^{-/-}$ and TBK1$^{-/-}$ + TRE3G-TBK1 motor neurons from (a) are shown. Quantifications are normalized to control human motor neurons. (c) Lysosome enzymatic activity assay in control, TBK1$^{-/-}$, and TBK1$^{-/-}$ + TRE3G-TBK1 motor neurons. The self-quenched substrate is used as endocytic cargo, and the fluorescence signal generated by lysosomal degradation is proportional to the intracellular lysosomal activity. (d) Quantifications of the relative fluorescent intensity from (c) are shown.

Next, we examined whether restoring TBK1 could alleviate TDP-43 pathology and early-stage neurodegenerative phenotypes in TBK1$^{-/-}$ motor neurons. We performed ICC analysis using endogenous TDP-43 antibody and calculated the correlation coefficient of TDP-43 to DAPI staining in control, TBK1$^{-/-}$, and the TBK1 restoration (TBK1$^{-/-}$ + TRE3G-TBK1) motor neurons (Figure 4.4 a,b). Despite the loss of TBK1 activity in the mutant motor neurons, the subsequent restoration of TBK1 expression attenuated the cytoplasmic localization of TDP-43 (p<0.0001) (Figure 4.4 a,b). In addition, TBK1 restoration almost completely rescued the insoluble TDP-43 accumulations in TBK1$^{-/-}$ motor neurons upon lysosomal stress (Figure 4.4 c,d). Therefore, our results show that the expression level of TBK1 negatively correlates with the TDP-43 pathology, and TDP-43 pathology is a functional consequence of TBK1 deficiency. In addition, restoration of TBK1 rescued TDP-43 pathology in the TBK1 loss-of-function models.
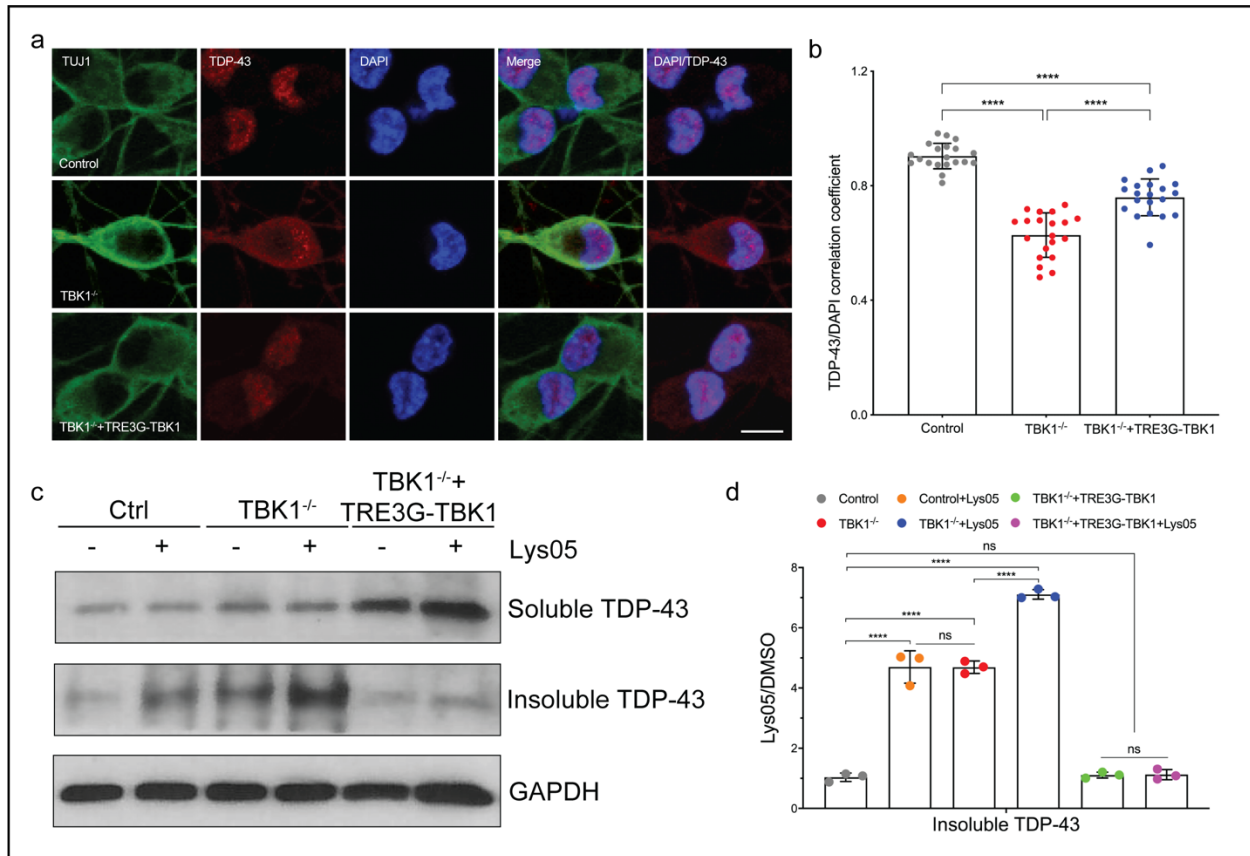
Figure 4.4 Restoration of TBK1 rescues TDP-43 pathology in the loss-of-function models.

(a) Representative images of control, TBK1$^{-/-}$, and TBK1$^{-/-}$ + TRE3G-TBK1 motor neurons for quantification of TDP-43 localization. All cells are stained by DAPI, TDP-43, and neuronal marker TUJ1. Scale bar, 20 µm. (b) Quantifications of the TDP-43/DAPI correlation coefficient from (a) are shown. (c) Western blot analysis of control, TBK1-/-, and TBK1-/- + TRE3G-TBK1 motor neurons treated with DMSO or Lys05. Accumulations of TDP-43 proteins are shown in the soluble (RIPA) and insoluble (urea) fractions. GAPDH in the soluble fraction is used as the loading control for normalization. (d) Quantifications of insoluble TDP-43 expression between DMSO and Lys05 treated hMNs are shown.

111

We next tested whether decreased motor neuron survival upon Baf A1 treatment and the early-stage neurodegenerative phenotypes found in TBK1$^{-/-}$ motor neurons could be alleviated by restoring TBK1 expression. To do this, we treated motor neurons with DMSO or 100 nM Baf A1 on Day 2, and the cell survival assay was performed on Day 5 (Figure 4.5 a). Remarkably, although Baf A1 treatment sensitized TBK1$^{-/-}$ motor neurons to neuronal death, partial restoration of TBK1 significantly re-sustained the motor neuron survival ($p<0.0001$) (Figure 4.5 b). Thus, restoration of functional TBK1 activity protected the vulnerable motor neurons from degeneration under stress. In addition, the mean firing ($p<0.0001$) and bursting frequency ($p<0.05$) were reduced in the TBK1$^{-/-}$ hyperexcitable motor neurons (Figure 4.5 c), indicating TBK1 restoration re-sustained the electrophysiological properties in motor neurons.

To confirm if TBK1 restoration could also rescue the axonal repair, the axotomy experiment was conducted on Day 9 after motor neuron differentiation (Figure 4.5 d). Restoration of TBK1 promoted motor neurons' ability to regenerate after axotomy in TBK1$^{-/-}$ motor neurons ($p<0.0001$) (Figure 4.5 e,f). Therefore, restoring TBK1 in the loss-of-function model re-sustained endo-lysosomal functions, TDP-43 homeostasis, and the physiological function of motor neurons. Our results suggest that the TDP-43 pathology and the functional consequences caused by TBK1 deficiency are reversible in human motor neurons, and functional TBK1 restoration could potentially rescue disease pathology in ALS patients with TBK1 mutations.
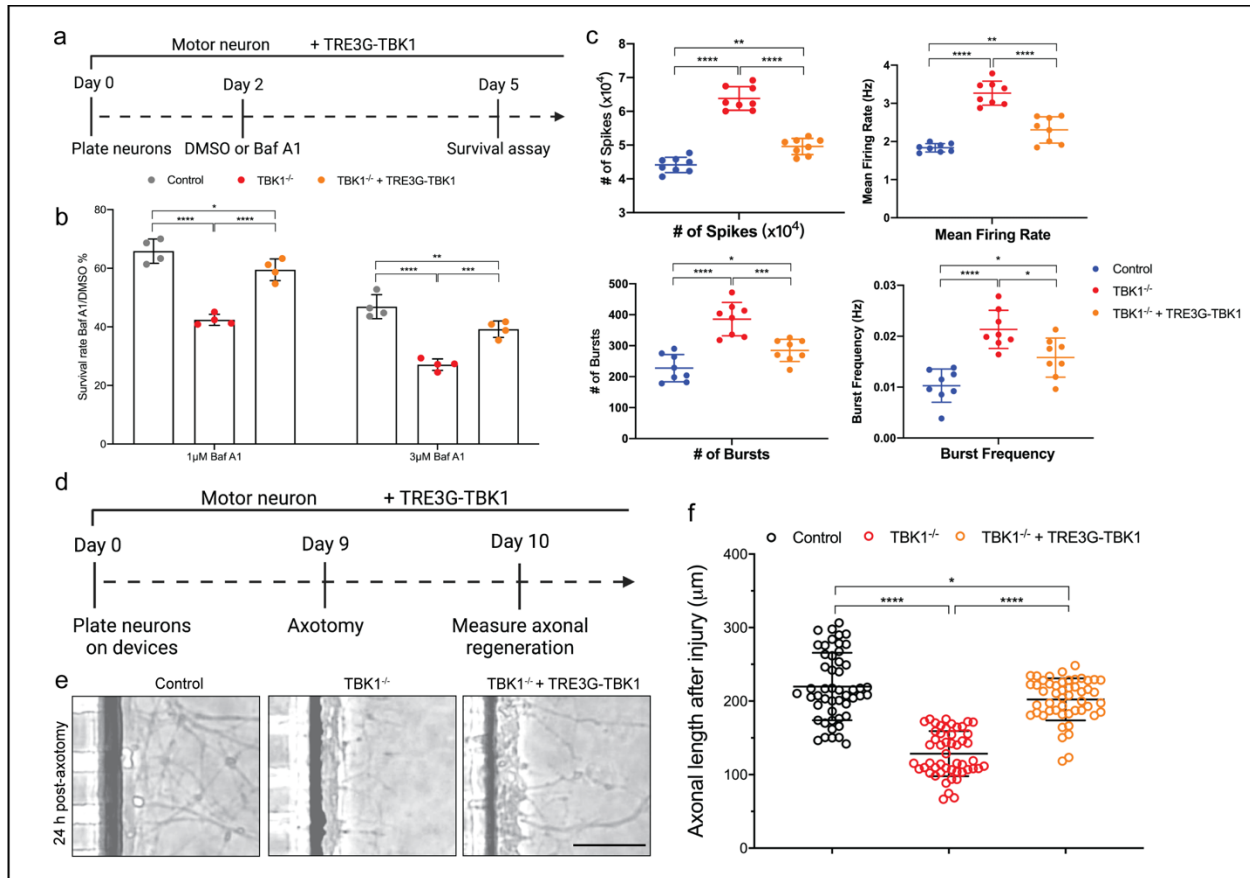
Figure 4.5 TBK1 restoration rescued the physiological functions of human motor neurons.

(a) Experimental outline of cell survival assays in hMNs. Motor neurons are differentiated, and DMSO or 100 mM Baf A1 is added on Day 2. Cell survival assay is performed on Day 5. (b) The number of living cells is measured on Day 5 for survival assay. The survival rate of cells treated with Baf A1 is normalized to the DMSO control. (c) Analysis of MEA recordings on Day 28 in culture. Compared to TBK1$^{-/-}$ motor neurons, spike numbers and mean firing rate are reduced in TBK1$^{-/-}$ + TRE3G-TBK1 motor neurons. (d) Experimental outline of axotomy assays in human motor neurons. (e) Representative images of axonal sprouting in control, TBK1$^{-/-}$, and TBK1$^{-/-}$ + TRE3G-TBK1 motor neurons from both pre- and post-axotomy conditions. Scale bar: 500 μm. (f) Quantifications of axonal regrowth length for control, TBK1$^{-/-}$, and TBK1$^{-/-}$ + TRE3G-TBK1 motor neurons are shown.

4.3.2 TBK1 patient motor neurons did not show TDP-43 pathology

In the previous chapter, our results suggested the crucial role of TBK1 in maintaining TDP-43 homeostasis and motor neuron health and showed that loss of TBK1 activity is sufficient to drive ALS-associated phenotypes in human motor neurons. However, homozygous mutations of TBK1 are embryonic lethal, and TBK1 is haploinsufficient in ALS and FTD patients [9]. To determine whether haploinsufficiency of TBK1 in patient motor neurons was sufficient to recapitulate ALS disease pathology, we generated induced pluripotent stem cells (iPSCs) from two ALS patients (MGH-138 and MGH-142) with TBK1 mutations and induced them into motor neurons (Figure 4.6 a). Sanger sequencing confirmed the missense mutation of p.Leu306Ile (L306I) and deletion of p.Glu463Serfs (E463Sfs) in MGH-138a and MGH-142a, respectively (Figure 4.6 b). Both mutations showed reduced p-TBK1 expression, confirming the TBK1 haploinsufficiency model (Figure 4.6 c). In addition, p62 was increased in both 138a and 142a motor neurons, suggesting defects of autophagy in both patient cell lines (Figure 4.6 c). To further investigate if p62 showed a similar accumulation pattern as in our TBK1 deficiency models, we performed ICC for p62 in control, 138a, and 142a motor neurons (Figure 4.6 d). Consistent with our previous results, p62 puncta was accumulated in TBK1 patient motor neurons (Figure 4.6 e), suggesting haploinsufficiency of TBK1 is sufficient to cause impaired autophagy activity in human motor neurons.

Notably, the TBK1$^{-/-}$ cells with TBK1 restoration also showed about 50% of TBK1 protein expression, however, these two cell lines were inherently different in the expression pattern of TBK1. The TBK1-/- cells with TBK1 restoration express 50% of normal TBK1 proteins, while the iPSCs express 50% of normal TBK1 proteins and 50% of mutant or inactive forms of TBK1 proteins. The inactive forms of TBK1 proteins might be more pathological than no TBK1 expression [10].
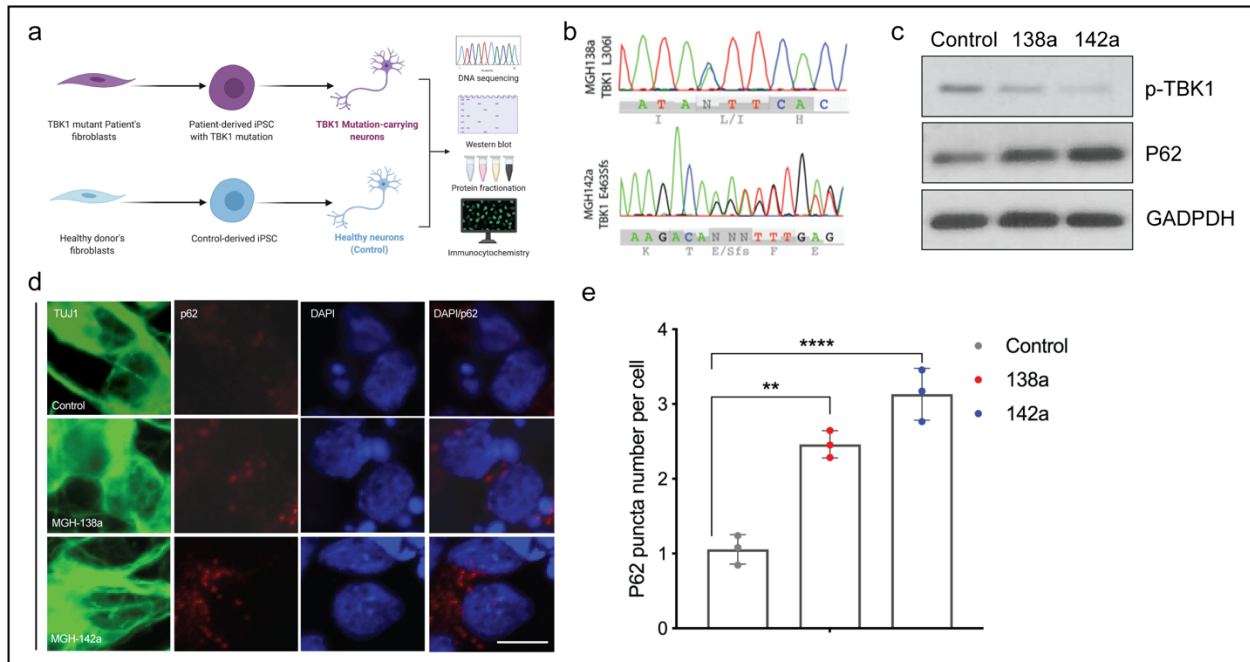
Figure 4.6 Impaired endosomal trafficking in TBK1$^{-/-}$ motor neurons identified by phospho-proteomics.

(a) Schematic illustration showing the generation of iPSCs and induced hMNs from TBK1 mutant patients and healthy controls. (b) Sanger sequencing validation of MGH-138a and MGH-142a patient-derived iPSCs. (c) Western blot analysis of p-TBK1 and p62 expression in healthy controls and TBK1 patient (138a and 142a) motor neurons. (d) Immunostaining of p62 for control, 138a, and 142a motor neurons. Scale bar, 20 μm. (e) Quantifications of p62 puncta number per cell in control, 138a, and 142a motor neurons.

To investigate whether haploinsufficiency of TBK1 could trigger TDP-43 pathology or motor neuron death in human motor neurons, we examined the localization and accumulation of TDP-43 in both TBK1 patient motor neurons compared to healthy controls (MGH-15b, 17a, 18a). We first performed ICC for endogenous TDP-43 in control, 138a, and 142a motor neurons. Surprisingly, the TBK1 patient-derived motor neurons did not display TDP-43 mislocalization as was shown in our TBK1 deficient motor neurons (Figure 4.7 a,b). In addition, we investigated the insoluble TDP-43 accumulations in control, 138a, and 142a motor neurons by immunoblotting.

Reduced TBK1 activity in both patient-derived lines showed a similar level of insoluble TDP-43 as in control motor neurons, indicating that haploinsufficiency of TBK1 could not induce TDP-43 pathology in human motor neurons. Furthermore, to determine if reduced TBK1 activity recapitulates motor neuron degeneration in ALS processes, we examined the survival of patient and control hMNs. Consistent with our previous results, haploinsufficiency of TBK1 in patient-derived hMNs did not affect neuronal survival in culture (Figure 4.7 e).
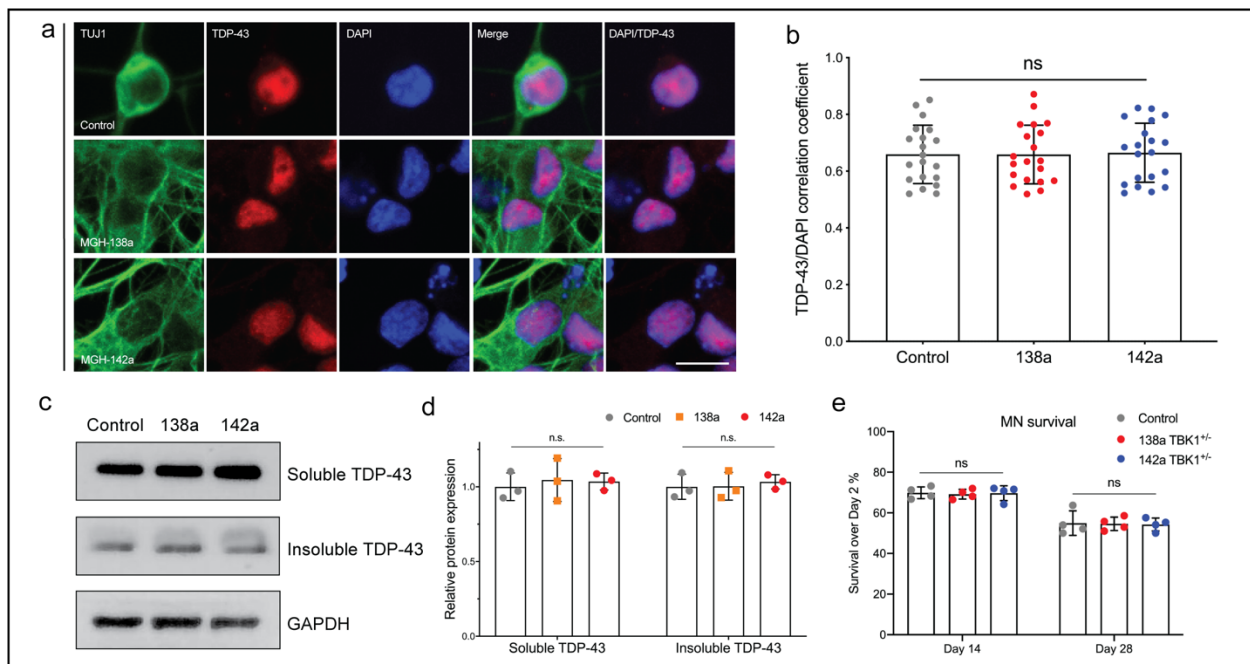
Figure 4.7 TBK1 patient-derived motor neurons do not show TDP-43 pathology or neurodegeneration.

(a) Immunostaining of endogenous TDP-43 for control, 138a, and 142a motor neurons. Scale bar, 20 µm.

(b) Quantifications of the TDP-43/DAPI correlation coefficient from (a) are shown. (c) Western blot analysis of soluble and insoluble TDP-43 expression in control and TBK1 patient (138a and 142a) motor neurons.

(d) Quantifications of soluble and insoluble TDP-43 in control, 138a, and 142a motor neurons. (e) The survival rate of control, 138a TBK1^{+/-}, and 142a TBK1^{+/-} hMNs on Day 14 and Day 28 compared to Day 2.

4.3.3 TBK1 mutations sensitized motor neurons to lysosomal stress

In the previous chapter, we found that TBK1 interacted with EEA1 and was needed for the endosome-lysosome pathway in motor neurons, and TBK1 deficiency leads to the accumulations of toxic proteins that are inadequately cleared by lysosomes. To confirm the critical role of the endo-lysosomal pathway in TDP-43 pathology, we stimulated the motor neuron cultures with lysosomal stress (1 µM Lys05, 48 hr treatment). This treatment initiated a significant increase of RAB5-positive vesicles in patient-derived, but not in control, motor neurons ($p<0.0001$) (Figure 4.8 a,b), suggesting that the endo-lysosomal pathway was more vulnerable to lysosomal stress in TBK1 mutant motor neurons. In addition, we investigated TDP-43 pathology in control and TBK1 mutant motor neurons under lysosomal stress. Surprisingly, lysosomal stress sensitized TBK1 mutant motor neurons to TDP-43 mislocalization and insoluble accumulations compared to control motor neurons (Figure 4.8 c-e). Notably, to investigate whether lysosomal stress could sensitize TBK1 mutant motor neurons to neurodegeneration, the most important end-point disease phenotype in ALS, we assayed the cell survival rate for control, 138a, and 142a motor neurons with Lys05 treatment at different doses. Lys05 treatment had little effect on the survival of control human motor neurons (Figure 4.8 f). However, TBK1 patient-derived motor neurons showed diminished cell survival under lysosomal stress in a dose-dependent manner (Figure 4.8 f), suggesting that lysosomal stress could be a key environmental factor that might affect TDP-43 homeostasis and the survival of motor neurons with TBK1 mutations.
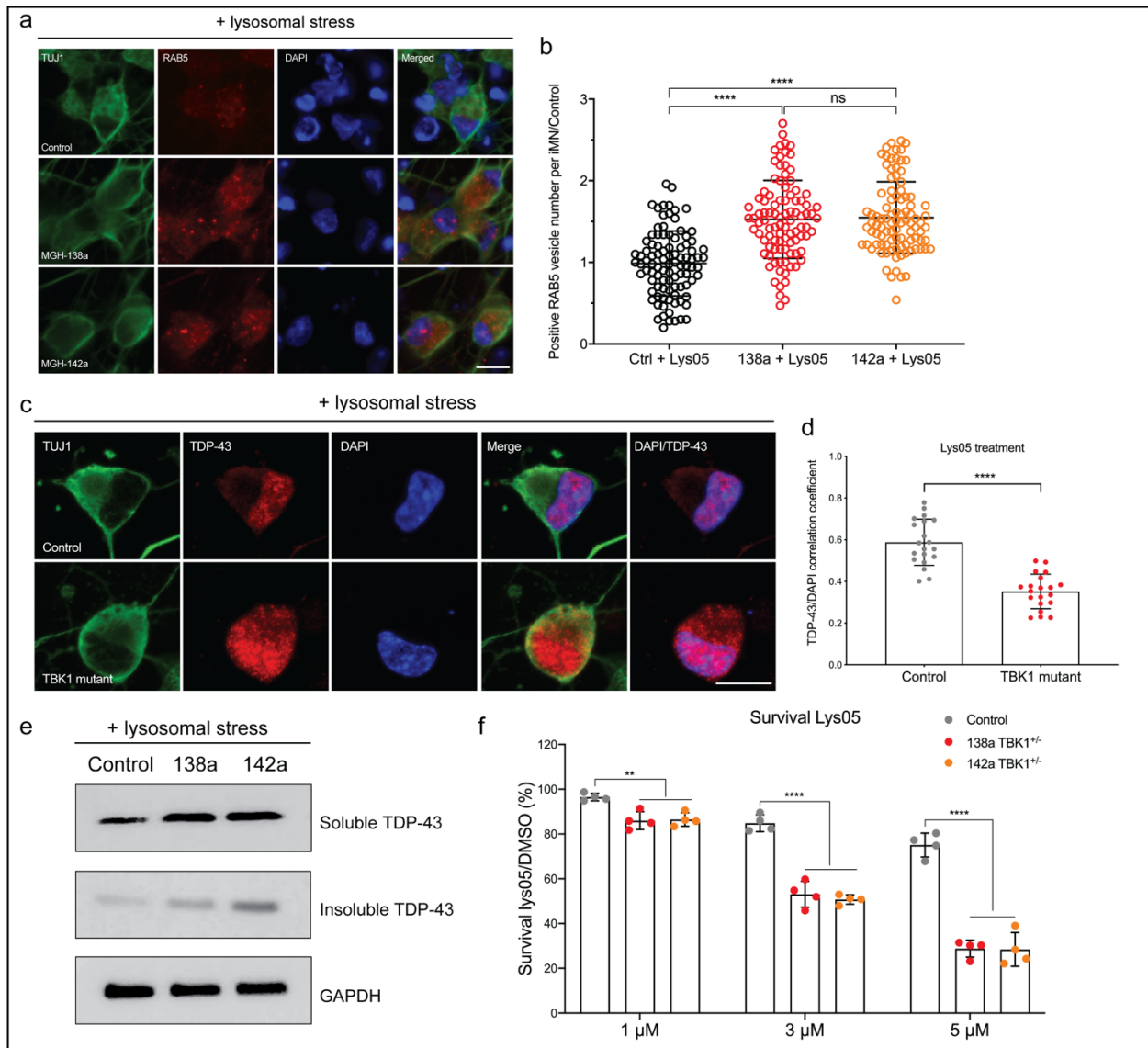
Figure 4.8 Lysosomal stress sensitizes TBK1 patient motor neurons to TDP-43 pathology and neurodegeneration.

(a) Representative images of control, 138a, and 142a motor neurons treated with Lys05 for vesicle number quantification of RAB5. All cells are stained by DAPI and neuronal marker TUJ1. Scale bar, 20 μm. (b) Quantifications of the positive RAB5 vesicle numbers in TBK1$^{-/-}$ hMNs from (a) are shown. (c) Representative images of control and TBK1 mutant motor neurons treated with Lys05 for endogenous TDP-43. All cells are stained by DAPI and neuronal marker TUJ1. Scale bar, 20 μm. (d) Quantifications of the TDP-43/DAPI correlation coefficient from (c) are shown. (e) Western blot analysis of soluble and insoluble TDP-43 expression in healthy controls and TBK1 patient (138a and 142a) motor neurons under lysosomal

stress. (f) The survival rate of control, 138a, and 142a motor neurons under lysosomal stress on Day 14 and Day 28 compared to Day 2.

4.3.4 TBK1 patient motor neuron pathology could be rescued by PIKFYVE inhibition

To confirm the link between impaired lysosomal functions and motor neuron degeneration, we use a small molecule, Apilimod, for targeting endosomal maturation and lysosomal functions. Apilimod is a PIKFYVE kinase inhibitor which inhibits the conversion of phosphatidylinositol 3-phosphate (PI3P) into phosphatidylinositol (3,5)-bisphosphate (PI(3,5)P2) [11]. PI3P anchors EEA1 to early endosomes to promote endosomal maturation and drives the fusion of lysosomes with autophagosomes and endosomes [12,13]. Thus, the inhibition of PIKFYVE kinase could promote endo-lysosomal functions and might compensate for reduced TBK1 activity-mediated motor neuron pathology (Figure 4.9 a). To confirm whether PIKFYVE inhibition could restore the endo-lysosomal pathway impaired in TBK1 mutant motor neurons under stress, we examined the RAB5 vesicles in TBK1 mutant motor neurons with and without apilimod, a PIKFYVE inhibitor, under lysosomal stress. The addition of Apilimod reduced the accumulated RAB5 vesicles, indicating the restoration of endosomal fusion and lysosomal degradation (Figure 4.9 b).

To further determine whether TDP-43 pathology and patient motor neuron survival could be rescued by restoring the endo-lysosomal pathway rather than the autophagy induction pathway, we examined the TDP-43 pathology in *TBK1* mutant motor neurons with Rapamycin. This autophagy inducer is being used in ongoing ALS trials, or with Apilimod. Interestingly, cytoplasmic TDP-43 localization was rescued by Apilimod, but not by Rapamycin, in TBK1 patient motor neurons (Figure 4.9 c,d), further confirming the critical role of the endo-lysosomal pathway in maintaining TDP-43 homeostasis. In addition, the insoluble form of TDP-43 that was found to be accumulated in TBK1 mutant motor neurons under stress could be rescued by Apilimod rather than Rapamycin (Figure 4.9 e).

Next, we tested the neuronal survival for stressed control and patient motor neurons

treated with Apilimod and Rapamycin treatment. Apilimod almost completely rescued patient-derived motor neuron survival under lysosomal stress, while Rapamycin treatment had no effect on the survival of stressed patient motor neurons (Figure 4.9 f). Therefore, the enhanced endo-lysosomal pathway by PIKFYVE kinase inhibition could rescue TDP-43 pathology and neurodegeneration caused by lysosomal stress in the TBK1 patient motor neurons, further supporting the endo-lysosomal mechanism of disease pathology caused by TBK1 deficiency. Furthermore, the fact that TDP-43 pathology and neurodegeneration could not be rescued by autophagy induction provided guidance for future therapeutic targets in *TBK1* mutant ALS patients.
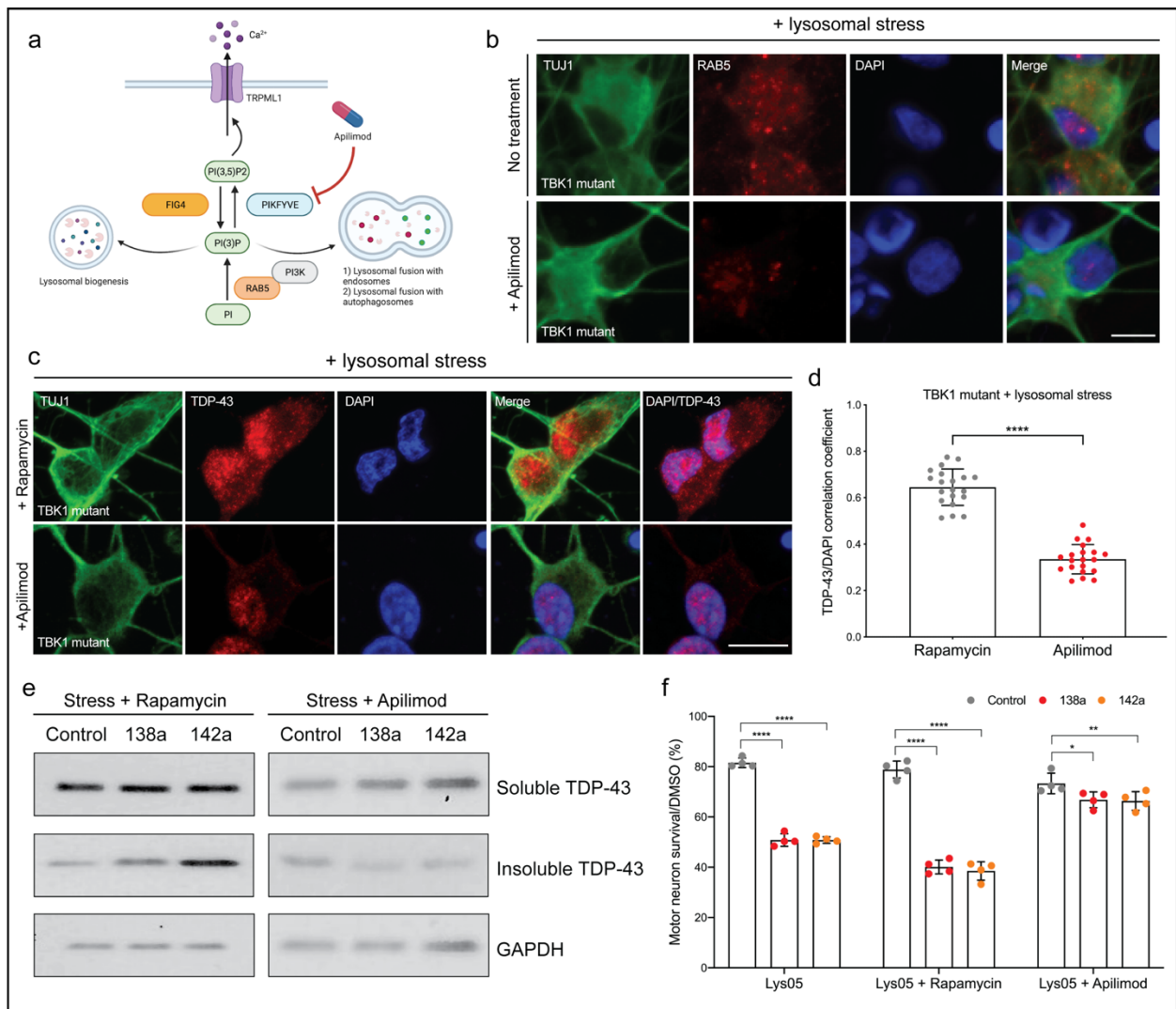
Figure 4.9 TDP-43 pathology and neurodegeneration can be rescued by PIKFYVE kinase inhibitor in TBK1 patient motor neurons.

(a) The mechanistic activity of Apilimod in regulating vesicle trafficking and lysosomal functions. (b) Representative images of stressed TBK1 mutant motor neurons treated with and without Apilimod for vesicle number quantification of RAB5. All cells are stained by DAPI and neuronal marker TUJ1. Scale bar, 20 μm. (c) Representative images of stressed TBK1 mutant motor neurons treated with Rapamycin or Apilimod for endogenous TDP-43. All cells are stained by DAPI and neuronal marker TUJ1. Scale bar, 20 μm. (d) Quantifications of the TDP-43/DAPI correlation coefficient from (c) are shown. (e) Western blot analysis of soluble and insoluble TDP-43 expression in stressed control and TBK1 patient (138a and 142a) motor neurons treated with Rapamycin or Apilimod. (f) The survival rate of stressed control, 138a, and 142a motor neurons treated with Rapamycin or Apilimod on Day 14.

4.4 Discussion and implications

In this chapter, we explored the methods for rescuing TBK1 deficiency-induced pathology in motor neurons. To this end, we first tried to restore TBK1 expression in our loss-of-function model. TBK1 restoration rescued TDP-43 pathology and the physiological properties of motor neurons that were disrupted by TBK1 deficiency. The TBK1 restoration results first confirmed that the detrimental effects observed in our loss-of-function model were the consequences of TBK1 deficiency, not of some off-target effects caused by gene editing. In addition, the fact that TBK1 deficiency induced TDP-43 pathology and motor neuron physiology could be reversed by TBK1 restoration-is more encouraging for future therapeutics in the ALS field. Previous research showed that mutations or abnormal post-translational modifications of TDP-43 could lead to the formation of irreversible aggregation via liquid-solid phase separation [14]. Our results demonstrated that the mislocalization of TDP-43 and its insoluble aggregation could, at least in part, be reversed by restoring functional TBK1 activity in TBK1 deficient motor neurons, providing evidence for future therapeutics to target TBK1 or downstream mechanisms in ALS patients.

In addition, we derived iPSCs from ALS patients with TBK1 mutations to study the effect of TBK1 haploinsufficiency on TDP-43 pathology and neurodegeneration. Haploinsufficiency of TBK1 did not cause TDP-43 pathology or neurodegeneration in human motor neurons, which is consistent with previous research using mouse models [15]. In our TBK1 patient motor neurons, haploinsufficiency was sufficient to cause impaired autophagy but could not initiate TDP-43 pathology, indicating that inducing autophagy might not be an ideal therapy for ALS patients. However, when motor neurons were under lysosomal stress, the TBK1 patient motor neurons displayed TDP-43 pathology and increased neurodegeneration compared to control motor neurons. These results supported our previous claim that TDP-43 pathology might be induced by impaired endo-lysosomal pathway when TBK1 was deficient.

The strong connections between impaired endo-lysosomal pathway and TDP-43 pathology in human motor neurons inspired us to explore potential therapeutic targets for TDP-43 pathology and ALS patients. A previous study has suggested the role of LAM-002 (Apilimod), an inhibitor of the PIKfyve kinase, in clearing toxic protein aggregates within lysosomes [16]. Mechanistically, LAM-002 is a RAB5 effector, and it activates the transcription factor EB, which in turn promotes endosomal maturation by increasing PI3P levels [17]. Therefore, modulating the RAB5 effector could potentially enhance the endo-lysosomal pathway and might compensate for the detrimental effects caused by reduced TBK1 activity. To validate our hypothesis, we compared the effects of Apilimod, together with Rapamycin, on rescuing TDP-43 pathology and the neurodegeneration phenotype observed in stressed TBK1 patient motor neurons. Intriguingly, Apilimod almost completely rescued the TDP-43 pathology and the neurodegeneration phenotype in the TBK1 patient motor neurons with stress, while Rapamycin had no therapeutic effect on these disease-relevant pathologies. Our results provided strong evidence for supporting pre-clinical validations of PIKfyve inhibitors in ALS patients with TBK1 mutations. In addition, Rapamycin and other autophagy inducers have been used in ongoing clinical trials to treat ALS

patients, while our results suggest the opposite. We should consider the genetic background of the patients, such as with TBK1 mutations, for more targeted therapeutics and better treatment outcomes.

4.5 Experimental procedures

Human pluripotent stem cell lines

The HUES3 Hb9::GFP and iPSC control 11a, 15b, 17a, and 18a used in this study were previously approved by the institutional review boards of Harvard University. Patient fibroblasts of MGH-138a and 142a were obtained from Massachusetts General Hospital (MGH) and converted into iPSCs at Harvard Stem Cell Institute. Specific point mutations were confirmed by PCR amplification followed by Sanger sequencing. Our lab screens for mycoplasma contamination weekly using the MycoAlert kit (Lonza), with no cell lines used in this study testing positive. The use of these cells at Harvard was further approved and determined not to constitute Human Subjects Research by the Committee on the Use of Human Subjects in Research at Harvard University.

Cell Culture and differentiation

Pluripotent stem cells were cultured with mTeSR plus medium (Stem Cell Technologies) on Matrigel (BD Biosciences) coated tissue culture dishes. Stem cells were maintained in 5% CO_2 incubators at 37 °C and passaged as small aggregates after 1mM EDTA treatment. After dissociation, 10 µM ROCK inhibitor (Sigma, Y-27632) was added to cell culture for 24 hr to prevent cell death, and then incubated with lentiviruses (FUW-M2rtTA, TetO-Ngn2-Puro). The HUES3 Hb9::GFP cell line has been previously described [18]. Motor neurons were differentiated using a modified protocol based on previous strategies [19,20]. This protocol relies on neural induction through NGN2 programming, SMAD inhibition through small molecules, and motor neuron

patterning through retinoic activation and Sonic Hedgehog signaling. In brief, hESCs were dissociated into single cells using accutase (Stem Cell Technologies), and then plated on Matrigel-coated culture dish at a density of 80,000 cells per cm^2 with mTeSR plus medium (Stem Cell Technologies) supplemented with 10 µM ROCK inhibitors (Sigma, Y-27632). When cells reached confluency, medium was changed to N2 medium (DMEM-F12 (Life Technologies) supplemented with ×1 Gibco GlutaMAX (Life Technologies), ×1 N-2 supplement (Gibco), × 0.3% Glucose) on Day 1-3. For small molecule treatment, 10 µM SB431542 (Custom Synthesis), 100 nM LDN-193189 (Custom Synthesis), 1 µM retinoic acid (Sigma), 1 µM SAG (Custom Synthesis) were added on Day 1-3. For NGN2 induction and neuron selection, 20 mg/ml Doxycycline and 10 mg/ml puromycin were added on Day 2-3. On Day 4-7, the N2 medium was changed to Neurobasal (Neurobasal (Life Technologies) supplemented with ×1 N-2 supplement (Gibco), ×1 B-27 supplement (Gibco), ×1 Gibco GlutaMAX (Life Technologies) and 100 µM non-essential amino-acids: NEAA) along with 1 µM retinoic acid, 1 µM SAG, 20 mg/ml Doxycycline, 10 mg/ml puromycin, and 10 ng/ml of neurotrophic factors: glial cell-derived neurotrophic factor (GDNF), ciliary neurotrophic factor (CNTF) and brain-derived neurotrophic factor (BDNF) (R&D). For post-mitotic cell selection, 10 mM 5-Fluoro-2'-deoxyuridine thymidylate synthase inhibitor (FUDR, Sigma) was added on Day 5-7. From Day 8, media was changed to the motor neuron maintenance media containing Neurobasal (Neurobasal (Life Technologies) supplemented with ×1 N-2 supplement (Gibco), ×1 B-27 supplement (Gibco), ×1 Gibco GlutaMAX (Life Technologies) and 100 µM non-essential amino-acids: NEAA) supplemented with 10 ng/ml of neurotrophic factors (GDNF, CNTF, and BDNF) and 10 mM FUDR. Half of the maintenance media was changed every two days.

Cell viability assay

Motor neuron viability assay was performed based on the CellTiter-Glo luminescent for each sample according to the manufacturer's recommendations (Promega G7570). In brief, motor

neurons were plated in triplicate onto 96-well plates. After treatment incubation, motor neurons were incubated for 10 min with CellTiter-Glo reagent at room temperature, and luminescence was measured using the Cytation imaging reader (BioTek). Background luminescence was measured using medium without cells and then subtracted from experimental values.

Immunocytochemistry and imaging

For immunocytochemistry, cells were fixed with 4% PFA for 20 min, and were subject to permeabilization with 0.25% Triton-X in PBS for 40 min. After that, cells were blocked using 10% donkey serum supplemented with 0.1% Triton-X in PBS (blocking buffer) for 1 hr at room temperature. Primary antibody diluted in blocking buffer was used for cell incubation overnight at 4 °C. At least three washes (5 min incubation each) with PBS were carried out, before incubating the cells with secondary antibodies (diluted in blocking buffer) for 1 hr at room temperature. Nuclei was stained with DAPI. The following antibodies were used in this study: TBK1 (1:200, Abcam ab109735), SQSTM1 / p62 (1:200, Abcam ab56416), TDP-43 (1:200, Proteintech Group 10782 & Cell Signaling Technology 3448S), Islet1 (1:500, Abcam ab20670), MAP2 (1:10,000, Abcam ab5392), TUJ1 (1:1,000, R&D Systems MAB NL493), EEA1 (1:100, Cell Signaling Technology 3288 & BD Biosciences 610456), RAB5 (1:100, Cell Signaling Technology 46449S), RAB7 (1:100, Cell Signaling Technology 9367S), LAMP1 (1:100, Abcam ab25630), phospho-TBK1 (1:200, Cell Signaling Technology 13498S). Secondary antibodies used (488, 555, and 647) were AlexaFluor (1:1,000, Life Technologies). Images were acquired using a Zeiss LSM 880 confocal microscope or a Nikon Eclipse Ti microscope. Images were analyzed using ImageJ or NIS- Elements (Nikon).

Western blot assays

For protein extraction, cells were lysed using 1% SDS lysis buffer (PhosphoSolutions, 100-LYS) with a brief sonication. For insoluble protein extraction, cells were lysed using RIPA buffer (Life Technology, 89900) with protease inhibitors (Life Technology, 78425) for 20 min on ice. After

centrifuge, the supernatant was collected as soluble fraction, and the insoluble fraction was collected from the pellet using 8M urea with 4% CHAPS, 40 mM Tris, and 0.2% Bio-Lyte 3/10 ampholyte (Bio-Rad, 1632103). For subcellular fractionation, cells were subject to sequential extract using the subcellular fractionation kit for cultured cell (Thermo Scientific, 78840) according to manufacturer instructions. After sample preparation, equivalent amount of 5-10 µg protein from each ample were subjected to electrophoresis using 4–20% SDS-PAGE (Bio-Rad, 4561096) and then transferred to a PVDF membrane (Thermo Fisher, 88518). The membrane was blocked with 3% Bovine Serum Albumin (Sigma, A9647) for 1 hr at room temperature, and incubated with primary antibodies overnight at 4°C. The next day, membrane was washed in TBST X3, 10 min each, and then incubated with HRP-conjugated secondary antibodies for 1 hr at room temperature. After that, membrane was washed in TBST X3, 10 min each, and then developed using ECL Western Blotting Detection System (VWR, 95038) and blotting films (Genesee Scientific, 30-810).

TDP-43 localization assay

For analysis of correlation coefficient of TDP-43 and nuclei, motor neurons were stained for TDP-43 (Cell Signaling Technology), TUJ1 (R&D Systems), and counterstained with DAPI. TUJ1 staining was used to determine the neuronal cell body, and the Pearson's correlation coefficient was calculated using NIS-Elements (Nikon) for TDP-43 and DAPI with at least 50 neurons being analyzed. Cells were segmented into the nuclear (DAPI positive) and cytoplasmic (DAPI negative) regions by NIS. The TDP-43 intensity in these two regions were used to determine the nuclear to cytoplasmic ratio (correlation coefficient) for TDP-43 fluorescent intensity.

Multi-electrode array (MEA) recordings

Recordings from 64 extracellular electrodes were made using a Maestro (Axion BioSystems) MEA recording amplifier with a head stage that maintained a temperature of 37 °C. In brief, 12-well MEA plates (Axion Biosystems, M768-GL1-30Pt200) were coated with PDL and

laminin. Motor neurons were seeded at a density of 500,000 cells per well and were fed with the motor neuron maintenance media supplemented with 10 ng/ml of neurotrophic factors (GDNF, CNTF, and BDNF) 2-3 times per week. Neuronal activity was measured weekly for 5 min using the Maestro 12-well 64 electrodes per well micro-electrode array (MEA) plate system (Axion Biosystems, Atlanta, GA). Data were sampled at 12.5 kHz, digitized, and analyzed using the Axion Integrated Studio software (Axion Biosystems) with a 200 Hz high pass and 2.5 kHz low pass filter and an adaptive spike detection threshold set at 5.5 times the SD for each electrode with 1 s binning. For each data point presented, four replicates were used for one experiment with 5 minutes recording. These standard settings were maintained for all Axion MEA recording and analysis. We confirmed that we obtained similar results across a wide range of action potential threshold and cluster similarity radius settings. Data was analyzed using the Axion Integrated Studio 2.4.2 and the Neural Metric Tool (Axion Biosystems). For retigabine dose-response experiment, 1 min of recording in each concentration of retigabine were performed. Mean firing rate were detected using the Axion Integrated Studio 2.4.2 with the default settings and analyzed with the Neural Metric Tool.

Axotomy

Standard neuron microfluidic devices (SND150, XONA Microfluidics) were mounted on glass coverslips coated with 0.1 mg/ml poly-L-ornithine (Sigma-Aldrich) and 5 µg/ml laminin (Invitrogen). Motor neurons were cultured on the devices at a concentration of around 250,000 cells per device for 7 days. Axotomy was performed by repeated vacuum aspiration and reperfusion using PBS in the axonal side of the device until all axons were diminished without disturbing the soma side cells. For the experiment, two independent replicates were performed with at least 20 neurites measured.

Lysosomal enzyme activity assay

Control and TBK1$^{-/-}$ motor neurons were incubated with Self-Quenched Substrate (Abcam Cat No. ab234622) following manufacturer's instructions. Briefly, cells were incubated with the substrate for 1hr and fixed with 4% PFA at room temperature for 20 min. After washing with PBS, cells were stained with DAPI and then mounted for imaging with Zeiss LSM880 Confocal Laser Scanning microscope. Images were analyzed using ImageJ. Mean fluorescence intensity was quantified in control and TBK1$^{-/-}$ motor neurons.

TBK1 cDNA plasmid transfection

For TBK1 rescue experiments, targeting vector with doxycycline inducible system was generated. EGFP was replaced with WT TBK1 cDNA (Addgene: #82285) in AAVS1-TRE3G-EGFP (Addgene: #52343) using MluI/SalI sites. The resulting vector was transfected together with TALEN vectors (Addgene: #52341/52342) targeting AAVS locus. TBK1$^{-/-}$ cells were transfected using Neon Transfection System with the vector and screened by puromycin for at least 2 weeks.

Data presentation and statistical analysis.

Comparisons were made between control and TBK1$^{-/-}$ motor neurons using t tests (two-tailed, unpaired)/ANOVA for continuous data and rank tests for nonparametric data. For multiple comparisons, one-way ANOVA to normalize variance and post hoc Tukey tests were used. In all figure elements, bars and lines represent the median with error bars representing standard deviation. The box and whisker plots display the minimum to maximum. Data distribution was assumed to be normal, but this was not formally tested. Significance was assumed at $P < 0.05$. Error bars represent the SD unless otherwise stated. Analysis was performed with the statistical software package Prism 8 (Graph Pad).

References:

1   Hergesheimer, R. C. *et al.* The debated toxic role of aggregated TDP-43 in amyotrophic lateral sclerosis: a resolution in sight? *Brain* **142**, 1176-1194, doi:10.1093/brain/awz078 (2019).

2   Fornai, F. *et al.* Autophagy and amyotrophic lateral sclerosis: The multiple roles of lithium. *Autophagy* **4**, 527-530, doi:10.4161/auto.5923 (2008).

3   Mandrioli, J. *et al.* Rapamycin treatment for amyotrophic lateral sclerosis: Protocol for a phase II randomized, double-blind, placebo-controlled, multicenter, clinical trial (RAP-ALS trial). *Medicine (Baltimore)* **97**, e11119, doi:10.1097/MD.0000000000011119 (2018).

4   Rubinsztein, D. C. The roles of intracellular protein-degradation pathways in neurodegeneration. *Nature* **443**, 780-786, doi:10.1038/nature05291 (2006).

5   Bose, J. K., Huang, C. C. & Shen, C. K. Regulation of autophagy by neuropathological protein TDP-43. *J Biol Chem* **286**, 44441-44448, doi:10.1074/jbc.M111.237115 (2011).

6   Wang, X. *et al.* Degradation of TDP-43 and its pathogenic form by autophagy and the ubiquitin-proteasome system. *Neurosci Lett* **469**, 112-116, doi:10.1016/j.neulet.2009.11.055 (2010).

7   Scotter, E. L. *et al.* Differential roles of the ubiquitin proteasome system and autophagy in the clearance of soluble and aggregated TDP-43 species. *J Cell Sci* **127**, 1263-1278, doi:10.1242/jcs.140087 (2014).

8   Kim, E. *et al.* Systematic Functional Interrogation of Rare Cancer Variants Identifies Oncogenic Alleles. *Cancer Discov* **6**, 714-726, doi:10.1158/2159-8290.CD-16-0160 (2016).

9   Freischmidt, A. *et al.* Haploinsufficiency of TBK1 causes familial ALS and fronto-temporal dementia. *Nat Neurosci* **18**, 631-636, doi:10.1038/nn.4000 (2015).

10   Taft, J. *et al.* Human TBK1 deficiency leads to autoinflammation driven by TNF-induced cell death. *Cell* **184**, 4447-4463 e4420, doi:10.1016/j.cell.2021.07.026 (2021).

11   Cai, X. *et al.* PIKfyve, a class III PI kinase, is the target of the small molecular IL-12/IL-23 inhibitor apilimod and a player in Toll-like receptor signaling. *Chem Biol* **20**, 912-921,

doi:10.1016/j.chembiol.2013.05.010 (2013).

12   Lemmon, M. A. Membrane recognition by phospholipid-binding domains. *Nat Rev Mol Cell Biol* **9**, 99-111, doi:10.1038/nrm2328 (2008).

13   Ikonomov, O. C., Sbrissa, D. & Shisheva, A. Localized PtdIns 3,5-P2 synthesis to regulate early endosome dynamics and fusion. *Am J Physiol Cell Physiol* **291**, C393-404, doi:10.1152/ajpcell.00019.2006 (2006).

14   Maharana, S. *et al.* RNA buffers the phase separation behavior of prion-like RNA binding proteins. *Science* **360**, 918-921, doi:10.1126/science.aar7366 (2018).

15   Gerbino, V. *et al.* The Loss of TBK1 Kinase Activity in Motor Neurons or in All Cell Types Differentially Impacts ALS Disease Progression in SOD1 Mice. *Neuron* **106**, 789-805 e785, doi:10.1016/j.neuron.2020.03.005 (2020).

16   Choy, C. H. *et al.* Lysosome enlargement during inhibition of the lipid kinase PIKfyve proceeds through lysosome coalescence. *J Cell Sci* **131**, doi:10.1242/jcs.213587 (2018).

17   Kim, G. H., Dayam, R. M., Prashar, A., Terebiznik, M. & Botelho, R. J. PIKfyve inhibition interferes with phagosome and endosome maturation in macrophages. *Traffic* **15**, 1143-1163, doi:10.1111/tra.12199 (2014).

18   Han, S. S., Williams, L. A. & Eggan, K. C. Constructing and deconstructing stem cell models of neurological disease. *Neuron* **70**, 626-644, doi:10.1016/j.neuron.2011.05.003 (2011).

19   Nehme, R. *et al.* Combining NGN2 Programming with Developmental Patterning Generates Human Excitatory Neurons with NMDAR-Mediated Synaptic Transmission. *Cell Rep* **23**, 2509-2523, doi:10.1016/j.celrep.2018.04.066 (2018).

20   Amoroso, M. W. *et al.* Accelerated high-yield generation of limb-innervating motor neurons from human stem cells. *J Neurosci* **33**, 574-586, doi:10.1523/JNEUROSCI.0906-12.2013 (2013).

CHAPTER 5: Discussion, Implications, and Future Directions

5.1 Discussion and implications

5.1.1 TBK1 mutations in ALS: loss of function and ALS relevant pathologies

The advance of next-generation sequencing techniques has led to the discovery of multiple new ALS genes [1], and the heterozygous loss-of-function mutations of TBK1 have been reported to associate with ALS and FTD [2]. However, evaluation of the loss-of-function mutations of TBK1 is halted by the incomplete understanding of TBK1 related pathology in human motor neurons, which prevents the development of more targeted therapeutics [3]. In Chapter 2, we generated a human stem cell model with homozygous loss-of-function mutations of *TBK1*. Our *TBK1* loss-of-function model successfully recapitulated TDP-43 pathology found in most ALS patients. Therefore, our model could be utilized to study the cell-autonomous mechanisms of TDP-43 pathology in human motor neurons.

In addition to TDP-43 pathology, we performed a series of functional assays on motor neuron homeostasis with TBK1 deficiency. Consistent with previous animal experiments [4,5], loss of TBK1 in human motor neurons does not show overt motor neuron death. However, our results revealed some disrupted motor neuron homeostatic functions in TBK1$^{-/-}$ motor neurons. Specifically, loss of TBK1 activity leads to motor neuron hyperexcitability, an early pathogenic phenotype occurring before molecular or anatomical symptoms of neurodegeneration in ALS. The motor neuron hyperexcitability could be explained by at least two mechanisms. First, reduced TBK1 activity causes impaired autophagic flux, which has been found to associate with neuronal hyperexcitability [6]. Similarly, in ATG7-deficient neurons, lysosomal delivery of endocytosed Kir2 channels is disrupted, and the Kir2 channels are elevated on the plasma membrane with reduced activity [7]. These inactivated channels result in decreased Kir2 currents in the absence of autophagy, correlating with the intrinsic hyperexcitability caused by defective autophagic flux [7]. Second, loss of TBK1 results in TDP-43 pathology, which is associated with deficits in RNA processing. Previous studies have revealed that mislocalization or dysfunction of TDP-43 drives intrinsic hyperexcitability of both cortical and motor neurons [8,9]. Although the detailed mechanisms

of TDP-43 dysfunction induced hyperexcitability remained unknown, possible interpretations include perturbations in ion channels and reduction in the magnitude of voltage-activated currents caused by deficits in RNA processing. In addition, we have previously identified the impaired regeneration of motor axons caused by dysfunctional TDP-43 [10]. Loss of TBK1 also induced impaired axonal repair upon axotomy, a marker of early-stage neurodegeneration. One intriguing mechanism for this phenotype could be explained by the central role of TBK1 in maintaining microtubule dynamics. Previous research had demonstrated the role of TBK1 in regulating microtubule dynamics [11], which was essential for axonal growth and regrowth in motor neurons. Another potential mechanism for impaired axonal regeneration in TBK1 deficient cells could be the impaired autophagy activity. Inhibition of autophagy had been shown to impair axonal growth [12], and autophagy induction could promote motor axonal regeneration after spinal cord injury [13]. Thus, although the loss of TBK1 did not cause motor neuron degeneration in culture, TBK1 deficiency and the induced TDP-43 pathology could be linked to disrupted motor neuron physiological properties, like hyperexcitability and impaired axonal repair, suggesting that loss of TBK1 activity could contribute to ALS relevant pathologies in motor neurons.

5.1.2 TDP-43 pathology: highlighting the endo-lysosomal pathway

TDP-43 pathology is a universal hallmark and a prominent feature of ALS. The aggregated form of TDP-43 had been shown to interact with normal TDP-43 and other proteins and impair their normal functions. Previous research had evidenced that TDP-43 mutations or induced TDP-43 pathology were sufficient to cause motor neuron cytotoxicity [14]. Therefore, pathological TDP-43 can pose detrimental effects on motor neurons and subsequently cause motor neuron death in ALS, and figuring out the most disease-relevant target of TDP-43 pathology could be therapeutically beneficial.

The "autophagy theory" has always been intriguing in terms of TDP-43 pathology in ALS. TDP-43 had been shown to regulate ATG7 mRNA stability, which was involved in the process of

autophagosome formation [15]. In addition, several mutations in genes involved in autophagy have been identified to associate with ALS, like p62, OPTN, VCP, and UBQLN2, and all of them include the finding of TDP-43 pathology in patients [16]. Moreover, several research groups have demonstrated the therapeutic effects against TDP-43 aggregates by inducing autophagosome formation with Rapamycin [17,18].

Although accumulating evidence had shown the potential link between TDP-43 pathology and autophagy induction, many studies challenged the "autophagy theory" regarding the therapeutic potential of autophagy induction for TDP-43 pathology. One study by Scotter and others questioned the ability of autophagy induction on clearing pathological TDP-43 in HEK293 cells [19]. Another study also reported that autophagy inducers had no effect on pathological TDP-43 clearance and no reduction of toxicity in yeast models [20]. In addition, Leibiger and colleagues reported the detrimental effect of autophagy induction in yeast when wild-type TDP-43 was overexpressed [21]. Therefore, whether autophagy induction could be a potential therapeutic target against TDP-43 pathology remained debatable, and elucidating the detailed mechanism of TDP-43 pathology in our human motor neuron models could provide novel insights into this debate.

In Chapter 3, our data using human motor neurons suggested that autophagosome formation inhibition by ATG7 deletion did not trigger insoluble TDP-43 accumulations or TDP-43 mislocalization, suggesting pathways independent of autophagy induction in TBK1 deficiency-induced TDP-43 pathology. Therefore, in contrast to the previous recognition that autophagy inhibition is a disease-causing mechanism of TBK1 mutations [22,23], our data provided the first evidence that defective autophagosome formation failed to initiate TDP-43 pathology, a key disease-relevant phenotype, in human motor neurons. In addition, with the phospho-proteome data, we established a mechanistic link between TDP-43 pathology and the impaired endo-lysosomal pathway. Loss of TBK1 induced impaired endo-lysosomal pathway through disrupted endosomal maturation. In addition, inhibition of lysosomal activity was sufficient to trigger TDP-43 mislocalization and its insoluble accumulations. Our results suggested that TBK1 induced

pathological TDP-43 in human motor neurons were mainly cleared by the endo-lysosomal pathway and reduced lysosomal activity could pose detrimental effects on motor neurons (Figure 5.1).
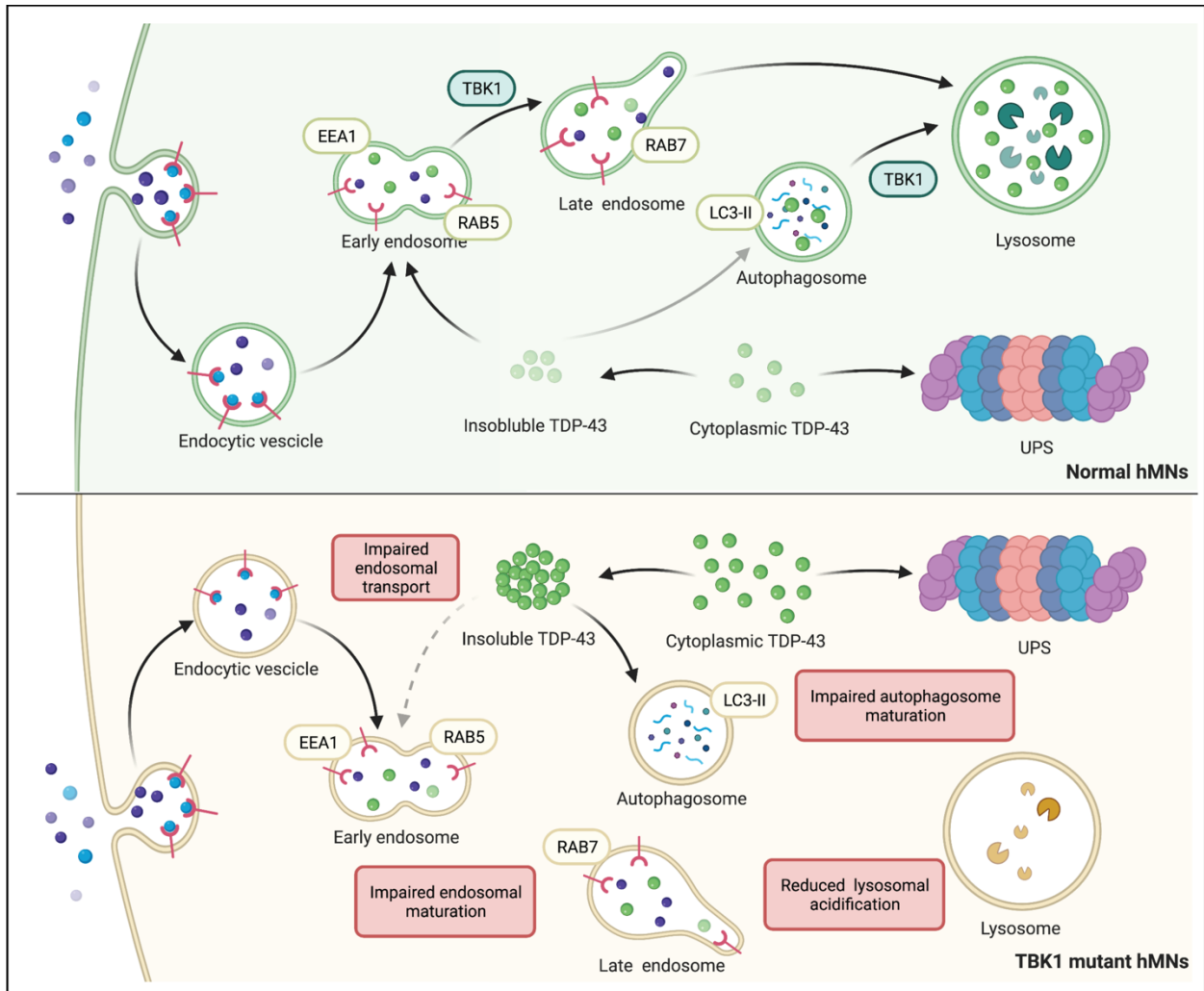
Figure 5.1 TBK1 deficiency induces TDP-43 pathology through the impaired endo-lysosomal pathway in human motor neurons.

Schematic illustration of TBK1-mediated pathological TDP-43 clearance by the endo-lysosomal pathway. Cytoplasmic TDP-43 and their insoluble accumulations are cleared primarily by the endo-lysosomal pathway in normal human motor neurons. Autophagy supplements that clearance function. In human motor neurons with loss of TBK1 activity, impaired endosomal maturation and subsequent lysosomal dysfunction

lead to the accumulation of pathological TDP-43.

5.1.3 TBK1 and endo-lysosomal pathway: implications for potential therapeutics

Our results highlighted the importance of TBK1 activity in TDP-43 and motor neuron pathology, making TBK1 an attractive therapeutic target for ALS and FTD patients with TBK1 mutations. We established a new approach for rescuing the TDP-43 pathology and neurodegeneration induced by reduced TBK1 function: restoring or replacing TBK1 activity. Our results demonstrated that the mislocalization of TDP-43 and its insoluble aggregation could, at least in part, be reversed by restoring functional TBK1 activity in TBK1 deficient motor neurons. In addition, the physiological properties provide evidence for future therapeutics to target TBK1 or downstream mechanisms in ALS patients.

Our results showed that loss of TBK1 in motor neurons was related to TDP-43 pathology and neurodegenerative phenotypes. However, TBK1 is haploinsufficient in ALS patients with the mutations. To determine whether the identified mechanism is universal in clinical settings, we generated human patient iPSCs and induced motor neurons harboring TBK1 mutations to address the clinical relevance of reduced TBK1 activity and ALS disease pathology. Our results showed that TBK1 patient motor neurons were more sensitive to lysosomal stress, highlighting the role of lysosomal activity in ALS progression. Notably, reduced lysosomal acidification and functions had been found to associate with natural aging, which would pose enormous risks to the motor neurons of individuals with TBK1 mutations.

Since TBK1 is needed for the endosome-lysosome pathway in motor neurons, mutations of TBK1 lead to the accumulations of toxic proteins that are inadequately cleared in lysosomes. In contrast to most theories that TBK1 functions through the autophagy initiation pathway in protein degradation, we identified the more critical roles of the endo-lysosomal mechanism in maintaining physiological TDP-43 recycling. A previous study has suggested the role of LAM-002 (Apilimod), an inhibitor of the PIKfyve kinase, in clearing toxic protein aggregates within

lysosomes [24]. We found that Apilimod treatment almost completely rescued the response of TBK1 patient motor neurons to lysosomal stress and re-sustained the motor neuron homeostasis and survival. The fact that PIKFYVE inhibitor, which activates RAB5-induced endosomal trafficking, could restore TBK1 mutant motor neuron function further validated this mechanism. In addition, previous research also showed that PIKFYVE inhibitors could reverse C9ORF72 deficiency-induced neurodegeneration [25], highlighting the mechanistic convergence of endosomal trafficking perturbation in a large portion of ALS. Therefore, our results, combined with previous research, may provide novel insights into the more general and universal therapeutics of ALS and FTD and possibly other neurodegenerative disorders.

5.2 Future directions

5.2.1 Animal studies

This thesis presented evidence supporting a mechanistic link between TBK1 deficiency and TDP-43 pathology in cultured human motor neurons. However, the motor system is highly complex, with diverse cell types and tissues involved, and it is still unclear whether the endo-lysosomal pathway and TDP-43 pathology are true *in vivo*. Previous research using *TBK1* mutant mice showed no evidence for neurodegeneration [4], similar to our results using iPSCs. However, we identified that environmental factors, like lysosomal stress, could pose huge risks to motor neurons with *TBK1* mutations. Recent studies also highlighted the role of environmental factors combined with genetic factors in ALS progression [26,27].

We can use the TBK1 mutant mice as our animal model and stress them with lysosomal inhibitors, like Lys05, to see whether the TBK1 mutations with lysosomal stress affect motor system functions. The Lys05 injection experiment has been established as previously described [28]. In addition, reduction of lysosomal function has been found to occur with natural aging, and the Lys05 experiments will allow us to access the effect of aging posed on TBK1 mutant animals.

We can perform a series of behavior assays on the mice to examine if they display defects in motor system functions, including hanging wire and rotarod [29].

5.2.2 Investigating TBK1 functions in other relevant cell types

The loss-of-function mutation of TBK1 in hESCs established in this project is a valuable tool to investigate the functions of TBK1 in almost any type of cell. Considering the various function of TBK1 and the complexity of ALS disease, we hypothesize that TBK1 may have distinct functions, and the loss of TBK1 may cause diverse functional consequences in different cell types. Mutations of *TBK1* in mice have been shown to affect microglia activation and neuroinflammation [30]. In addition, TBK1 deficiency has been reported to reduce interferon response in astrocytes and microglia [4]. The neuroinflammation pathway is an intriguing mechanism that has been shown to associate with ALS. Loss of TBK1 affected the production of proinflammatory cytokines in the myeloid lineage of cells (like macrophages) [31]. Therefore, it would be interesting to investigate if TBK1 deficiency contributes to ALS through motor neuron non-autonomous mechanisms. With the established protocol for directed stem cell differentiation, we could differentiate our *TBK1* mutant stem cells into a particular cell type and study the functions of TBK1 and the consequences of TBK1 deficiency in that model system.

5.2.3 Novel mechanisms of TBK1 for ALS progression

As discussed in this Chapter 3, TBK1 deficiency leads to the downregulated phosphorylation state of many proteins. Besides the reduced endosomal trafficking pathway, many other interesting mechanisms are also included. For example, reduced phosphorylation also affects RNA splicing and nuclear transport pathways. The dysregulation of alternative splicing of RNA has recently been identified as a major contributor to ALS pathogenesis. Indeed, TDP-43 and FUS are RNA-binding proteins and are involved in RNA processing such as alternative

splicing [32,33]. It will be interesting to investigate whether the dysregulated RNA splicing is caused directly by TBK1 deficiency. In addition, figuring out whether the TDP-43 pathology is induced by aberrant RNA processing or vice versa could be beneficial for more targeted therapeutics for TDP-43 pathology.

The nuclear transport pathway would be another intriguing mechanism in TBK1 deficient motor neurons. Previous studies have shown that the C9orf72 repeat expansion could disrupt the nucleocytoplasmic transport [34,35]. It would be interesting if this could also be observed in motor neurons with *TBK1* mutations. TBK1 shares many similarities with C9orf72 in contributing to ALS pathology, including the disrupted autophagy and endo-lysosomal pathway. However, TBK1 has been reported to affect motor neuron health through the loss-of-function mechanism, while C9orf72 has shown to have both loss-of-function and gain-of-function mechanisms. The disrupted nucleocytoplasmic transport in *C9orf72* mutants has mainly resulted from the gain-of-function mechanism. We can use the TBK1 deficiency model to test the nucleocytoplasmic transport in motor neurons. In addition, it would also be very fascinating to compare the mechanism of TBK1 and *C9orf72* mutations, as there seems to be mechanistic convergence in both genes. A better understanding of the function of regulatory mechanisms of TBK1 could provide us with novel therapeutic insights into this complicated disease and offer us a greater chance for universal therapeutics to cure this disease.

5.3 Concluding remarks

In summary, we generated the first TBK1 loss-of-function model in hESCs by gene editing. When induced into human motor neurons, TBK1 deficiency led to TDP-43 pathology and impaired physiological properties, like hyperexcitability and impaired axonal repair. These findings suggest that our TBK1 deficiency model recapitulated key disease hallmarks and caused disease-relevant pathologies, which could be utilized as a model to study the contribution of TBK1 deficiency to ALS and TDP-43 pathology.

Previous recognition linked TBK1 deficiency-related proteinopathy to impaired autophagy, and ongoing clinical trials were using autophagy inducers to treat ALS patients. We showed that inhibition of autophagy induction failed to reproduce the TDP-43 pathology in human motor neurons, suggesting a mechanism independent of autophagy induction. Using phospho-proteomics data, we identified the disrupted endosomal trafficking pathway that might associate with dysregulated TDP-43 degradation. In fact, TBK1 deficiency led to the impaired endo-lysosomal pathway, and TDP-43 pathology was, at least in part, the consequence of impaired endo-lysosomal pathway. Together, our results suggested the mechanism of TDP-43 pathology induced by TBK1 deficiency in human motor neurons and the potential therapeutic targets independent of autophagy induction.

Meanwhile, we used TBK1 patient-derived iPSCs and investigated the role of TBK1 haploinsufficiency in disease progression and pathologies. Under normal conditions, haploinsufficiency of TBK1 did not display TDP-43 pathology or neurodegenerative phenotypes. However, these patient-derived motor neurons were more sensitive to lysosomal stress, which could occur during natural aging. TBK1 patient motor neurons showed increased TDP-43 pathology and even neurodegeneration under lysosomal stress. Our results suggest that loss of lysosomal function during aging will pose huge risks to individuals with *TBK1* mutations, and modulating RAB5 effectors, which are upstream of endo-lysosomal pathway, could rescue the disease pathologies.

In addition, our results using post-mortem spinal tissues from sporadic ALS patients suggested a potential link between ALS pathology and p-TBK1 levels, providing preliminary evidence that p-TBK1 level could be a potential biomarker for sporadic ALS patients with TDP-43 pathology.

In closing, we investigated the role of TBK1 deficiency in contributing to ALS pathology and identified the key mechanism for TDP-43 pathology. Manipulating this mechanism, rather than the autophagy induction mechanism, could potentially benefit patients with TDP-43

pathology or *TBK1* mutations.

References:

1   Cirulli, E. T. *et al.* Exome sequencing in amyotrophic lateral sclerosis identifies risk genes and pathways. *Science* **347**, 1436-1441, doi:10.1126/science.aaa3650 (2015).

2   Freischmidt, A. *et al.* Haploinsufficiency of TBK1 causes familial ALS and fronto-temporal dementia. *Nat Neurosci* **18**, 631-636, doi:10.1038/nn.4000 (2015).

3   Freischmidt, A., Muller, K., Ludolph, A. C., Weishaupt, J. H. & Andersen, P. M. Association of Mutations in TBK1 With Sporadic and Familial Amyotrophic Lateral Sclerosis and Frontotemporal Dementia. *JAMA Neurol* **74**, 110-113, doi:10.1001/jamaneurol.2016.3712 (2017).

4   Gerbino, V. *et al.* The Loss of TBK1 Kinase Activity in Motor Neurons or in All Cell Types Differentially Impacts ALS Disease Progression in SOD1 Mice. *Neuron* **106**, 789-805 e785, doi:10.1016/j.neuron.2020.03.005 (2020).

5   Brenner, D. *et al.* Heterozygous Tbk1 loss has opposing effects in early and late stages of ALS in mice. *J Exp Med* **216**, 267-278, doi:10.1084/jem.20180729 (2019).

6   McMahon, J. *et al.* Impaired autophagy in neurons after disinhibition of mammalian target of rapamycin and its contribution to epileptogenesis. *J Neurosci* **32**, 15704-15714, doi:10.1523/JNEUROSCI.2392-12.2012 (2012).

7   Lieberman, O. J. *et al.* Cell-type-specific regulation of neuronal intrinsic excitability by macroautophagy. *Elife* **9**, doi:10.7554/eLife.50843 (2020).

8   Dyer, M. S. *et al.* Mislocalisation of TDP-43 to the cytoplasm causes cortical hyperexcitability and reduced excitatory neurotransmission in the motor cortex. *J Neurochem* **157**, 1300-1315, doi:10.1111/jnc.15214 (2021).

9   Devlin, A. C. *et al.* Human iPSC-derived motoneurons harbouring TARDBP or C9ORF72 ALS mutations are dysfunctional despite maintaining viability. *Nat Commun* **6**, 5999, doi:10.1038/ncomms6999 (2015).

10   Klim, J. R. *et al.* ALS-implicated protein TDP-43 sustains levels of STMN2, a mediator of motor neuron growth and repair. *Nat Neurosci* **22**, 167-179, doi:10.1038/s41593-018-0300-4 (2019).

11   Pillai, S. *et al.* Tank binding kinase 1 is a centrosome-associated kinase necessary for microtubule dynamics and mitosis. *Nat Commun* **6**, 10072, doi:10.1038/ncomms10072 (2015).

12   Ban, B. K. *et al.* Autophagy negatively regulates early axon growth in cortical neurons. *Mol Cell Biol* **33**, 3907-3919, doi:10.1128/MCB.00627-13 (2013).

13   He, M. *et al.* Autophagy induction stabilizes microtubules and promotes axon regeneration after spinal cord injury. *Proc Natl Acad Sci U S A* **113**, 11324-11329, doi:10.1073/pnas.1611282113 (2016).

14   Suk, T. R. & Rousseaux, M. W. C. The role of TDP-43 mislocalization in amyotrophic lateral sclerosis. *Mol Neurodegener* **15**, 45, doi:10.1186/s13024-020-00397-1 (2020).

15   Bose, J. K., Huang, C. C. & Shen, C. K. Regulation of autophagy by neuropathological protein TDP-43. *J Biol Chem* **286**, 44441-44448, doi:10.1074/jbc.M111.237115 (2011).

16   Maurel, C. *et al.* Causative Genes in Amyotrophic Lateral Sclerosis and Protein Degradation Pathways: a Link to Neurodegeneration. *Mol Neurobiol* **55**, 6480-6499, doi:10.1007/s12035-017-0856-0 (2018).

17   Mandrioli, J. *et al.* Rapamycin treatment for amyotrophic lateral sclerosis: Protocol for a phase II randomized, double-blind, placebo-controlled, multicenter, clinical trial (RAP-ALS trial). *Medicine (Baltimore)* **97**, e11119, doi:10.1097/MD.0000000000011119 (2018).

18   Zarogoulidis, P. *et al.* mTOR pathway: A current, up-to-date mini-review (Review). *Oncol Lett* **8**, 2367-2370, doi:10.3892/ol.2014.2608 (2014).

19   Scotter, E. L. *et al.* Differential roles of the ubiquitin proteasome system and autophagy in the clearance of soluble and aggregated TDP-43 species. *J Cell Sci* **127**, 1263-1278, doi:10.1242/jcs.140087 (2014).

20   Liu, G. *et al.* Endocytosis regulates TDP-43 toxicity and turnover. *Nat Commun* **8**, 2092,

doi:10.1038/s41467-017-02017-x (2017).

21   Leibiger, C. *et al.* Endolysosomal pathway activity protects cells from neurotoxic TDP-43.
Microb Cell **5**, 212-214, doi:10.15698/mic2018.04.627 (2018).

22   Oakes, J. A., Davies, M. C. & Collins, M. O. TBK1: a new player in ALS linking autophagy
and neuroinflammation. *Mol Brain* **10**, 5, doi:10.1186/s13041-017-0287-x (2017).

23   Catanese, A. *et al.* Retinoic acid worsens ATG10-dependent autophagy impairment in
TBK1-mutant hiPSC-derived motoneurons through SQSTM1/p62 accumulation. *Autophagy* **15**,
1719-1737, doi:10.1080/15548627.2019.1589257 (2019).

24   Choy, C. H. *et al.* Lysosome enlargement during inhibition of the lipid kinase PIKfyve
proceeds through lysosome coalescence. *J Cell Sci* **131**, doi:10.1242/jcs.213587 (2018).

25   Shi, Y. *et al.* Haploinsufficiency leads to neurodegeneration in C9ORF72 ALS/FTD human
induced motor neurons. *Nat Med* **24**, 313-325, doi:10.1038/nm.4490 (2018).

26   Bozzoni, V. *et al.* Amyotrophic lateral sclerosis and environmental factors. *Funct Neurol*
31, 7-19, doi:10.11138/fneur/2016.31.1.007 (2016).

27   Oskarsson, B., Horton, D. K. & Mitsumoto, H. Potential Environmental Factors in
Amyotrophic Lateral Sclerosis. *Neurol Clin* **33**, 877-888, doi:10.1016/j.ncl.2015.07.009 (2015).

28   Xu, C. *et al.* SIRT1 is downregulated by autophagy in senescence and ageing. *Nat Cell
Biol* **22**, 1170-1179, doi:10.1038/s41556-020-00579-5 (2020).

29   Knippenberg, S., Thau, N., Dengler, R. & Petri, S. Significance of behavioural tests in a
transgenic mouse model of amyotrophic lateral sclerosis (ALS). *Behav Brain Res* **213**, 82-87,
doi:10.1016/j.bbr.2010.04.042 (2010).

30   Xu, D. *et al.* TBK1 Suppresses RIPK1-Driven Apoptosis and Inflammation during
Development and in Aging. *Cell* **174**, 1477-1491 e1419, doi:10.1016/j.cell.2018.07.041 (2018).

31   Gao, T. *et al.* Myeloid cell TBK1 restricts inflammatory responses. *Proc Natl Acad Sci U S
A* **119**, doi:10.1073/pnas.2107742119 (2022).

32   Buratti, E., Brindisi, A., Pagani, F. & Baralle, F. E. Nuclear factor TDP-43 binds to the

polymorphic TG repeats in CFTR intron 8 and causes skipping of exon 9: a functional link with disease penetrance. *Am J Hum Genet* **74**, 1322-1325, doi:10.1086/420978 (2004).

33   Polymenidou, M. *et al.* Misregulated RNA processing in amyotrophic lateral sclerosis. *Brain Res* **1462**, 3-15, doi:10.1016/j.brainres.2012.02.059 (2012).

34   Zhang, K. *et al.* The C9orf72 repeat expansion disrupts nucleocytoplasmic transport. *Nature* **525**, 56-61, doi:10.1038/nature14973 (2015).

35   Freibaum, B. D. *et al.* GGGGCC repeat expansion in C9orf72 compromises nucleocytoplasmic transport. *Nature* **525**, 129-133, doi:10.1038/nature14974 (2015).